1. Report No.	2. Government Accession No.	3. Recipient's Catalog No.
NASA CR- 134735		

4. Title and Subtitle	5. Report Date
Coatings for Directional Eutectics	October, 1974
	6. Performing Organization Code
7. Author(s)	8. Performing Organization Report No.
E.J. Felten, T.E. Strangman and N.E. Ulion	PWA-5091
	10. Work Unit No.
9. Performing Organization Name and Address	11. Contract or Grant No.
Pratt & Whitney Aircraft Division United Aircraft Corporation East Hartford, Connecticut	NAS3-16792
	13. Type of Report and Period Covered
12. Sponsoring Agency Name and Address	Contractor Report
National Aeronautics and Space Administration	14. Sponsoring Agency Code

15. Supplementary Notes

Project Manager, John P. Merutka, NASA Lewis Research Center, Cleveland, Ohio

16. Abstract

Eleven coating systems based on MCrAlY overlay and diffusion aluminide prototypes were evaluated to determine their capability for protecting the $\gamma/\gamma'-\delta$ (gamma/gamma prime-delta) directionally solidified eutectic alloy (Ni-20Cb-6Cr-2.5Al) in gas turbine engine applications. Furnace oxidation and hot corrosion, Mach 0.37 burner-rig, tensile ductility, stress-rupture and thermomechanical fatigue tests were used to evaluate the coated $\gamma/\gamma'-\delta$ alloy. The diffusion aluminide coatings provided adequate oxidation resistance at 1144°K (1600°F) but offered very limited protection in 1144°K (1600°F) hot corrosion and 1366°K (2000°F) oxidation tests. A platinum modified NiCrAlY overlay coating exhibited excellent performance in oxidation testing and had no adverse affects upon the eutectic alloy in tensile ductility, stress-rupture and thermomechanical fatigue tests.

17. Key Words (Suggested by Author(s))	18. Distribution Statement
Oxidation resistant coatings Hot corrosion resistant coatings Aluminide coatings Overlay coatings Directionally solidified eutectic superalloys	UNCLASSIFIED – UNLIMITED

19. Security Classif. (of this report)	20. Security Classif. (of this page)	21. No. of Pages	22. Price*
UNCLASSIFIED	UNCLASSIFIED	143	4.50

* For sale by the National Technical Information Service, Springfield, Virginia 22151

FOREWORD

This is the final report of the work performed by the Materials Engineering and Research Laboratory of the Pratt & Whitney Aircraft Division of United Aircraft Corporation, East Hartford, Connecticut under NASA-Lewis Research Center Contract NAS3-16792, entitled Coatings for Directional Eutectics, and conducted during the period March 30, 1973 to June 30, 1974.

Mr. John Merutka of the NASA-Lewis Research Center served as Project Manager for this program.

The Pratt&Whitney Aircraft personnel who contributed to the program are as follows :

Mr. Nicholas E. Ulion, Program Manager
Mr. Edward J. Felten, Principal Investigator
Mr. Thomas E. Strangman, Senior Materials Engineer

In this program, temperature, length and stress values were measured in units of degrees Farenheit, inches and pounds per square inch, respectively. In addition, all compositions are given in weight percent unless specified otherwise.

TABLE OF CONTENTS

LIST OF ILLUSTRATIONS

LIST OF ILLUSTRATIONS (Cont'd)

LIST OF ILLUSTRATIONS (Cont'd)

LIST OF ILLUSTRATIONS (Cont'd)

LIST OF ILLUSTRATIONS (Cont'd)

LIST OF ILLUSTRATIONS (Cont'd)

LIST OF ILLUSTRATIONS (Cont'd)

LIST OF ILLUSTRATIONS (Cont'd)

LIST OF TABLES

LIST OF TABLES (Continued)

I. SUMMARY

The objective of this program was to evaluate MCrAlY (M = Ni and/or Co) overlay and diffusion aluminide coatings for the γ/γ'-δ (gamma/gamma prime-delta) directionally solidified eutectic alloy. It is projected that this alloy will require coating protection on all surfaces for successful use as a gas turbine blade or vane. Therefore, in this program, MCrAlY overlay type coatings which are primary for external airfoil protection and diffusion aluminide type coatings for possible blade root and internal surface protection were evaluated.

Electron beam vapor deposition, sputtering, plasma spraying, electroplating and pack coating techniques, singly or in selected combinations, were employed to fabricate eleven candidate coating systems for protecting the γ/γ'-δ (gamma/gamma prime-delta) directionally solidified eutectic alloy (Ni-20Cb-6Cr-2.5Al). These coatings, which were based on MCrAlY overlay and diffusion aluminide-type systems, were initially screened with furnace oxidation and hot corrosion tests in order to evaluate their potential for protecting the γ/γ'-δ alloy. Fracture strains for selected coatings and the coated eutectic alloy were determined. Three of the most promising MCrAlY overlay coatings were then tested in a 1366°K (2000°F) cyclic oxidation burner rig (Mach 0.37) test for 1000 hours. The best one of these three overlay coatings was then evaluated for effects on stress-rupture and thermomechanical fatigue behavior of the γ/γ'-δ alloy. Visual, metallographic, electron beam microprobe and chemical analyses were conducted on appropriate specimens from the above tests.

The initial furnace tests clearly indicate that the diffusion aluminide coatings are unsatisfactory at high temperatures but may be useful for intermediate temperature protection. These coatings afforded inadequate protection in 1366°F (2000°F) cyclic furnace oxidation and 1144°K (1600°F) laboratory hot corrosion tests. However, in 1144°K (1600°F) cyclic oxidation testing, the aluminide coatings provided adequate protection. Overlay coating systems of all types were superior to the aluminides in these same tests. Many of the overlay coatings, particularly those based on NiCrAlY compositions, provided ample protection for 100 hours of furnace cyclic oxidation at 1478°F (2200°F). This indicates that the full temperature advantage anticipated with the D. S. eutectic alloy may be realized.

While the plasma sprayed overlay coatings adequately protected the γ/γ'-δ eutectic alloy in the furnace tests, they were not equivalent to the electron beam vapor deposited overlays. This was particularly evident in the 1366°K (2000°F) and higher temperature tests where the plasma sprayed coatings failed to form protective aluminum oxide scales.

Tensile testing of coated eutectic alloy specimens indicated that while fracture strains for each of the coatings evaluated were similar, substrate fracture strains varied considerably depending upon the particular coating utilized as illustrated in the following tabulation.

578°K Coating Fracture and γ/γ'-δ Specimen Failure Strains

Coating	Coating Fracture Strain (%)	Specimen Failure Strain (%)
Overlay		
NiCrAlY	0.40-0.70	0.70-0.74
CoNiCrAlY	0.40-0.48	0.47-0.48
NiCrAlY/Pt	0.60-0.81	1.24-1.97
NiCrAlY/Al	0.40-0.52	6.1 - >7.15
Diffusion Aluminide		
Cr/Al	0.51-1.02	2.28-4.04
Ni/Cr/Al	0.40-0.51	4.83-6.04

The data have been tentatively interpreted to indicate that the low strain, low temperature (578°K) failures of some coated γ/γ'-δ specimens are the result of a mechanical interaction between the coating and the substrate. Decreasing the thickness of the "strong" coating layer may provide an acceptable engineering solution for alleviating low strain substrate failures.

Three overlay-type coatings, Ni-20Co-18Cr-13Al-0.3Y, platinum modified Ni-18Cr-12Al-0.3Y, and pack aluminized Ni-18Cr-5Al-0.3Y, were selected for evaluation in the 1366°K (2000°F) burner rig test. The platinum modified NiCrAlY coating performed best; after 1016 hours in test this coating was still providing adequate protection for the eutectic alloy.

Stress-rupture and thermomechanical fatigue testing indicated that the presence of the platinum modified NiCrAlY coating caused no adverse effects on the γ/γ'-δ eutectic alloy properties. As illustrated in the following tabluation, the coated stress-rupture specimens exhibited the longest lives in both the aged and unaged conditions.

NiCrAlY/Pt Coated γ/γ'-δ Stress-Rupture Results
(1311°K - 151.7 MN/m^2 - Air)

Quantity	Coated	Furnace Aged (1366°K/500 hrs/Argon)	Time to Rupture (hours)
2	No	No	106.2, 122.9
2	No	Yes	114.7, 166.4
2	Yes	No	206.1, 206.2
2	Yes	Yes	213.4, 287.3
1	Yes	Yes (Air)	328.8

Failure of both of the NiCrAlY/Pt coated thermomechanical fatigue (700°K, + 0.25% strain; 1311°K, - 0.25% strain) specimens was associated with microstructural defects present in the γ/γ'-δ substrate. One specimen, which failed in 119 cycles, contained numerous oxide inclusions while the second, which failed in 593 cycles, exhibited cellular and lamellar

microstructural variations along the specimen length. Failure of the former specimen was associated with oxide inclusions and, for the latter specimen, localized deformation and failure occurred in a cellular region. The NiCrAlY/Pt coating was in generally excellent condition and was not contributory to specimen failure.

The results of this program demonstrate the fundamental capabilities of overlay type coatings, particularily the platinum modified NiCrAlY system, for protection of external airfoil surfaces of a $\gamma/\gamma' - \delta$ eutectic alloy gas turbine blade or vane. For first generation $\gamma/\gamma' - \delta$ turbine components, diffusion aluminide coatings may provide adequate protection for internal surfaces at intermediate temperatures. However, in hot corrosion environments and in higher temperature oxidation, improved diffusion aluminide coatings will be required.

II. INTRODUCTION

The increasing performance, durability and environmental demands on modern gas turbine engines for commercial service require the development of turbine materials with improved temperature and strength capabilities. Directionally-Solidified (D.S.) eutectics such as gamma/gamma prime-delta, ($\gamma/\gamma'-\delta$) (Ni-20Cb-6Cr-2.5Al) offer the potential of a 56 to 83°K (100 to 150°F) metal temperature advantage or a 50% strength improvement over the best currently-used nickel-base superalloys. These properties would permit the increased gas temperatures and rotor speeds required for advanced engines.

The oxidation characteristics of the $\gamma/\gamma'-\delta$ D.S. eutectic alloy have been sufficiently well determined to establish that oxidation resistant coatings are required over a wide range of temperatures. Thus, development of suitable coatings is an important factor necessary for successful application of eutectic alloy turbine components. The program described herein was directed at identifying coating systems to fulfill this need.

Prior to this investigation, a preliminary evaluation of the compatibility and oxidation resistance of selected diffusion and overlay coatings on eutectic alloys was performed at Pratt & Whitney Aircraft. The 1366°K (2000°F) cyclic oxidation burner rig test, which provided the basis for this initial evaluation, indicated that the diffusion coatings examined did not provide any significant protection for the $\gamma/\gamma'-\delta$ alloy at this temperature. One specimen failed after nine hours due to melting while the remaining specimens were severely oxidized after 140 hours of exposure, or less. In contrast to the diffusion coatings, a NiCrAlY overlay coating on $\gamma/\gamma'-\delta$ had experienced only moderate degradation after exposure for 700 hours in this test. A CoCrAlY overlay coating on a $\gamma'-\delta$ (Ni-23Cb-4.4Al) alloy exhibited cracking in the as-coated (fully processed) condition. Such cracking was attributed to formation of a brittle phase at the coating-alloy interface and/or thermal expansion mismatch strains between the alloy and coating.

Data from these initial P&WA evaluations provided the basis for formulating those coating systems which were evaluated in this program. While the diffusion aluminide coatings appeared to be unsuitable for airfoil surfaces of turbine components, some consideration of these coatings was required since the oxidation characteristics of the uncoated alloy indicate that total surface protection is required. Because of the nature of overlay coating processing (line of sight deposition), protection of internal surfaces requires use of a diffusion aluminide type coating. For blade applications, some (if not all) of the root surfaces will also require protection. Since root areas and internal surfaces will operate at reduced temperatures relative to external airfoil surfaces, diffusion coatings may provide sufficient protection in these areas. In consideration of these factors, emphasis was given to overlay type coatings; however, limited evaluation of aluminide systems was performed in this program as well.

In addition to characterization of the oxidation and hot corrosion resistance of candidate coating systems, the influence of promising coatings on the metallurgical stability and mechanical properties of the eutectic alloy required evaluation. Potential undesirable effects due to coatings, such as reduction of substrate load carrying cross-section by interdiffusional effects at high temperatures, and coating brittleness at low to intermediate temperatures, must be determined and minimized, while beneficial effects, such as protectivity and possible enhancement of thermal fatigue and stress-rupture properties are maximized, to obtain the optimum combination of oxidation and mechanical properties of the coating-eutectic system. Consequently, after D.S. eutectic alloy coupons coated with eleven candidate coating systems (nine overlay and two diffusion aluminide) were evaluated in various furnace oxidation and hot corrosion tests, six coating systems (including the two diffusion aluminides) were subsequently screened to determine fracture strains of both the coatings and coated substrates. Collectively, these data were used to select three coating systems for a 1000 hour/2000°F cyclic oxidation burner rig evaluation. Based on the results of this test, an overlay coating system was selected for additional characterization in stress-rupture and thermomechanical fatigue tests, which were used to determine the influence of the coating upon eutectic alloy properties.

The $\gamma/\gamma'-\delta$ D.S. eutectic alloy specimens required in this program were obtained from various geometry bars cast by the United Aircraft Research Laboratories or the Casting Development Section of the P&WA Materials Engineering and Research Laboratory (MERL). All specimens utilized were machined from cast bars except for the burner rig specimens which were cast to size. All coatings were prepared by the MERL Coatings Group. Electron beam (e.b.) vacuum vapor deposition, sputtering, plasma spraying and electroplating techniques, singly or in selected combinations, were employed to produce the various overlay type systems. For one system, the initial e.b. coating was subsequently partially diffusion aluminized; this system is classified as an overlay type system, however. The diffusion aluminide type coatings were produced by conventional pack cementation techniques; however, one of these systems incorporated a prior electroplated layer, as well.

III. FURNACE OXIDATION EVALUATION

Initially, eleven candidate coatings, consisting of nine MCrAlY overlay and two diffusion aluminide prototypes, were evaluated as protective systems for the directionally solidified $\gamma/\gamma'-\delta$ eutectic alloy (Ni-20Cb-6Cr-2.5Al)* in a series of furnace tests. Previous data from a preliminary P&WA test program indicated that candidate coatings should be principally of the overlay type, since these systems had shown the most promising results for elevated temperature applications. However, diffusion aluminide coatings were included since the oxidation characteristics of the eutectic alloy indicate that root and internal surfaces of turbine hardware would also require protection.

A. CANDIDATE COATING SYSTEMS

The candidate coating systems selected for evaluation in this program are listed in Table I. In order to obtain the desired coating compositions and microstructures, it was necessary to employ a variety of processing techniques, including electron beam evaporation, sputtering, plasma spraying, electroplating and pack cementation. The processing techniques and sequence of utilization are also indicated in Table I.

*All compositions are given in weight percent.

TABLE I

CANDIDATE COATING SYSTEMS

a) 25.4μ (1 mil) nickel (electroplate) plus 127μ (5 mils) Co-18Cr-11Al-0.6Y (electron beam)

b) 12.7μ (0.5 mils) tungsten (sputter) plus 127μ (5 mils) Co-18Cr-11Al-0.6Y (electron beam)

c) 127μ (5 mils) Co-33Ni-18Cr-15Al-0.6Y (electron beam)

d) 127μ (5 mils) Ni-18Cr-12Al-0.3Y (electron beam)

e) 12.7μ (0.5 mils) tungsten (sputter) plus 127μ (5 mils) Ni-18Cr-12Al-0.3Y (electron beam)

f) 127μ (5 mils) Ni-18Cr-5Al-0.3Y (electron beam) plus 63.5μ (2.5 mil) diffusion aluminide (pack)

g) 127μ (5 mils) Co-18Cr-11Al-5Ta-0.3Y (plasma spray)

h) 127μ (5 mils) Ni-18Cr-12Al-2Si-0.3Y (plasma spray)

i) 127μ (5 mils) Ni-18Cr-12Al-0.3Y (electron beam) plus 6.3μ (0.25 mils) platinum (sputter)

j) 50.8 to 76.2μ (2 to 3 mils) ductile diffusion aluminide (pack)

k) 76.2μ (3 mils) nickel (electroplate) plus chromized (pack) plus diffusion aluminide (pack)

A brief summary of the reasons for choosing each coating system follows:

a) 25.4μ (1 mil) nickel (electroplate) plus 127μ (5 mils) Co-18Cr-11Al-0.6Y (electron beam)

b) 12.7μ (0.5 mil) tungsten (sputter) plus 127μ (5 mils) Co-18Cr-11Al-0.6Y (electron beam)

c) 127μ (5 mils) Co-33Ni-18Cr-15Al-0.6Y (electron beam)

In view of the extensive experience that has been accumulated at P&WA with CoCrAlY coatings on conventional nickel-base superalloys, including detailed examination of the mechanical behavior of this coating, and its superior resistance to hot corrosion attack, these systems were included in the program. Since prior experience has shown that CoCrAlY coatings on γ'-δ (Ni-23Cb-4.4Al) exhibited cracking in the coated (fully processed) condition, evaluation of the CoCrAlY coating was proposed in conjunction with nickel and tungsten interlayers which might suppress brittle phase formation or reduce the effects of expansion coefficient mismatch. Tungsten was of particular interest since it had been reported[1] to inhibit interdiffusion between coatings and nickel alloy substrates. Selection of the CoNiCrAlY composition was based on the results of other P&WA development programs related to coatings for conventional nickel-base alloys. Experience in these programs indicated that additions of nickel to CoCrAlY improved diffusional stability, high temperature oxidation resistance, and coating ductility and also possibly reduced thermal expansion mismatch. Therefore, it seemed reasonable to assume that CoNiCrAlY coatings could possibly provide improved compatibility with the γ/γ'-δ substrate without use of an interlayer.

d) 127μ (5 mils) Ni-18Cr-12Al-0.3Y (electron beam)

Considerable experience for a range of NiCrAlY compositions which had been generated in other P&WA programs concerned with conventional superalloys, indicated that these coatings offered superior elevated temperature oxidation resistance and interdiffusional stability on nickel-base superalloys. In addition, preliminary experience at P&WA with NiCrAlY systems on γ/γ'-δ had been very encouraging.

e) 12.7μ (0.5 mils) tungsten (sputter) plus 127μ (5 mils) Ni-18Cr-12Al-0.3Y (electron beam)

Although the diffusional stability of the NiCrAlY coatings are relatively good when compared to other coatings on nickel-base superalloys, it was reported that a tungsten interlayer could be effective in reducing interdiffusion to lower levels[1]. Such effects could be important relative to overtemperature capability for the alloy-coating system.

f) 127μ (5 mils) Ni-18Cr-5Al-0.3Y (electron beam) plus 63.5μ (2.5 mils) diffusion aluminide (pack)

Since it had been established that total surface protection of the $\gamma/\gamma'-\delta$ alloy was required, it was assumed that, for internal surfaces or possibly blade roots, a diffusion aluminide coating could be necessary in conjunction with any airfoil overlay coating developed. Subsequent aluminizing of a previously deposited low aluminum overlay coating appeared to offer a unique processing advantage in that all surfaces could be coated while simultaneously increasing the protectivity of the overlay to a more desirable level. Indeed, results[2] reported in the literature have shown that aluminizing of overlay coatings can be an effective method to increase coating life. Alternatively, a low aluminum overlay coating might be suitable for protection of root surfaces. In this situation, the overlay coating on the root would be masked and only the overlay coated airfoil and the internal surfaces would be aluminized.

g) 127μ (5 mils) Co-18Cr-11Al-5Ta-0.3Y (plasma spray)

h) 127μ (5 mils) Ni-18Cr-12Al-2Si-0.3Y (plasma spray)

Tantalum in CoCrAlY [3,4] and silicon in NiCrAl[2,5,6] had been reported to improve the oxidation performance of these alloys. In addition, such modified compositions could offer improved mechanical or physical properties and/or improved overtemperature capability. Both of these overlay compositions are difficult to fabricate via available vapor deposition (e.b.) techniques. While the plasma spray process is relatively new as a turbine coating processing technique, it offers potential for reducing coating costs and presents essentially unlimited flexibility in the selection of overlay coating compositions.

i) 127μ (5 mils) Ni-18Cr-12Al-0.3Y (electron beam) plus 6.3μ (0.25 mils) platinum (sputter)

It has been shown[7,8] that additions of precious metals such as platinum to aluminide coatings on nickel-base superalloys have significantly increased the useful lives of these coatings in high temperature oxidation. Laboratory evaluations conducted at P&WA had shown that additions of 5 to 10 w/o Pt to NiCrAl(Y) alloys provided improved oxidation and sulfidation performance. A duplex process to fabricate the coating was employed since it was not possible to employ vapor deposition techniques or considered economical to plasma spray such a coating. A subsequent heat treatment was employed to interdiffuse the platinum. Improvements in mechanical, physical, or overtemperature characteristics by virtue of the platinum modification appeared possible.

Results for the oxidation of uncoated eutectic alloys[9] indicated that coatings would be required for $\gamma/\gamma'-\delta$ exposed to temperatures as low as 1033°K (1400°F). Thus, it appears that internal passages of air-cooled hardware and possibly the root surfaces of turbine blades will require protective coatings. Since MCrAlY overlay coatings are limited to line-of-sight deposition, diffusion aluminide type coatings would be necessary to protect internal passages. With this in mind, the Cr/Al and Ni/Cr/Al diffusion coatings identified below, were included in this Program.

j) 50.8 to 76.2μ (2 to 3 mils) ductile diffusion aluminide - chromize (pack) plus aluminide (pack)

To provide total surface protection of the alloy, it appeared that suitable diffusion aluminide coatings had to be developed for the $\gamma/\gamma'-\delta$ alloy to coat internal surfaces and perhaps root surfaces as well. Particularly for a blade application, it appeared that considerably more ductility would be required of the internal airfoil or cooling hole coating than was presently available with conventional aluminides. Current information indicated that the $\gamma/\gamma'-\delta$ alloy was compatible with processing at temperatures as high as 1366°K (2000°F). Pack coating processing at elevated temperatures (to 1366°K) or lower temperature packs (1033°K) in conjunction with subsequent elevated temperature heat treatments appeared to offer potential for providing a ductile diffusion aluminide coating.

k) 76.2μ (3 mils) nickel (electroplate) plus chromize (pack) plus aluminide (pack)

UARL experience[10] indicated that nickel plating and chromizing prior to aluminizing of the $\gamma'-\delta$ alloy produced the most successful diffusion aluminide coating yet evaluated. Limited P&WA experience with conventional aluminides on the $\gamma/\gamma'-\delta$ alloy had not been encouraging (based on coating performance in 1366°K (2000°F) burner rig cyclic oxidation testing). Therefore, the nickel plating, chromizing and aluminizing approach was included in the program, primarily as a point of reference. The ability to employ such a coating process to protect internal and hole surfaces could be severely restricted. In any case, this system appeared to be worthy of consideration since its evaluation could serve to define requirements and limitations associated with development of a suitable diffusion coating for the $\gamma/\gamma'-\delta$ system.

B. PREPARATION OF FURNACE TEST SPECIMENS

Directionally solidified $\gamma/\gamma'-\delta$ (Ni-20Cb-6Cr-2.5Al) eutectic alloy bars 31.7 cm (1.25 inch) diameter by approximately 15.2 cm (6 inches) long were procured from the United Aircraft Research Laboratories. Master melts of the eutectic composition were initially made in alumina crucibles and chill cast into copper molds of appropriate diameter. The resulting castings were then placed in 31.7 cm (1.25 inch) diameter,

99.7% purity, recrystallized alumina cylindrical crucibles and unidirectionally solidified vertically (i.e. Ni_3Cb phase parallel to longitudinal axis) under a dynamic argon atmosphere utilizing the high-gradient apparatus depicted in Figure 1. The solidification rate was 3 cm/hr and each casting was prepared to allow metallographic inspection by polishing a longitudinal flat approximately .05 cm (0.02 inch) deep along the length of the specimen.

The 31.7 cm (1.25 inch) diameter bars were surface ground using flood coolant to produce rectangular blocks approximately 2.22 cm (0.875 inch) by 2.22 cm (0.875 inch) by 7.6 cm (3 inches) long. These blocks were cut into approximately 2.22 cm (0.875 inch) lengths, and the resultant cubes were cut to provide 2.22 cm (0.875 inch) square by approximately 0.15 cm (0.060 inch) thick coupons, using a 0.08 cm (0.031 inch) thick aluminum oxide wheel with flood coolant. The coupons were then surface ground to finish dimension, 0.15 cm (0.060±0.005 inch), using a light grinding method and flood coolant to minimize surface stresses. Finally, all specimens were polished through 600 grit silicon carbide paper to eliminate any residual disturbed surface affects introduced during machining. In addition, edges and corners of each coupon were radiused. The coupons were machined so that the longitudinal direction of the D.S. eutectic resided in the plane defined by the 2.22 cm (0.875 inch) by 2.22 cm (0.875 inch) coupon faces.

Following final surface preparation, several coupons were visually examined and found to contain cracks. Fluorescent Penetrant Inspection (FPI) of all coupons was subsequently performed and the number, location and length of cracks recorded. The cracking occurred during the machining operation. It was originally believed that the machining technique may have been too agressive; however, subsequent experience in this and other programs with the larger diameter 31.7 cm (1.25 inch) bars indicates that residual stresses associated with this size casting are principally responsible for the cracking which occurred.

While the cracking was undesirable, the specimens were considered suitable for the purpose of screening the candidate coatings. Appropriate disposition of these coupons resulted in the specimens being used to screen coatings as originally planned. Based on FPI and visual examination, coupons were segregated into three groups. Coupons with the largest cracks were used to document the pre-test coating conditions for each of the candidate coating systems. Coupons with no cracks or very limited cracks (cracks confined to edges or to one face only) constituted the second group, while specimens with limited to moderate cracking constituted the third group. The specimens were distributed in such a manner that each candidate overlay coating system contained approximately equal numbers of coupons from groups 2 and 3. Coupons used for diffusion aluminide coating evaluation were of the group 2 category. For each candidate coating system, coupons from group 2 were used as the primary specimens for each exposure condition and it is felt that representative weight change data was obtained with these specimens. Coupons from group 3 were used as the duplicate test specimens. Weight change data from these specimens was perhaps less reliable; however, the metallurgical examination of candidate coating systems constituted the primary source of information in interpreting the performance of any given system.

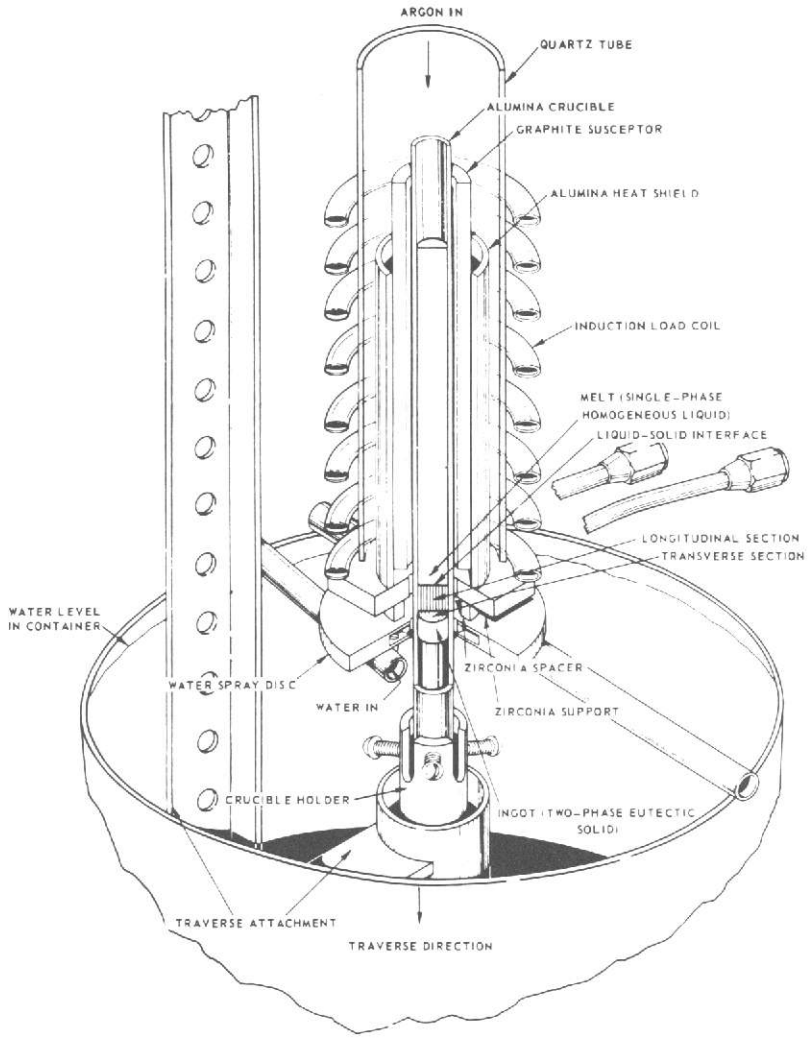

Figure 1 UARL High Thermal Gradient Directional Solification Apparatus

A support rod, which is required for fixturing during the coating operation, was attached to coupons to be overlay coated. Strips of TD-NiCrAl sheet approximately 0.32 cm (0.125 inch) wide by approximately 0.15 cm (0.060 inch) thick and approximately 5 cm (2 inches) long were resistance welded to a corner of each coupon. Prior to test most of the support rod was removed, however, a small portion adjacent to the weld was allowed to remain, thereby minimizing exposed substrate areas.

Ingots of the appropriate MCrAlY compositions were electron beam evaporated and deposited onto $\gamma/\gamma'-\delta$ coupons using techniques which have been described previously[11]. For those duplex coating systems which incorporated platinum or tungsten layers, in conjunction with e.b. coatings, d.c. cathode sputtering techniques similar to those described elsewhere [12,13] were utilized to deposit the elemental layer. Standard electroplating procedures were employed to deposit the nickel layers used in conjunction with the CoCrAlY e.b. coating and standard pack cementation procedures were employed to aluminize the outer half-thickness of the low aluminum NiCrAlY e.b. overlay coating.

Chemistries of the electron beam deposited coatings, obtained by analysis of condensate collected on titanium or iron-base sample plates coated simultaneously with the specimens they represented, are given in Table II. In those instances where two specimens were coated simultaneously, only one sample plate was analyzed.

All electron beam deposited coatings were glass bead peened and heat treated at 1353°K (1975°F) for 4 hours in a hydrogen atmosphere. It should be noted that the platinum modified NiCrAlY coating was peened but not heat treated until after the platinum layer was applied. Also the low aluminum e.b. NiCrAlY coating received only the post-coating heat treatment related to the pack aluminizing cycle (9 hours - 1297°K (1875°F) - argon; 10% Co_2Al_5, 1% Cr, 0.5% NH_4Cl, Balance 220 mesh Al_2O_3).

Following post-coating heat treatment of the W/CoCrAlY coated coupons, physical separation of the coating was observed. An extreme case of this condition is illustrated in Figure 2a. As shown in Figure 2b, separation occurred just above the sputtered tungsten layer in the zone where interdiffusion between the tungsten and CoCrAlY coating has occurred, resulting in a new phase. Electron microprobe analysis of this phase indicated it was rich in cobalt, chromium and tungsten. Subsequently, several chips of the phase were examined by x-ray diffraction analysis. Because of the small amount of material obtained, the quality of the diffraction data was poor; however, it did indicate that this phase was probably related to one of the topologically close packed (TCP) phases[14,15]. As a result of the adherence problem encountered with this system, it was deleted from further consideration in this program. The W/NiCrAlY system had no major adherence problems; however, some chipping at the coupon edges during glass bead peening was encountered. Since the chipping could have exposed the tungsten

TABLE II

CHEMICAL ANALYSIS OF TEST SAMPLE PLATES COATED BY ELECTRON BEAM VAPOR DEPOSITION

Coating Designation	Chemical Analysis (w/o) Ni	Co	Cr	Al	Y	Specimen Nos.
Co-18Cr-11Al-0.6Y		Bal.	17.2	10.9	0.35	233-4[a]/
(Group a - Table I)		Bal.	16.2	10.8	0.51	246-2[b]/246-1[c]
		Bal.	17.0	10.9	0.54	246-13[b]/239-21[c]
		Bal.	18.6	11.0	0.48	239-20[b]/233-18[c]
Ni-18Cr-12Al-0.3Y	76.5		10.3	11.2	>1	/239-16[a]
(Group d - Table I)	69.5		20.0	11.3	0.81	246-5[b]/239-42[c]
	74.4		15.3	11.7	0.37	246-20[b]/233-1[c]
	72.4		17.7	11.0	0.31	239-24[b]/239-34[c]
	74.4		15.4	11.4	0.63	246-29[b]/246-7[b]
Ni-18Cr-5Al-0.3Y	79.5		17.1	5.4	0.07	/239-41[a]
(Group f - Table I)	79.6		17.5	5.2	0.03	246-31[b]/246-22[c]
	78.2		16.9	5.2	0.02	246-24[b]/239-33[c]
	79.9		16.8	5.4	0.10	239-30[b]/239-37[c]
Co-33Ni-18Cr-15Al-0.6Y						
(Group c - Table I)	35.6	31.1	17.6	15.3	0.43	233-7[a]/
	35.4	30.8	18.3	15.1	0.45	246-8[b]/239-18[c]
	35.6	30.6	18.0	15.2	0.49	233-10[b]/246-15[c]
	35.9	30.8	17.8	15.0	0.53	239-36[b]/233-6[c]
	34.7	30.5	18.3	15.9	0.48	246-27[b]/246-9[b]
Ni-18Cr-12Al-0.3Y	70.6	----	16.1	12.0	0.24	246-3[b]/246-11[c]
(Group e - Table I)	70.7	----	15.1	12.4	0.32	246-17[b]/233-17[c]
	70.8	----	14.9	12.9	0.39	239-22[b]/239-25[c]
	70.2	----	18.6	12.0	0.43	233-5[a]/
Co-18Cr-11Al-0.6Y	----	69.7	18.5	11.0	0.24	/233-8[a]
(Group b - Table I)	----	69.9	18.4	10.8	0.29	246-4[b]/246-12[c]
	----	71.6	16.8	10.9	0.28	246-18[b]/233-3[c]
	----	71.2	17.7	10.9	0.36	239-23[b]/239-27[c]
Ni-18Cr-12Al-0.3Y	73.0	----	15.3	11.7	0.28	233-2[a]/
(Group i - Table I)	72.4	----	16.1	11.5	0.29	246-6[b]/249-19[c]
	72.7	----	16.4	11.4	0.38	246-21[b]/239-29[c]
	72.8	----	15.2	11.5	0.64	239-26[b]/239-35[c]

a - Pre-test cracked coupons
b - Excellent quality coupons
c - Good quality coupons

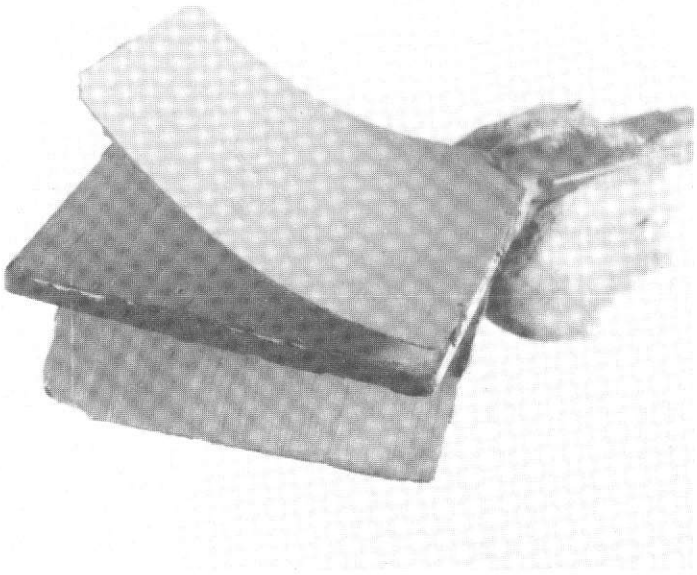

A

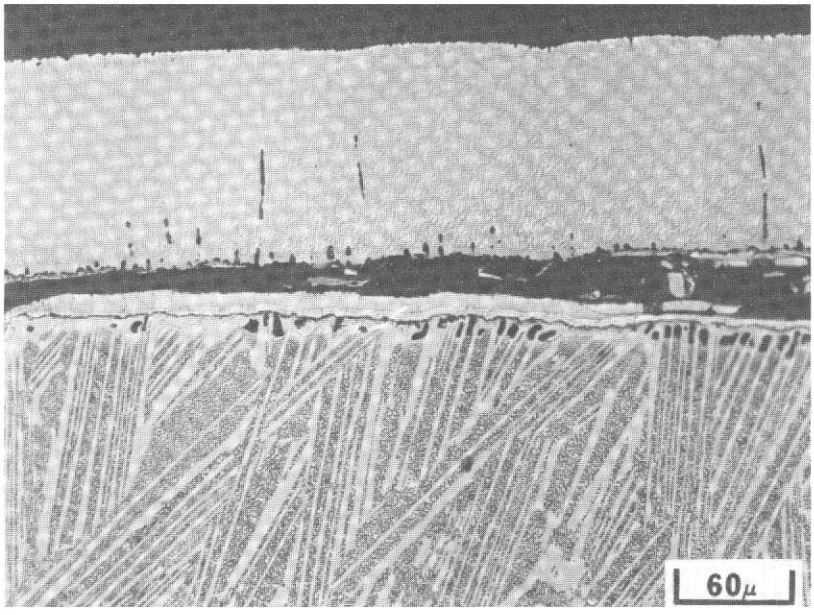

B

Figure 2 Coating debonding observed on γ/γ' - δ coupons which were sputter coated with $\sim 12.7\mu$ (0.5 mils) of tungsten and electron beam vapor deposited with $\sim 127\mu$ (5 mils) of nominal Co-18Cr-11Al-0.6Y; (A) coupon representative of an extreme degree of debonding and **(B)** transverse section of a coupon with less dramatic coating debonding. Note that separation has occurred in the tungsten-CoCrAlY interdiffusion zone. Voids beneath the tungsten layer appear to be associated with the γ/γ' regions of the substrate.

layer, it was decided to employ a slurry aluminide coating to locally repair the chipped areas. This was done and these coupons were used in the furnace evaluations. Typical pre-test microstructures for this and the other overlay type coatings evaluated are shown in Figure 3.

The two plasma sprayed coatings were produced with powders procured from Alloy Metals Incorporated, Troy, Michigan. Chemistry and particle size distribution for the CoCrAlTaY and NiCrAlSiY powders are given in Table III. These powders were applied using a Plasmadyne system employing an SG-100 (Mach 3) gun operating at 76.5 KW with argon and helium, primary and secondary gases, respectively. Spraying was performed in a chamber maintained at a pressure of 44 to 66 microns. Following spraying, coatings were heat treated at 1353°K (1975°F) for 4 hours in a hydrogen atmosphere and glass bead peened. Typical pre-test microstructures for the plasma sprayed coatings are shown in Figure 4. Compared with the electron beam vapor deposited systems, these coatings were less homogeneous and had poorer thickness uniformity.

The diffusion aluminide coatings were obtained by standard pack cementation techniques. The Ni/Cr/Al coating was prepared in three phases. Initially, approximately 76.2μ (3 mils) of nickel was applied to the coupons by standard electroplating techniques. Subsequently, the coupons were chromized (20% Cr, 1-2% NH_4Cl, Balance 120 mesh Al_2O_3 - 6 hours at 1311°K (1900°F)) and aluminized (10% Co_2Al_5, 2% Cr, 0.5-1% NH_4Cl, Balance 220 mesh Al_2O_3 - 12.5 hours at 1297°K (1875°F)). As shown in Figure 5, the thickness and microstructure of this coating varied somewhat depending on whether the coating was parallel or perpendicular to the alloy growth direction; it is possible that this thickness variation resulted from variations in the nickel plate thickness.

The Cr/Al or "ductile" aluminide coating (Figure 6) had surface aluminum contents of 15-17% which were obtained by using a post-pack anneal - 16 hours at 1353°K (1975°F). The chromizing cycle was the same as above; the aluminizing cycle consisted of a two hour exposure at 1297°K (1875°F) in argon with a pack mix consisting of 5% Co_2Al_5, 1% Cr, 0.5-1% NH_4Cl, and balance 220 mesh Al_2O_3.

TABLE III

NiCrAlSiY AND CoCrAlTaY PLASMA SPRAY POWDERS

Chemistry*

	Weight Percent								PPM		
Lot No.	Ni	Co	Cr	Al	Si	Ta	Y	C	O_2	H_2	N_2
3228	----	Bal.	17.53	11.06	----	5.19	0.34	0.011	509	20	86
3232	Bal.	----	17.31	12.09	2.07	----	0.32	0.011	334	9	77

Sieve Analysis**

Lot No.	-325 Mesh	-20 Microns
3228	100 w/o	51.1 w/o
3232	100 w/o	49.5 w/o

*National Spectrographic Laboratories, Inc., Cleveland, Ohio
**Alloy Metals, Inc., Troy, Michigan

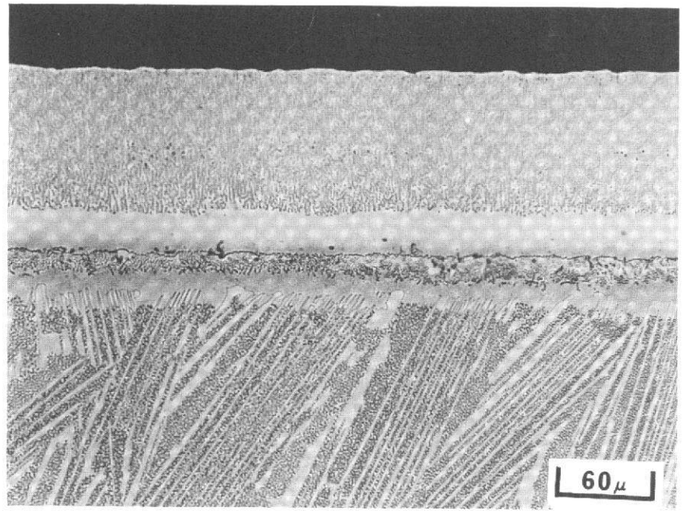

Ni/CoCrAlY

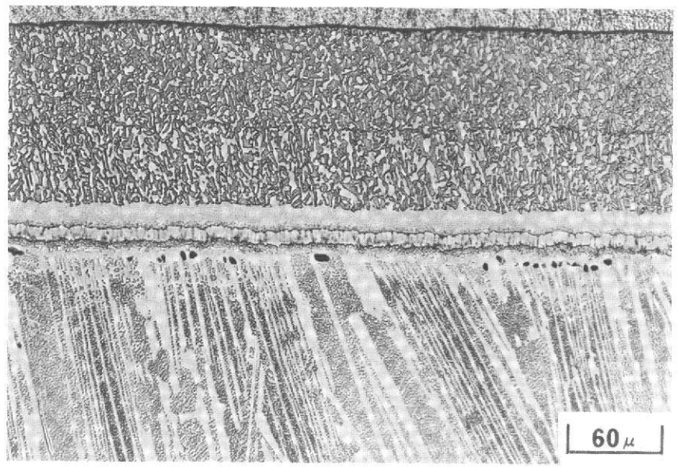

W/NiCrAlY

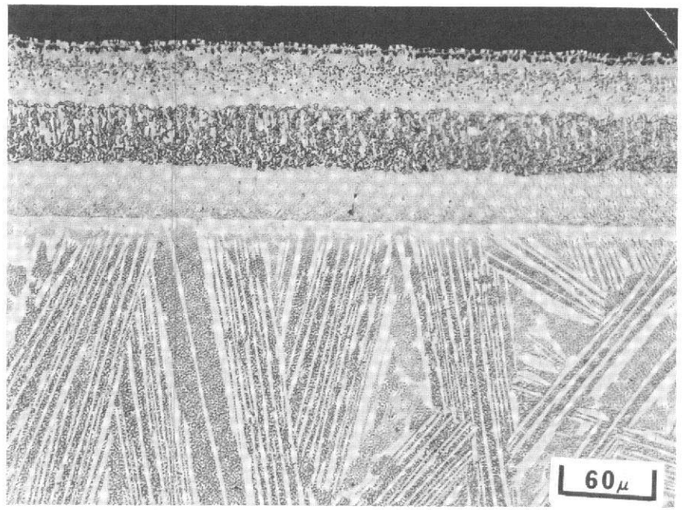

NiCrAlY

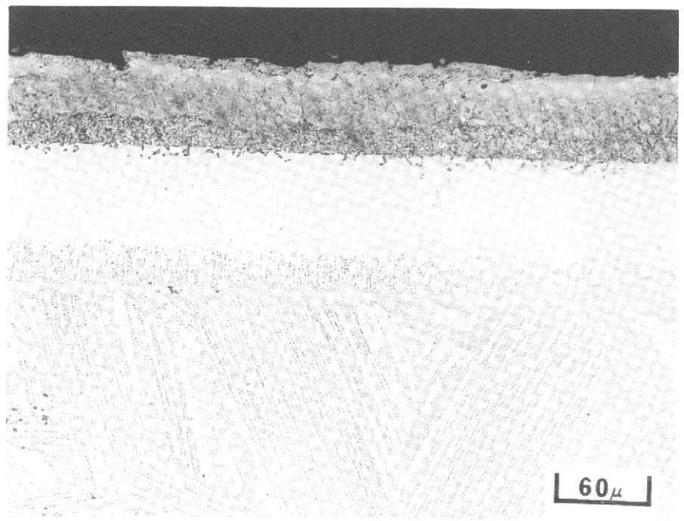

NiCrAlY/Al

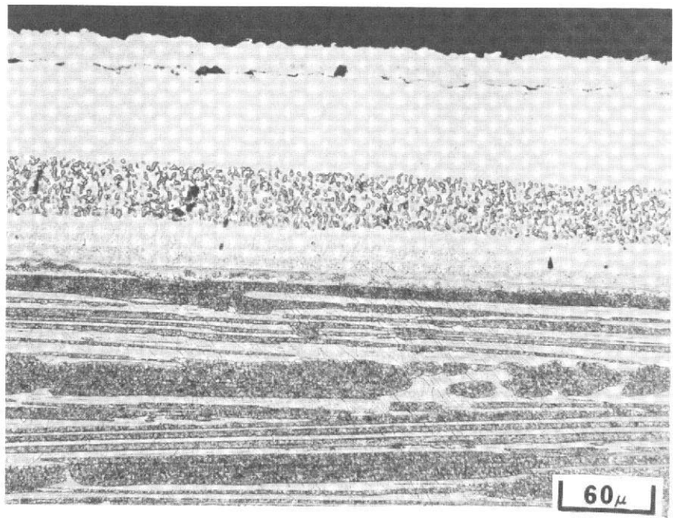

NiCrAlY/Pt

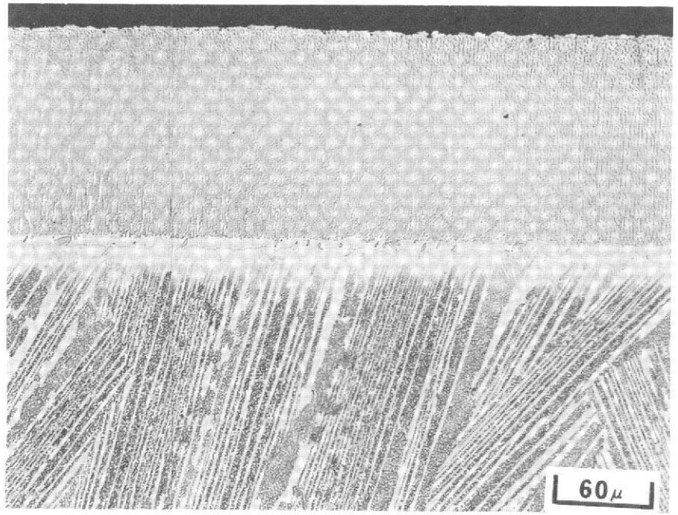

CoNiCrAlY

Figure 3 Metallographic Sections Illustrating Typical Pre-test Microstructural Conditions for Those Overlay Coatings Based on Electron Beam Deposition

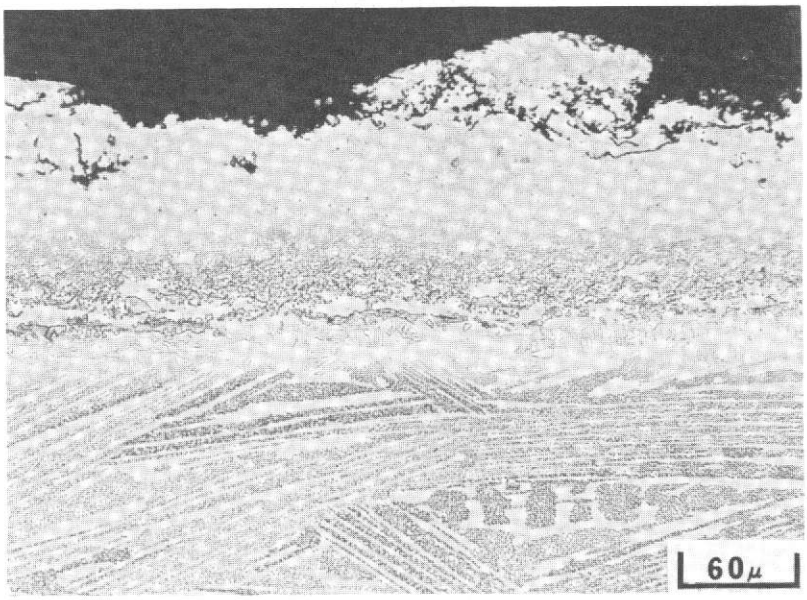

CoCrAlTaY

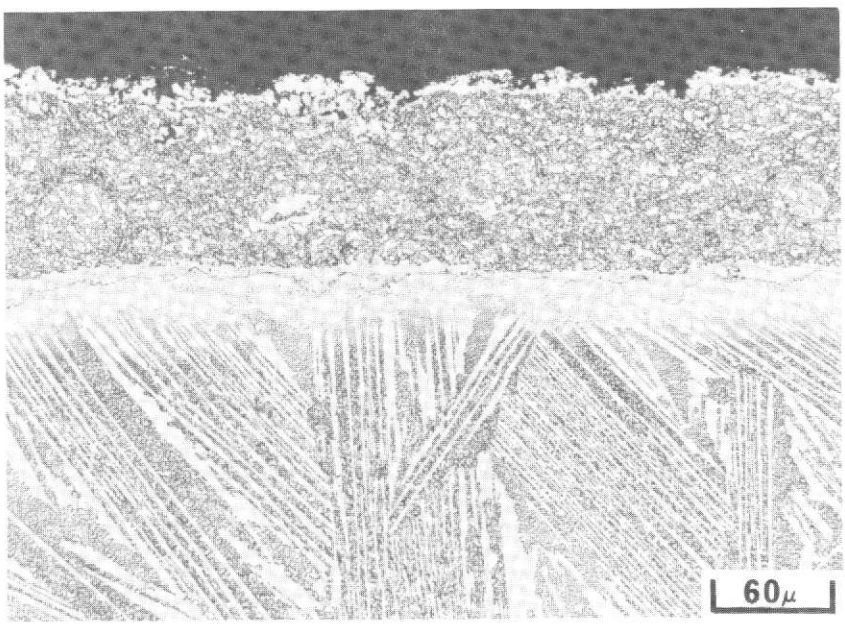

NiCrAlSiY

Figure 4 Metallographic Sections Illustrating Pre-test Microstructural Condition of Plasma Sprayed Overlay Coatings. While the overall coating quality is good note that the homogeneity and thickness uniformity are poorer than for a vapor deposited coating.

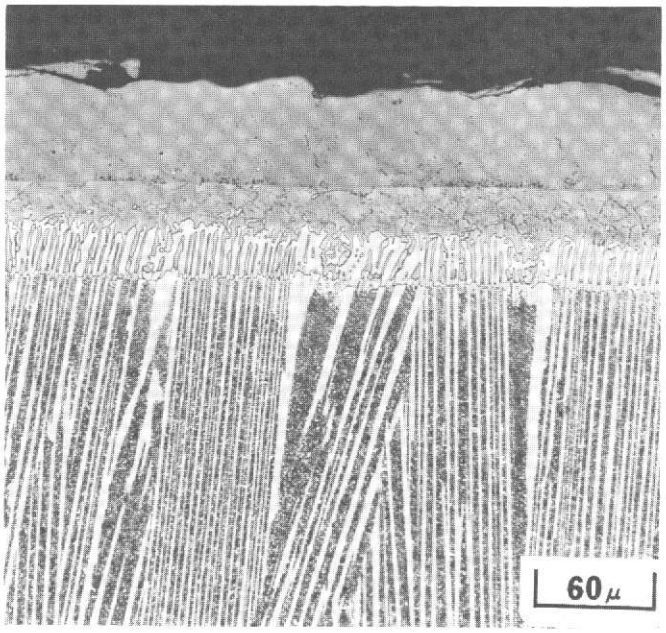

(a)

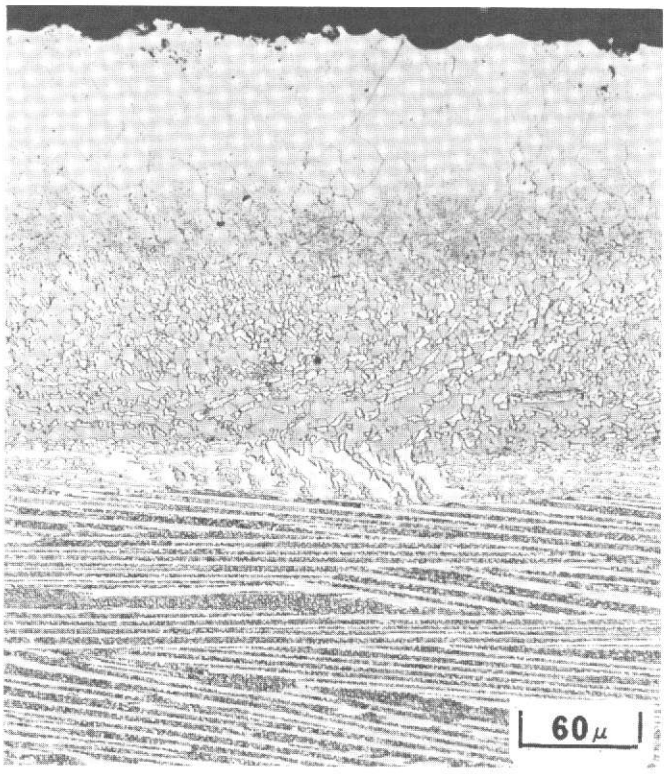

(b)

Figure 5 Transverse (A) and Longitudinal (B) Sections of a Eutectic Alloy Coupon Which Was Electroplated with 76.2μ (3 mils) Nickel, Chromized (6 Hours @ 1311°K) and Aluminized (12.5 Hours @ 1297°K). Note the difference in coating thickness for directions parallel and perpendicular to the alloy growth direction.

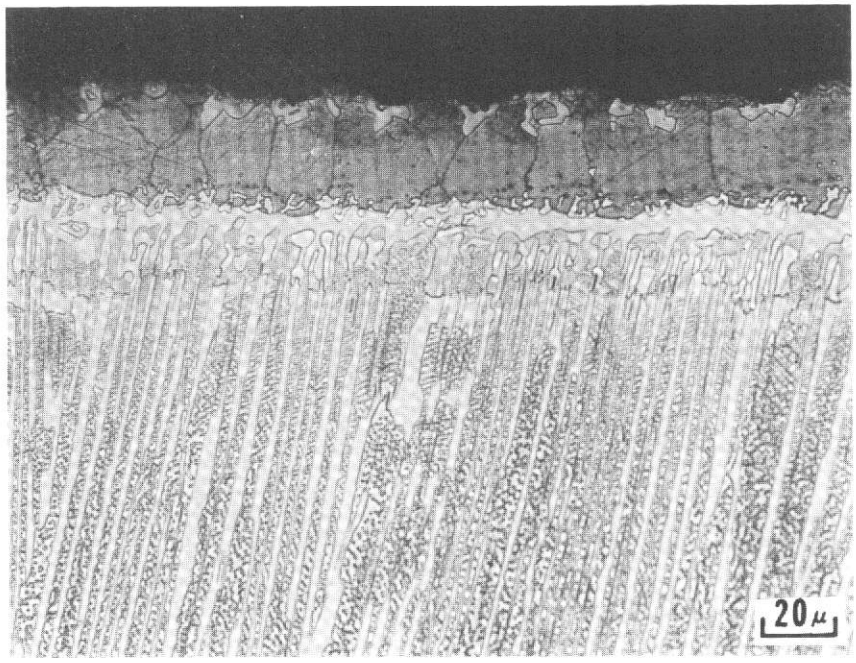

Figure 6 Pre-test Microstructure of the Pack Chromized and Aluminized γ/γ' - δ Eutectic Alloy Which Was Diffusion Annealed for 16 Hours at 1353°K (1975°F)

C. FURNACE TESTING PROCEDURE

The screening of candidate coatings consisted of cyclic oxidation furnace tests at 1144°K (1600°F), 1366°K (2000°F), 1422°K (2100°F) and 1478°K (2200°F), respectively, and a laboratory hot corrosion test at 1144°K (1600°F). Individual test conditions, as well as the systems evaluated in each test, are given in Table IV.

Oxidation specimens were suspended at about 2.54 cm (1 inch) intervals from a coated B-1900 rod in a horizontal tube furnace with a 20 to 25 cm (8-10 inch) hot zone controlled to ±5°K (9°F). Specimens were automatically cycled into and out of the furnace hot zone. The one hour cycles consisted of 55 minutes in the hot zone and 5 minutes of static air cooling at room temperature. Specimens were weighed at 16 to 20 hour intervals. For those systems evaluated, duplicate specimens were tested at 1144°K (1600°F) and 1366°K (2000°F). The overlay type systems were also tested at 1422°K (2100°F) and 1478°K (2200°F), but only single specimens were evaluated at these temperatures.

The hot corrosion test consisted of exposing specimens which were coated with 0.5 mg cm^{-2} of Na_2SO_4 for 20 hour intervals at 1144°K (1600°F). After the exposure interval, the specimens were washed, weighed and visually examined. Sodium sulfate was reapplied and testing continued in this manner for a total of 13 cycles (260 hours). All of the candidate systems were evaluated in duplicate in this test.

While the weight change data obtained in the various furnace tests was indicative of relative coating performance, the primary evaluation criteria was based upon the metallographic condition of the specimens following exposure. Where appropriate, selected specimens were examined using the electron beam microprobe.

D. FURNACE TEST RESULTS

Results of the oxidation and hot corrosion testing will be discussed as a function of increasing temperature. It should be recalled that 1144°K (1600°F) tests were selected for the purpose of screening the coatings for relatively low temperature conditions which are common to internal airfoil passages and blade roots while testing at 1366°K (2000°F) and above was used to evaluate the potential of these coatings for protecting external airfoil surfaces.

TABLE IV

COATING SYSTEMS EVALUATED IN FURNACE TESTING

	100 Hours of 1478°K (2200°F) Cyclic Oxidation	100 Hours of 1422°K (2100°F) Cyclic Oxidation	500 Hours of 1366°K (2000°F) Cyclic Oxidation	100 Hours of 1144°K (1600°F) Cyclic Oxidation	260 Hours of 1144°K (1600°F) Hot Corrosion*
(a) ~ 25.4μ (1 mil) nickel (electroplate) plus ~ 127μ (5 mils) Co-18Cr-11Al-0.6Y (electron beam)	X	X	X	---	X
(b) ~ 127μ (0.5 mil) tungsten (sputter) plus ~ 127μ (5 mils) Co-18Cr-11Al-0.6Y (electron beam)	Not Evaluated Because of Coating Adherence Problem				
(c) ~ 127μ (5 mils) Co-33Ni-18Cr-15Al-0.6Y (electron beam)	X	X	X	X	X
(d) ~ 127μ (5 mils) Ni-18Cr-12Al-0.3Y (electron beam)	X	X	X	X	X
(e) ~ 12.7μ (0.5 mil) tungsten (sputter) plus ~ 127μ (5 mils) Ni-18Cr-12Al-0.3Y (electron beam)	X	X	X	---	X
(f) ~ 127μ (5 mils) Ni-18Cr-5Al-0.3Y (electron beam) plus ~ 63.5μ (2.5 mils) diffusion aluminide (pack)	X	X	X	---	X
(g) ~ 127μ (5 mils) Co-18Cr-11Al-5Ta-0.3Y (plasma spray)	X	X	X	---	X
(h) ~ 127μ (5 mils) Ni-18Cr-12Al-2Si-0.3Y (plasma spray)	X	X	X	---	X
(i) ~ 127μ (5 mils) Ni-18Cr-12Al-0.3Y (electron beam) plus ~ 6.3μ (0.25 mil) platinum (sputter)	X	X	X	---	X
(j) ~ 50.8 to 76.2μ (2 to 3 mils) ductile diffusion aluminide (pack)	---	---	X	X	X
(k) ~ 76.2μ (3 mils) nickel (electroplate) plus chromized (pack) plus diffusion aluminide (pack)	---	---	X	X	X

*0.5 mg cm^{-2} Na_2SO_4 applied at 20 hour intervals.

Duplicate specimens representing all coating groups were evaluated in the 1144°K (1600°F) laboratory hot corrosion test, and duplicate specimens representing two overlay and two diffusion aluminide coatings were evaluated in the 1144°K (1600°F) cyclic oxidation test.

1144°K (1600°F) Laboratory Hot Corrosion Test (260 hours)

The results of the hot corrosion test are summarized in Table V. As suggested by the weight change results, all of the overlay coatings provided adequate protection during the course of this test. Moreover, in almost every instance, the reproducibility of the test results was excellent. Metallographic examination of the test specimens revealed attack to be minimal and uniform as illustrated in Figures 7 and 8.

The diffusion aluminide coatings of both types were subject to localized pitting failures. At sites where failure had occurred, it was generally observed that the coating had been completely oxidized and reaction with the substrate was observed as shown in Figure 9.

The results obtained with the uncoated $\gamma/\gamma'-\delta$ alloy at this temperature show that Na_2SO_4 accelerates attack of the alloy. It is worth noting that the weight change time relationships obtained in both tests at 1144°K (1600°F) show the degradation process to be gradual and controlled as shown in Figures 10a and 10b. In addition, no preferential attack of the δ phase was observed.

1144°K (1600°F) Furnace Cyclic Oxidation Test (100 hours)

The results of the 1144°K (1600°F) cyclic oxidation test are summarized in Table VI. All of the vapor deposited specimens performed extremely well in this test. While visual evidence of non-uniform oxidation was observed, results from the weight-change measurements and metallographic examinations showed that any influences on coating life due to this behavior were negligible. All of the coatings evaluated in the 1144°K (1600°F) cyclic oxidation test proved to be satisfactory at this temperature. Representative microstructures are illustrated in Figure 11 for the two diffusion aluminide and two of the e.b. overlay coatings following 100 hours of 1144°K (1600°F) furnace cyclic oxidation. The weight changes observed for all coated alloys were less than that observed for the uncoated $\gamma/\gamma'-\delta$ alloy. However, as in the previous test, the overlay coatings were superior to the diffusion aluminide coatings. In this test, the oxide formed on the latter coatings was adherent in contrast to their behavior at 1366°K (2000°F). In the absence of hot corrosion effects the aluminide coatings would, however, also provide significant protection for the $\gamma/\gamma'-\delta$ alloy at 1144°K (1600°F).

TABLE V

1144°K (1600°F) FURNACE CYCLIC HOT CORROSION BEHAVIOR OF COATED $\gamma/\gamma'-\delta$ EUTECTIC ALLOYS

Coating Type	Total Wt. Change[a] ($mg\ cm^{-2}$)	Comments
Ni/CoCrAlY	0.06 0.04	Both specimens were attacked to a minimal extent.
W/NiCrAlY	0.10 0.60	Weight change data affected by excessive attack at coating repair sites.
NiCrAlY	0.17 0.12	Both specimens were in excellent condition at the conclusion of the test.
NiCrAlY/Pt	0.11 0.03	Both specimens lost weight initially, but were in excellent condition at the conclusion of the test.
NiCrAlY/Al	0.36 0.43	Localized failure sites were observed at defects in the coating.
CoNiCrAlY	0.06 0.02	Both specimens were attacked only to a slight degree.
CoCrAlTaY	0.64 0.15	Both specimens were covered with a blue spinel oxide. Reproducibility was only fair.
NiCrAlSiY	0.02 0.01	The small final weight changes may be due to a combination of spalling and removal of Cr from the coating due to formation of soluble Na_2CrO_4.
Ductile Aluminide	1.47 1.57	Large weight gains due to selective attack at specimen corners.
Ni/Cr/Al	0.37 0.38	Localized failure sites were observed at defects in the coating.
Uncoated $\gamma/\gamma'-\delta$	4.90	Accelerated attack observed.

(a) Specimens coated with 0.5 mg cm^{-2} Na_2SO_4 (every 20 hours) and oxidized for 13-20 hour cycles (260 hours) at 1144°K (1600°F).

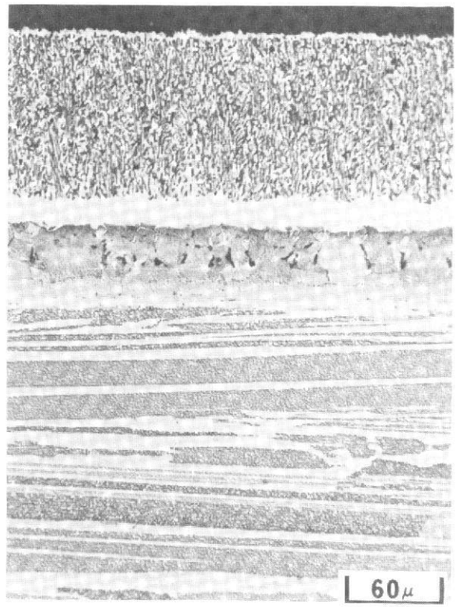

Ni/CoCrAlY

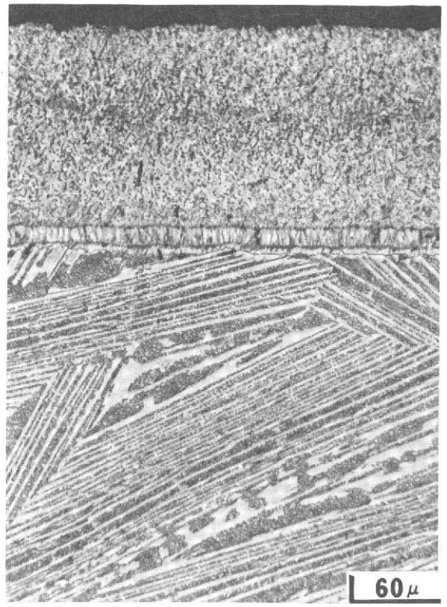

W/NiCrAlY

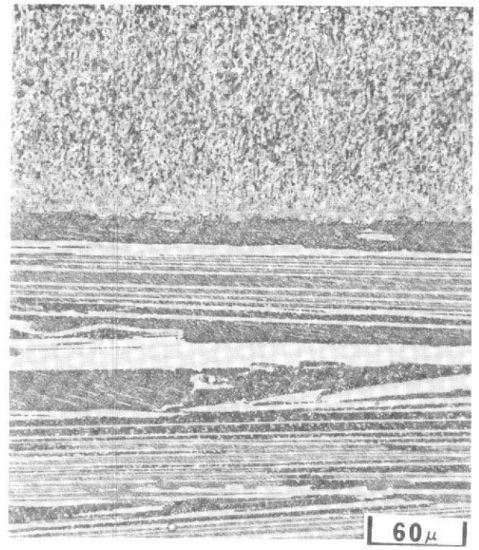

NiCrAlY

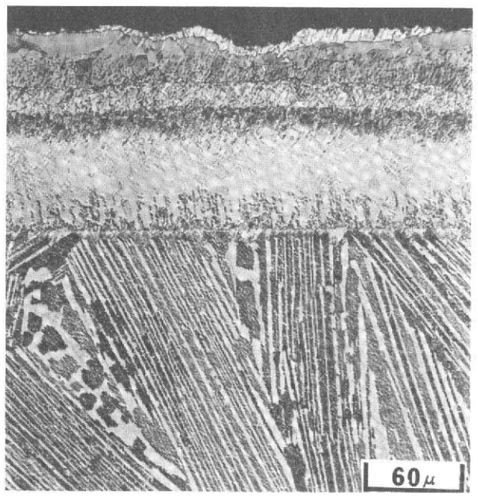

NiCrAlY/Al

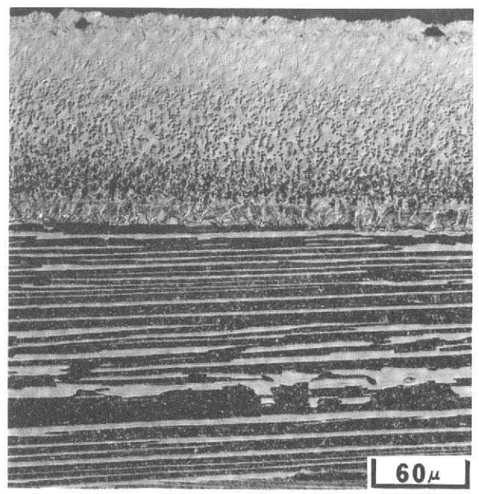

NiCrAlY/Pt

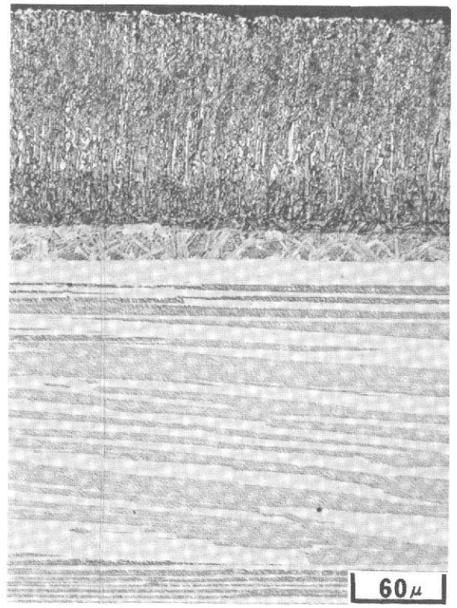

CoNiCrAlY

Figure 7 Post-Test Microstructural Condition of e.b. Overlay Coatings Which Were Exposed for 260 Hours in the 1144°K (1600°F) Laboratory Hot Corrosion Test

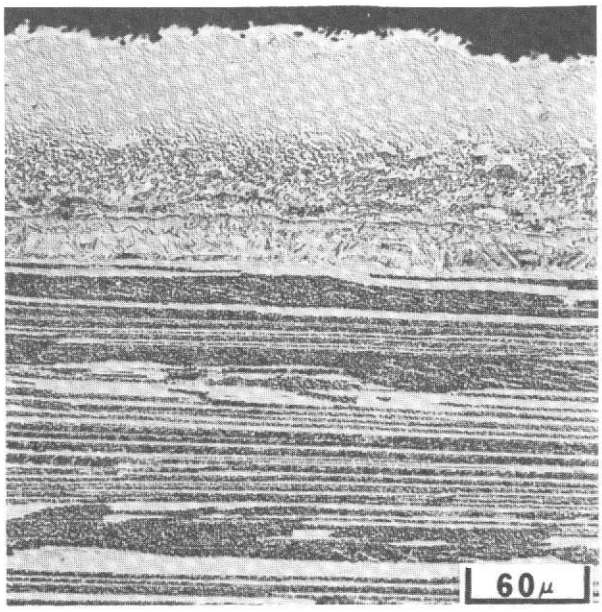

CoCrAlTaY

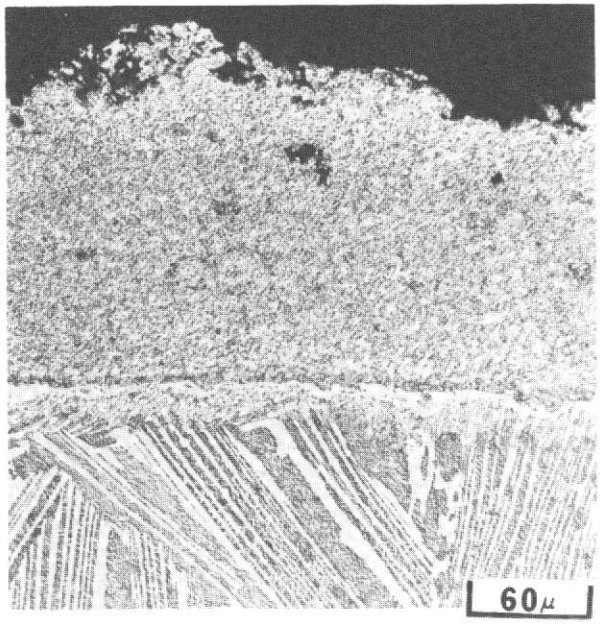

NiCrAlSiY

Figure 8 Post-Test Microstructures of Plasma Sprayed Overlay Coatings Which Were Exposed for 260 Hours in 1144°K (1600°F) Laboratory Hot Corrosion Test

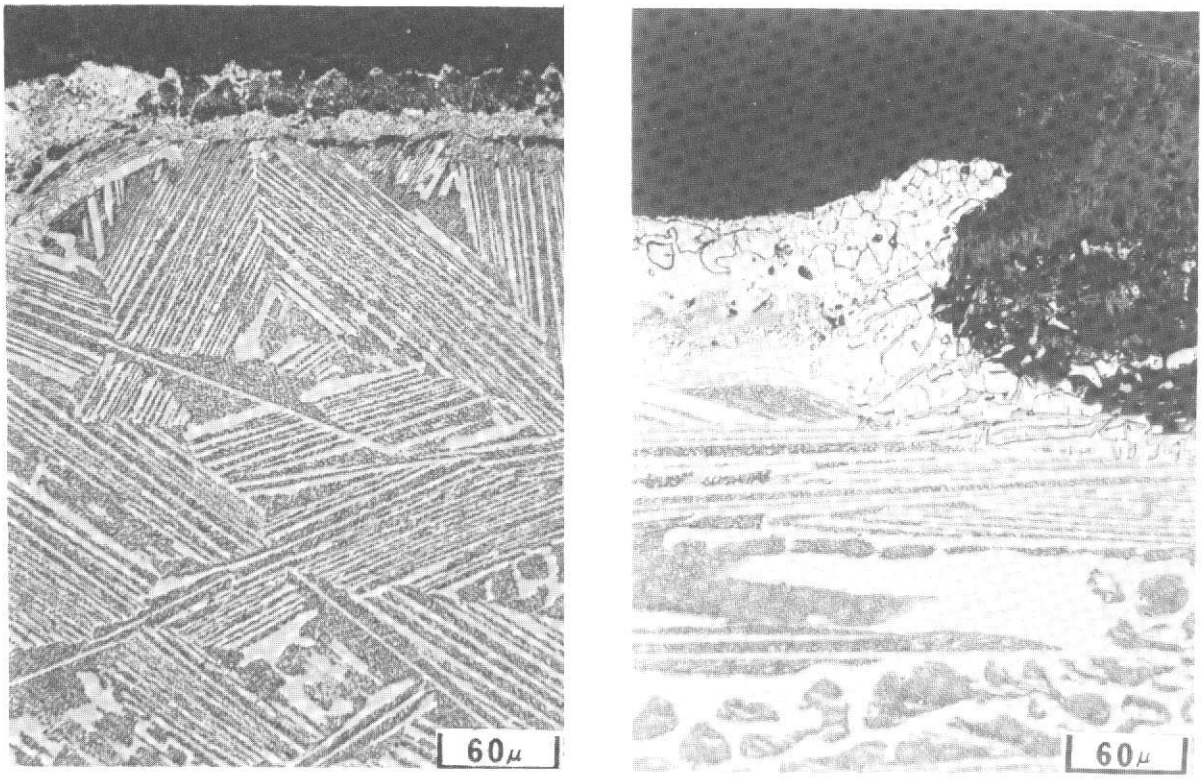

Cr/Al

Ni/Cr/Al

Figure 9 Post-Test Microstructures of Pack Coated Eutectic Alloy Specimens Which Were Exposed for 260 Hours in 1144°K (1600°F) Laboratory Hot Corrosion Test. Note the presence of localized coating failures and associated substrate attack.

TABLE VI

1144°K (1600°F) FURNACE CYCLIC OXIDATION OF COATED
$\gamma/\gamma'-\delta$ EUTECTIC ALLOYS

Coating Type	Total Wt. Change ($mg\ cm^{-2}$)	Comments
NiCrAlY	0.18 0.03	Generally uniform adherent Al_2O_3 scale formed on both specimens.
CoNiCrAlY	0.10 0.03	Generally uniform adherent Al_2O_3 scale formed on both specimens.
Ductile Aluminide (Cr/Al)	0.61 0.63	Adherent oxide was primarily Al_2O_3, but also contained some Cr-rich oxides.
Ni/Cr/Al	0.35 0.43	The oxide formed on these specimens appeared to be richer in Al_2O_3 than that formed in the ductile aluminide.
Uncoated $\gamma/\gamma'-\delta$	1.60	The external oxide scale was adherent NiO.

Specimens oxidized for 100 cycles

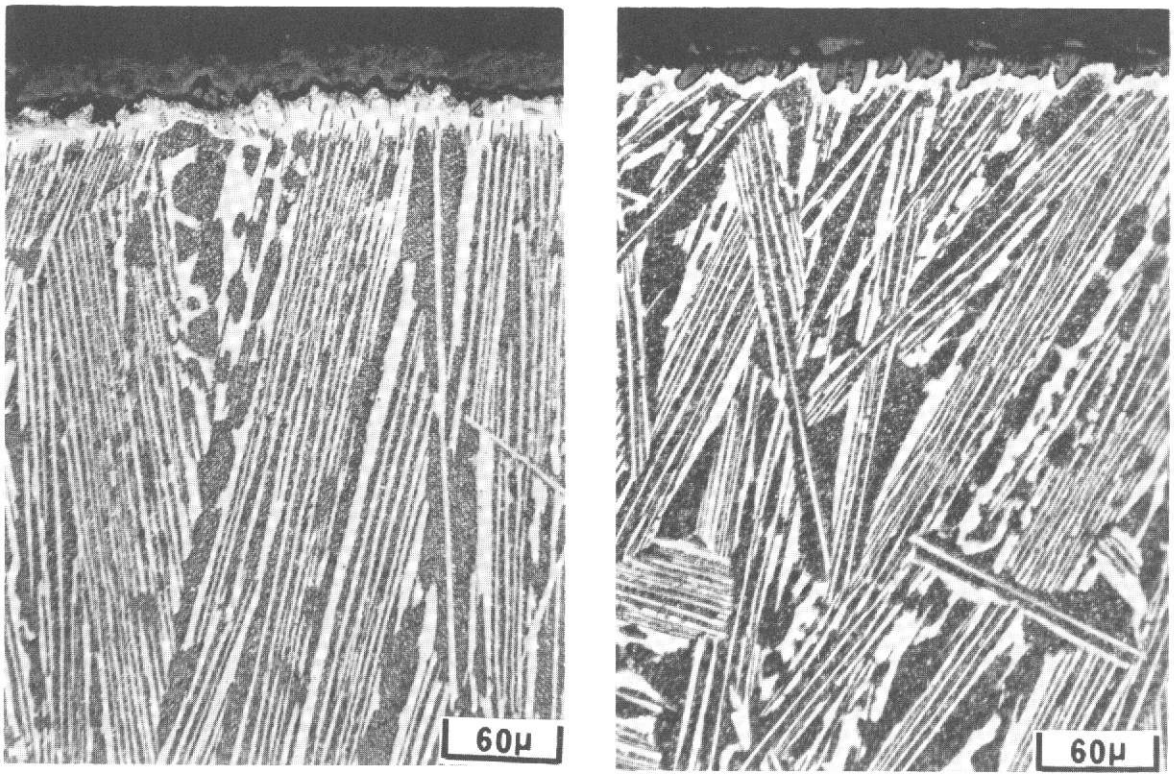

A B

Figure 10 Laboratory Hot Corrosion and Cyclic Oxidation Behavior of Uncoated γ/γ'-δ Eutectic Alloy. Alloy Condition After (A) 260 Hours of 1144°K (1600°F) Laboratory Hot Corrosion and (B) 100 Hours of 1144°K (1600°F) Cyclic Oxidation.

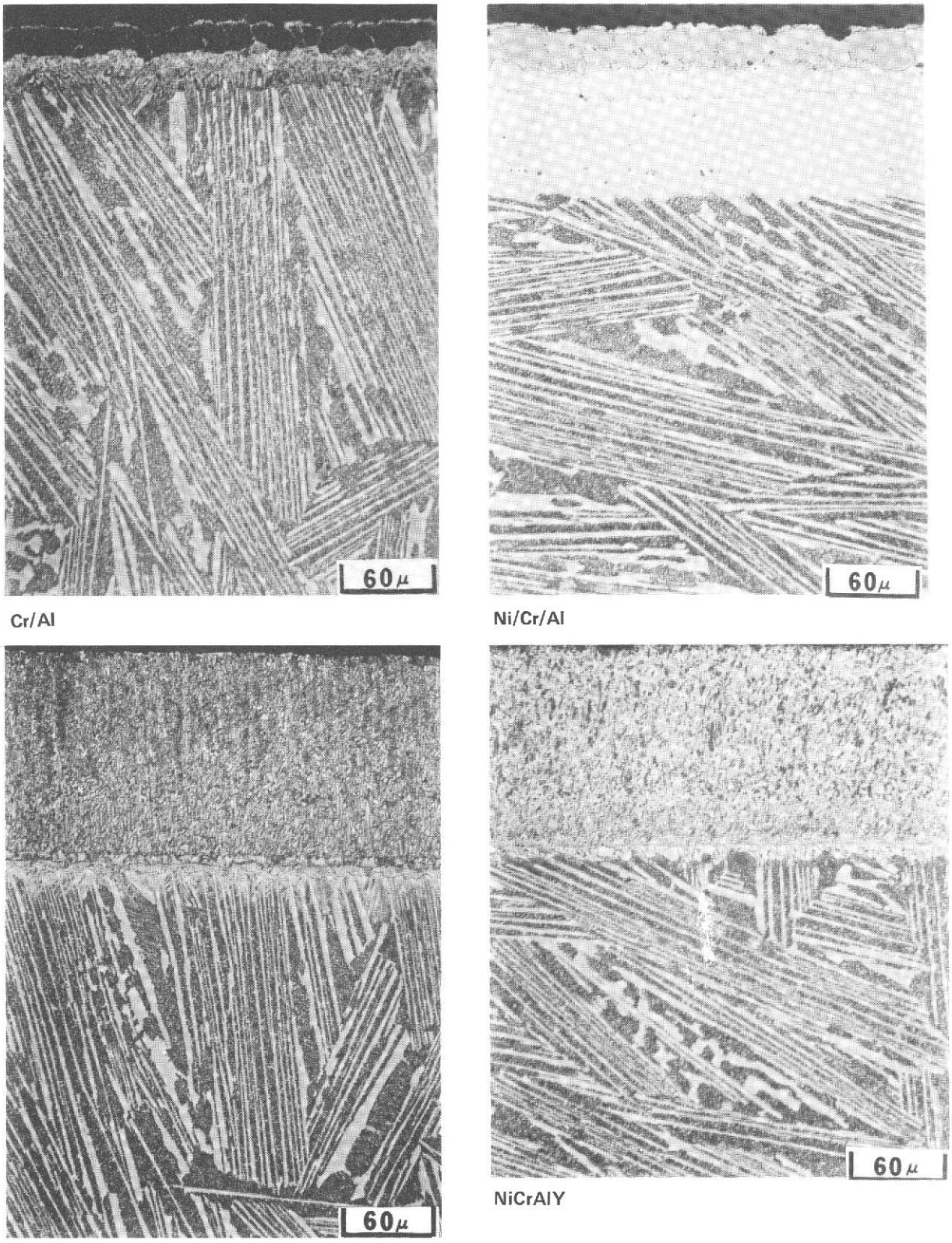

Figure 11 Post-Test Microstructures of Diffusion and e.b. Overlay Coatings on the Eutectic Alloy Which Were Exposed For 100 Hours In The 1144°K (1600°F) Cyclic Oxidation Test.

1366°K (2000°F) Furnace Cyclic Oxidation Test (500 hours)

The results of the 1366°K (2000°F) cyclic oxidation test are summarized in Table VII. The performances of the coatings in this test can be logically divided into three categories; e.b. vapor deposited overlay, plasma sprayed overlay, and diffusion aluminide coatings.

Coatings of the e.b. vapor deposited overlay type generally provided a significant amount of protection during the course of the test. The weight changes as a function of time for five of these coatings are presented in Figure 12. Of the coatings illustrated in this figure, the NiCrAlY/Pt and CoNiCrAlY coatings were judged to be most protective. The primary protective oxide formed on all these overlay coated specimens was Al_2O_3. The presence of yttrium in these coatings provided enhanced oxide adherence during the course of this test. Platinum, when present in the coating, is also believed to improve oxide adherence.

The plasma sprayed CoCrAlTaY and NiCrAlSiY coated specimens behaved in essentially the same manner, as illustrated in Figure 13. Formation of oxides other than Al_2O_3 on the surfaces of these coatings was observed. On the CoCrAlTaY-coated specimens a deep blue spinel, probably $CoAl_2O_4$, was the primary oxide while on the NiCrAlSiY-coated specimens both Al_2O_3 and $NiCr_2O_4$ were formed. Oxide spalling was responsible for the shapes of the weight gain time relationships observed in Figure 13. The plasma sprayed coatings provided some protection at 1366°K (2000°F), but were not equivalent to the vapor deposited overlay coatings.

The diffusion aluminide coatings provided inadequate protection at 1366°K (2000°F). As seen in Figure 14, these coatings are only marginally better in performance than the uncoated alloy. The oxide formed on these coatings, Al_2O_3, was non-adherent throughout the course of the experiment, leading to rapid degradation of the specimens. The absence of an active element, such as yttrium, is considered responsible for the poor performance of these coatings despite the fact that they are alumina formers, at least during the early stages of the test.

TABLE VII

1366°K (2000°F) FURNACE CYCLIC OXIDATION BEHAVIOR OF COATED γ/γ'-δ EUTECTIC ALLOYS

Coating Type	Cycles	Total Wt. Change ($mg\ cm^{-2}$)	Comments
Ni/CoCrAlY	500 300	2.45 3.11	The coating on both specimens was non-uniformly attacked with adherent Al_2O_3 formed over about 50% of the surface. In a patterned area spinel and CoO was observed in addition to spalling.
W/NiCrAlY	120 20	-0.20 2.58	The testing of both specimens was terminated prematurely due to separation of the coating from the substrate.
NiCrAlY	500 440	1.24 -1.13	On both specimens spalling occurred over about 75% of the surface in a non-uniform manner. On the remainder of the surface adherent Al_2O_3 had formed. A massive crack in the first specimen did not appear to seriously affect the performance of the specimen, but did result in the positive weight change observed.
NiCrAlY/Pt	500 420	0.58 -1.31	The oxide formed on both specimens was predominantly Al_2O_3, but contained small amounts of spinel. The oxide was adherent on both specimens. The coating on the second specimen delaminated in the vicinity of a crack in the base metal.
NiCrAlY/Al	500 440	0.28 0.37	The oxide formed on both specimens was Al_2O_3 which tended to spall in moderate amounts during the latter portion of testing.
CoNiCrAlY	500 500	0.32 0.52	The oxide formed on both specimens was predominantly Al_2O_3, but contained small amounts of spinel. A slight amount of spalling in localized areas was observed toward the end of testing.

TABLE VII (CONTINUED)

Coating Type	Cycles	Total Wt. Change ($mg\ cm^{-2}$)	Comments
CoCrAlTaY	500 400	-1.55 -1.75	The oxide formed on both specimens was predominantly spinel which spalled in moderate amounts throughout the course of the test.
NiCrAlSiY	500 500	-0.09 -0.05	The oxide formed on both specimens was predominantly Al_2O_3 initially. Increasing amounts of spinel and moderate spalling was observed during the latter portion of the test.
Ductile aluminide (Cr/Al)	100 20	-1.25 -3.00	The oxide formed on both specimens was yellow to brown in color and tended to spall throughout the test.
Ni/Cr/Al	120 140	-1.95 -5.72	The Al_2O_3 formed on these specimens was only semi-adherent. Spalling was observed at the conclusion of each of the 20 cycle increments.
Uncoated $\gamma/\gamma'-\delta$	40	-17.7	The oxide formed on this specimen was grey-green in color. A considerable amount of spalling was observed at the conclusion of each of the 20 cycle increments.

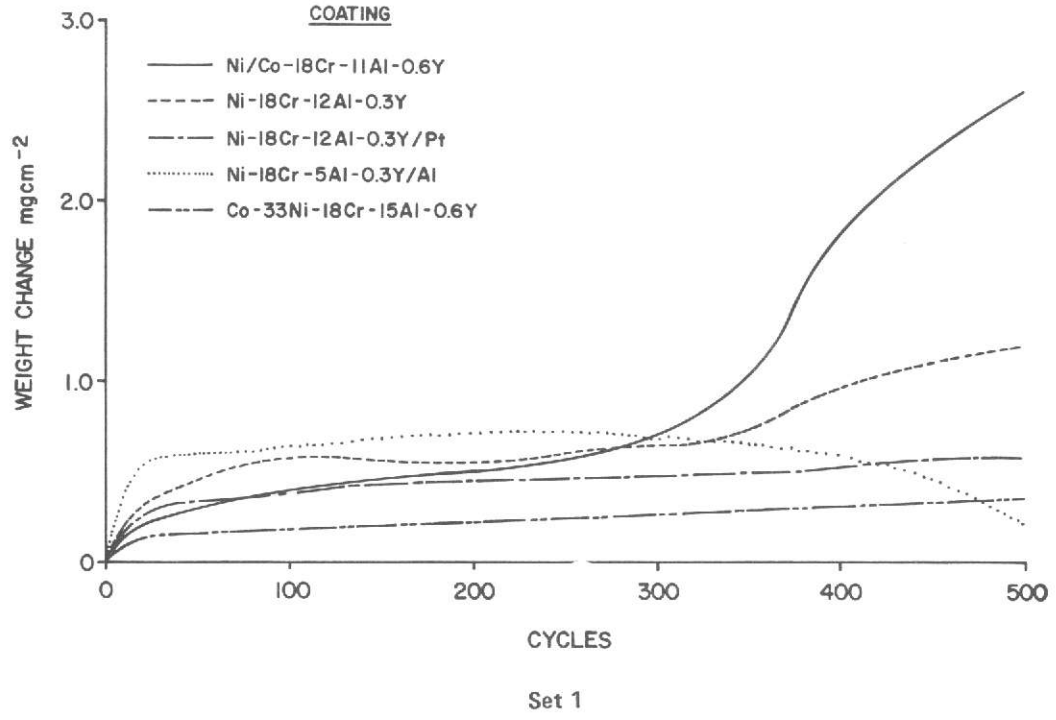

Set 1

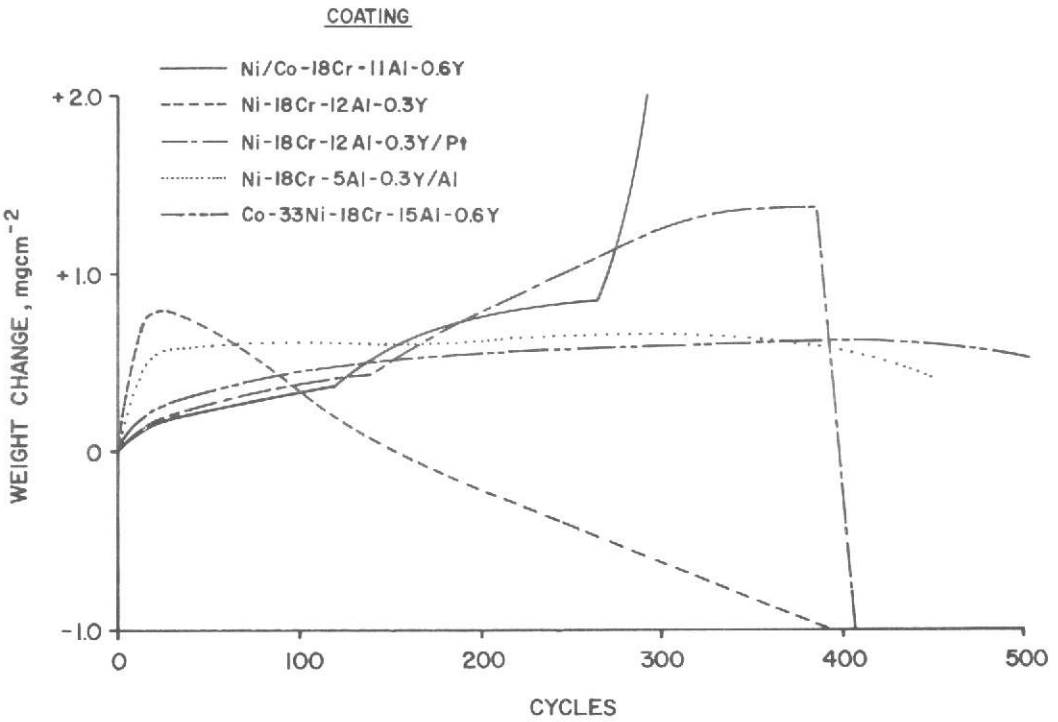

Set 2

Figure 12 1366°K (2000°F) Cyclic Oxidation Behavior of Eutectic Alloy Coupons Coated With eb Overlay Coatings. The Weight Change Data for the Second Set of Test Specimens is Not Fully Representative of Coating Performance Because of the Presence of Substrate Cracks.

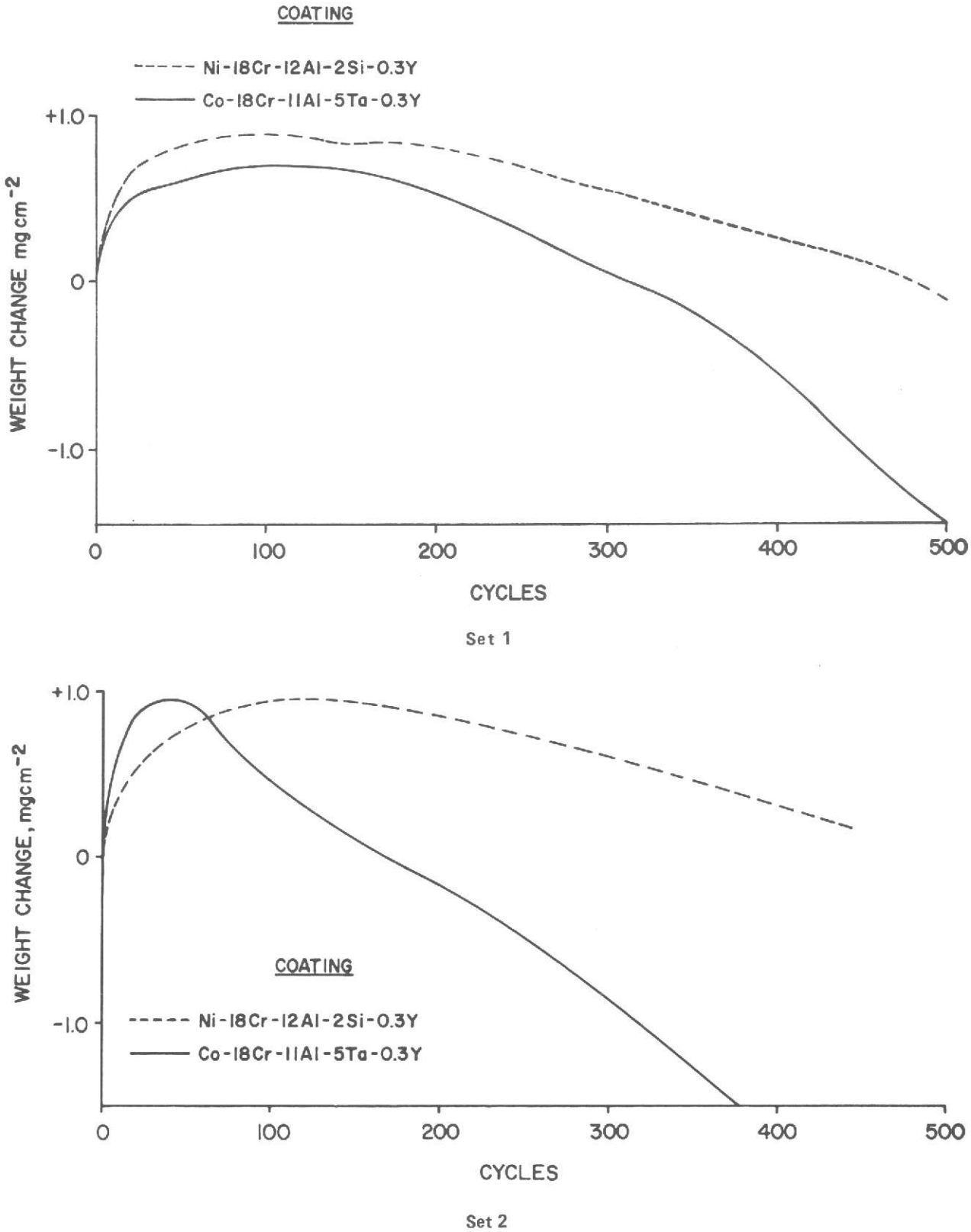

Figure 13 1366°K (2000°F) Cyclic Oxidation Behavior Of Plasma Spray Overlay Coated Eutectic Alloy Coupons.

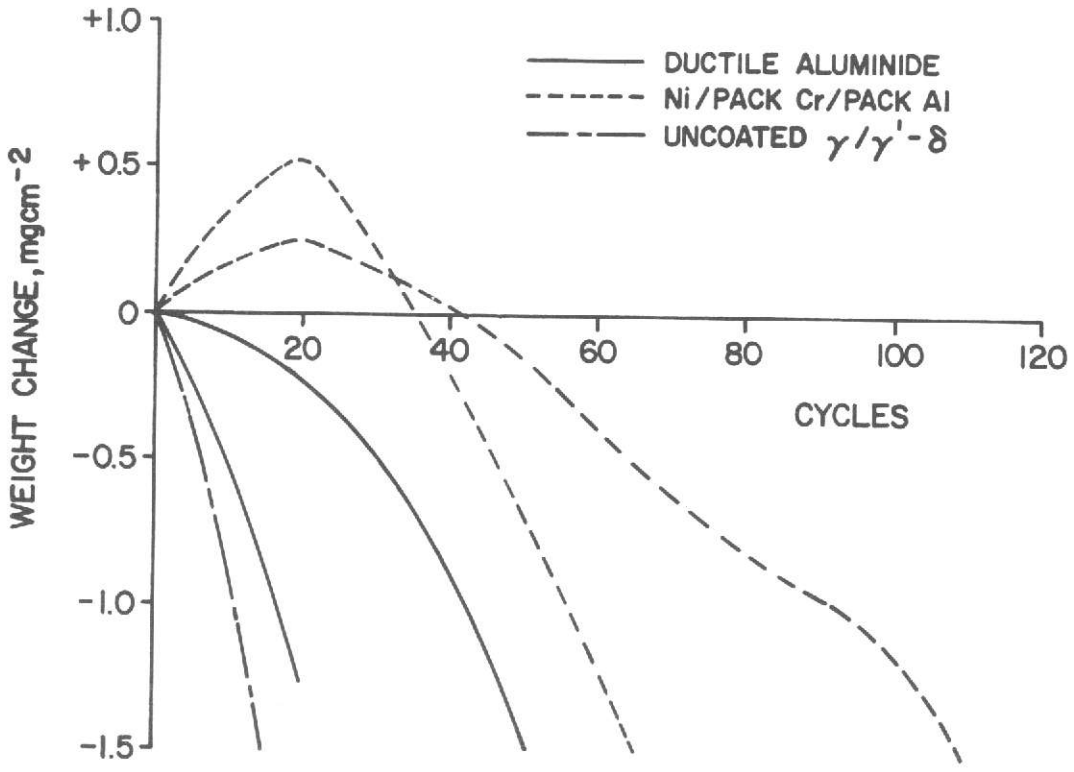

Figure 14 The 1366°K (2000°F) Cyclic Oxidation Behavior Of The $\gamma/\gamma'-\delta$ Eutectic Alloy, Uncoated And Coated With Two Diffusion Aluminide Coatings.

Metallographic examination of the vapor deposited overlay coatings was a primary means for evaluating behavior of those systems. In addition, these examinations indicated the effectiveness of interlayers (diffusion barriers) in conjunction with these coatings. This is illustrated in Figure 15 which shows the conditions of the Ni/CoCrAlY, W/NiCrAlY and NiCrAlY coatings after testing at 1366°K (2000°F). The Ni/CoCrAlY coating was severely depleted in aluminum after 500 cycles at 1366°K (2000°F) (Figure 15a); only a small amount of β-CoAl (the dark etching phase) remained and a significant amount of interdiffusion between the alloy and coating was evident. While coating failures were observed at local repair sites on the W/NiCrAlY, the major portion of the coating appeared to be of excellent quality after 120 cycles at 1366°K (2000°F) (Figure 15b). The outer portion of the coating consisted of γ-nickel (light etching phase) and β-NiAl (very dark etching phase) while the inner half of the coating consists of γ-nickel and γ'-Ni_3Al (grey etching phase). Additional comments concerning this system will be presented later. The NiCrAlY coating (Figure 15c) was only modestly degraded and was composed of a mixture of γ-nickel and γ'-Ni_3Al. The NiCrAlY coatings, with or without interlayers, are superior with regard to both oxidation resistance and diffusional stability compared to the Ni/CoCrAlY coating.

The NiCrAlY/Pt, CoNiCrAlY and NiCrAlY/Al coatings illustrated in Figure 16 also exhibited excellent thermal stability after 500 cycles at 1366°K (2000°F). The NiCrAlY/Pt coating (Figure 16a) consisted of γ-Ni (dark etching phase) and γ'-Ni_3Al (light etching phase). The CoNiCrAlY coating (Figure 16b) consists mainly of β-NiAl (dark etching phase) and γ-nickel solid solution in the outer portion of the coating. However, in some but not all areas γ'-Ni_3Al was also present. A mixture of γ-nickel and γ'-Ni_3Al was found in the inner portion of the coating. The NiCrAlY/Al coating (Figure 16c) consists of a continuous outer portion, which is predominately γ'-Ni_3Al (light etching phase) with remnants of β-NiAl (dark etching phase) present in some areas. The inner portion of the coating consists of a mixture of γ-Ni solid solution and γ'-Ni_3Al. A modest amount of interdiffusion between the coating and alloy is apparent.

Representative sections of the plasma sprayed CoCrAlTaY and NiCrAlSiY coatings are presented in Figure 17. Of these two coatings, the NiCrAlSiY coating has retained more aluminum as shown by the presence of γ'-Ni_3Al (dark grey etching phase) in the coating. However, there has been a considerable amount of diffusion between both coatings and the eutectic alloy substrate.

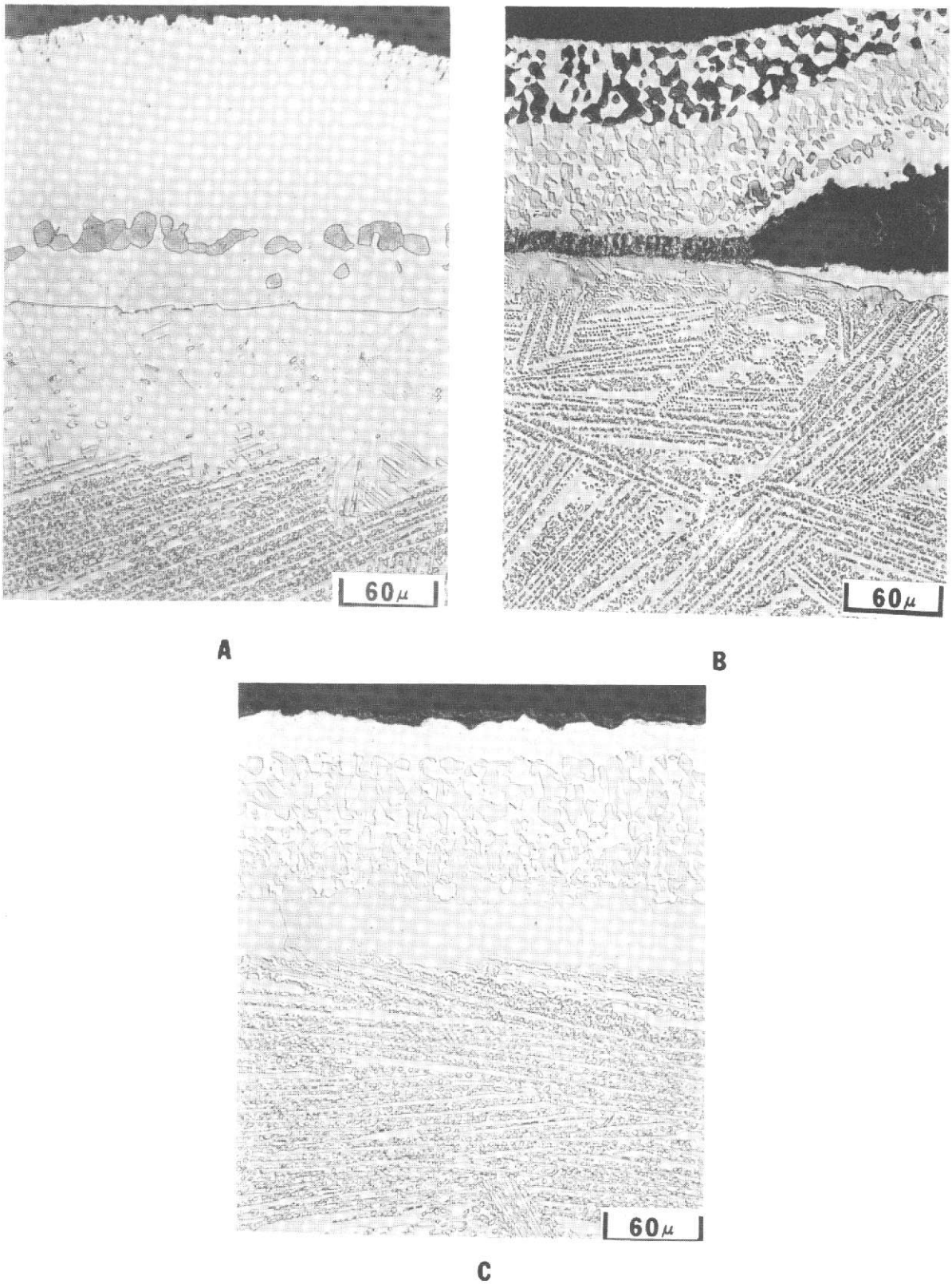

Figure 15 Representative Microstructures of (A) Ni/CoCrAlY After 500 Hours; (B) W/NiCrAlY After 120 Hours; and (C) NiCrAlY After 500 Hours of 1366°K (2000°F) Cyclic Oxidation

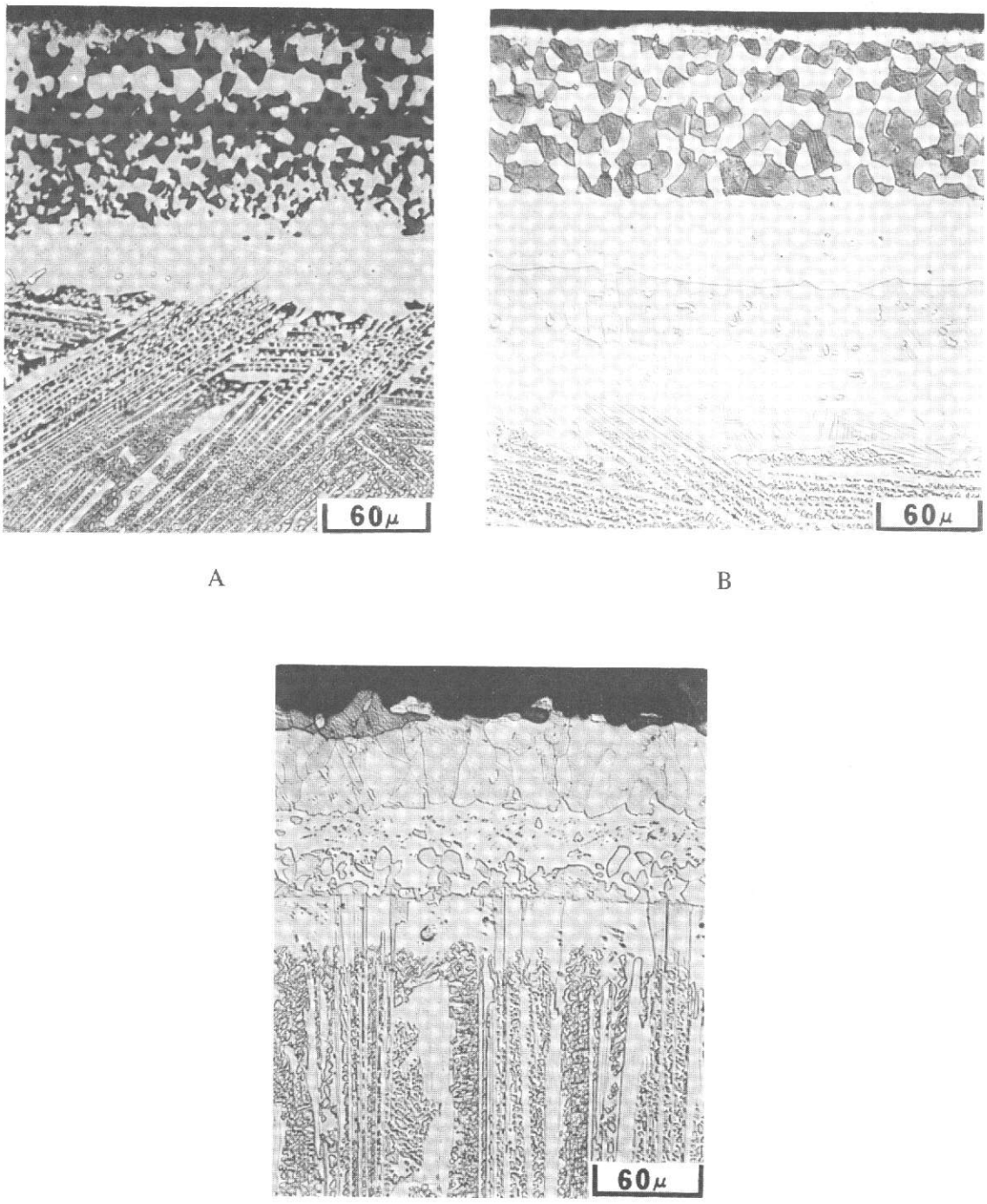

Figure 16 Representative Microstructures of (A) NiCrAlY/Pt,(B) CoNiCrAlY, and (C) NiCrAlY/Al Overlay Coatings on Eutectic Alloy Coupons Following 500 Hours of 1366°K (2000°F) Cyclic Oxidation.

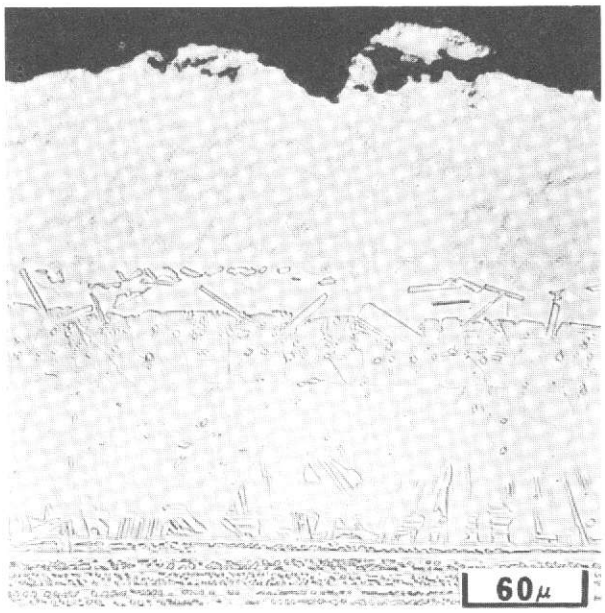

CoCrAlTaY

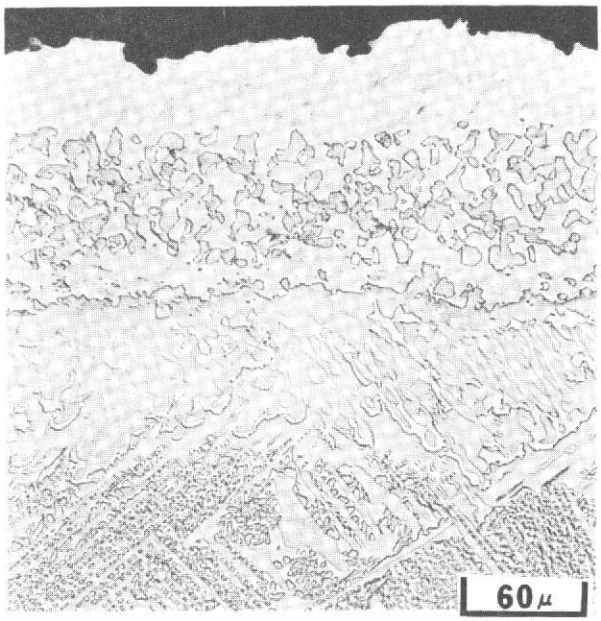

NiCrAlSiY

Figure 17 Representative Microstructures of Plasma Sprayed Coatings on Eutectic Alloy Coupons Following 500 Hours of 1366°K (2000°F) Cyclic Oxidation

The diffusion aluminide coatings were severely degraded after only relatively short exposures at 1366°K (2000°F). In fact, little or no ductile aluminide (Cr/Al) coating remained after only 100 cycles at 1366°K (2000°F). The Ni/Cr/Al coating was in somewhat better condition after 140 cycles, but certainly was not adequate at this temperature. This coating was the thicker of the two in the as-coated condition. Microstructures for these specimens and an uncoated eutectic alloy specimen which was exposed at 1366°K (2000°F) for 40 hours are shown in Figure 18.

1422°K (2100°F) and 1478°K (2200°F) Furnace Cyclic Oxidation (100 hours)

The weight change time relationships for the e.b. vapor deposited coatings oxidized for 100 one-hour cycles at 1478°K (2200°F) are presented in Figure 19. As indicated by the weight losses observed during the course of the test, oxide spallation was significant at this temperature for most of the coatings. A notable exception was the NiCrAlY/Pt coating on which the Al_2O_3 was generally adherent. The CoNiCrAlY and Ni/CoCrAlY coatings were removed from testing after 20 and 40 hours, respectively, because of visual evidence of incipient melting; subsequent metallographic examination confirmed that melting had occurred in the interdiffusion zone for both specimens.

The performances of the plasma sprayed coatings which were exposed in the 1478°K (2200°F) test are shown graphically in Figure 20. As in previous oxidation testing at 1366°K (2000°F), the performance of the NiCrAlSiY coating appeared to be better than that of the CoCrAlTaY coating. It is worth noting that the plasma sprayed CoCrAlTaY coating did not experience incipient melting, as did the Ni/CoCrAlY and CoNiCrAlY coatings, in this test. The 1478°K (2200°F) test results for the vapor deposited and plasma sprayed overlay coatings are summarized in Table VIII. The results obtained show that overlay coatings can be formulated upon which Al_2O_3 scales are still stable after 100 hours of furnace cyclic oxidation testing at 1478°K (2200°F).

The behavior of the coated specimens in the 1422°K (2100°F) cyclic oxidation test was generally consistent with the results obtained at 1478°K (2200°F). However, weight change data obtained exhibited more scatter between data points than that illustrated in Figure 19. The test results are summarized in Table IX.

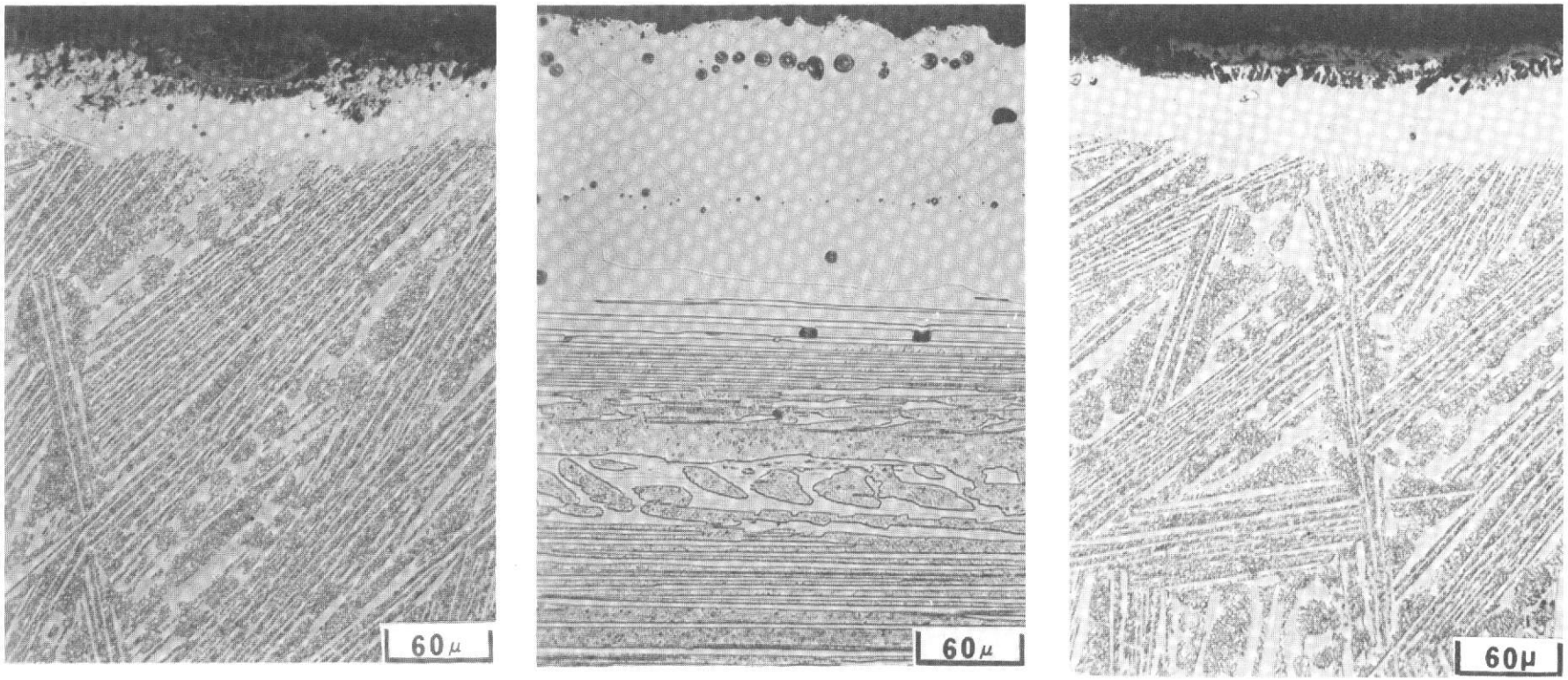

Cr/Al
100 HOURS

Ni/Cr/Al
140 HOURS

UNCOATED
40 HOURS

Figure 18 1366°K (2000°F) Cyclic Oxidation Behavior of Diffusion Aluminide Coated and Uncoated Eutectic Alloy Coupons After Exposure for the Times Indicated. The Ni/Cr/Al Coating was Initially Approximately Twice the Thickness of the Cr/Al Coating.

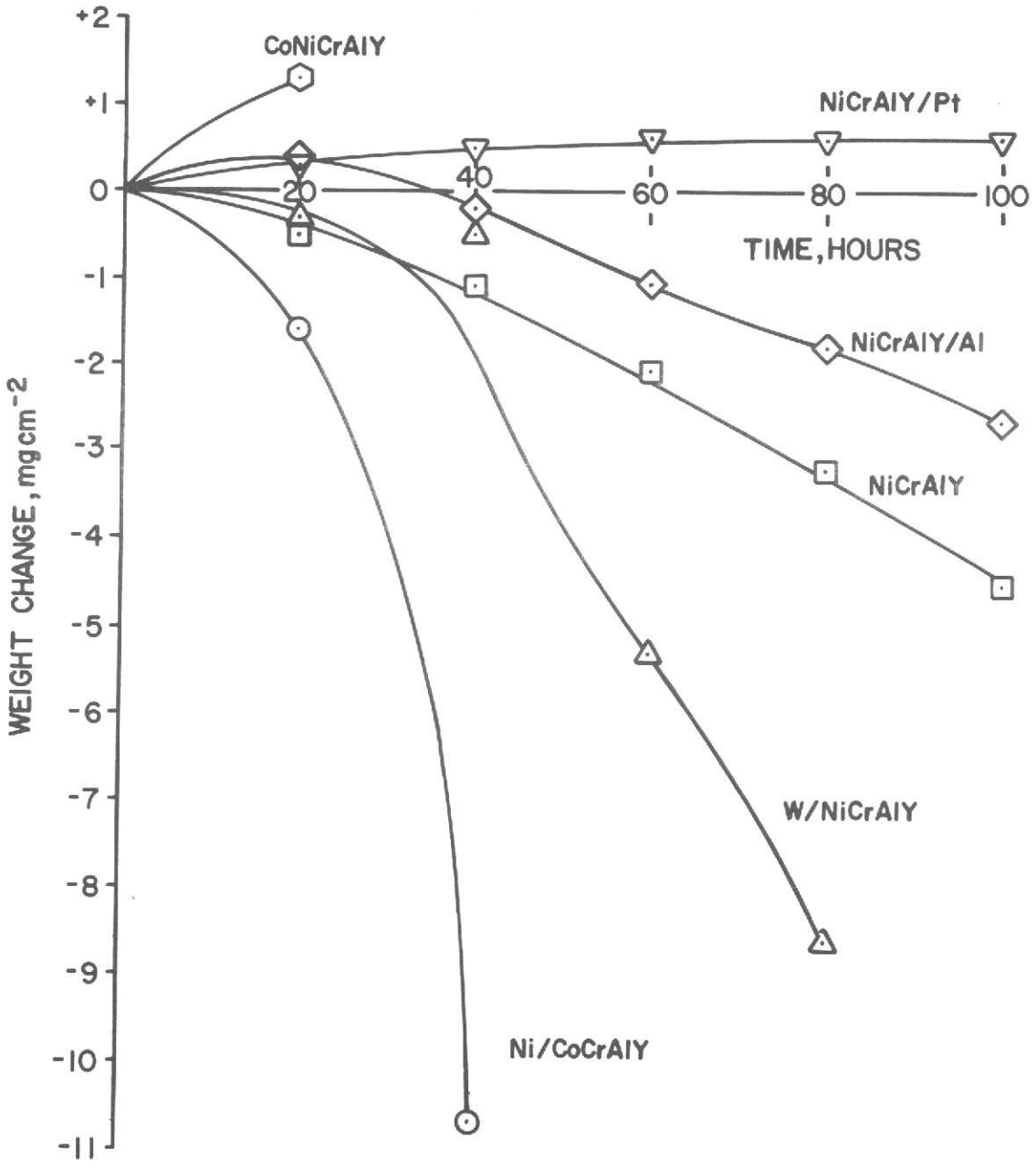

Figure 19 1478°K (2200°F) Cyclic Oxidation Behavior of Eutectic Alloy Coupons Coated With Vapor Deposited Overlay Coatings

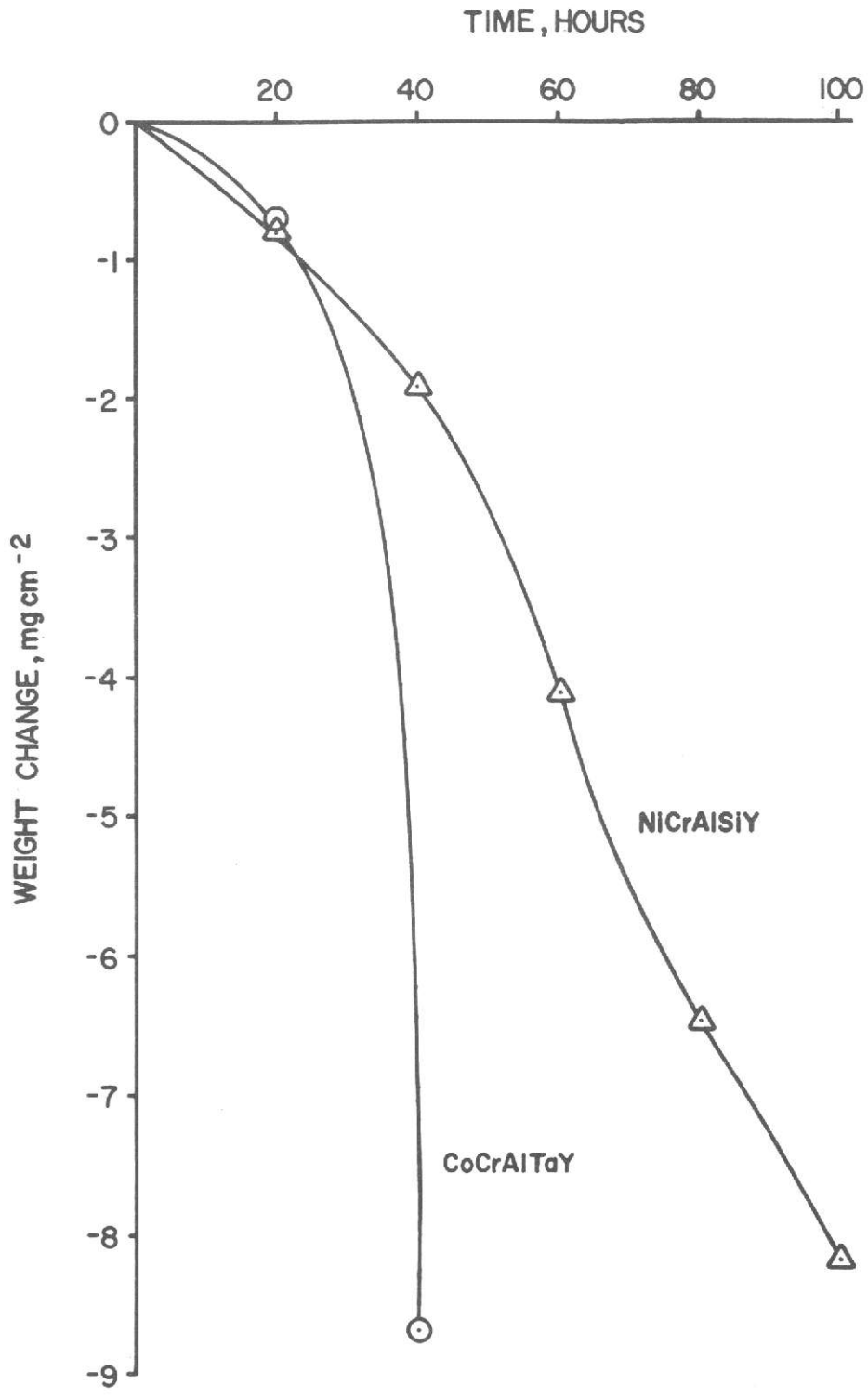

Figure 20 1478°K (2200°F) Cyclic Oxidation Behavior of Eutectic Alloy Coupons Coated With Plasma Sprayed Overlay Coatings

TABLE VIII

1478°K (2200°F) FURNACE CYCLIC OXIDATION BEHAVIOR OF COATED γ/γ'-δ EUTECTIC ALLOYS

Coating Designation	Cycles	Total Wt. Change ($mg\ cm^{-2}$)	Comments
Ni/CoCrAlY	40	-10.7	The oxide consisted of a mixture of Al_2O_3, spinel and CoO distributed non-uniformly. Considerable spalling and evidence of incipient melting was observed.
W/NiCrAlY	100	-11.6	The oxide formed was almost entirely Al_2O_3, which spalled to a considerable extent. A large amount of the weight loss was due to physical loss of the coating along the edges.
NiCrAlY	100	-4.5	The oxide formed was almost entirely Al_2O_3, which spalled to a considerable extent. Localized incipient melting was observed.
NiCrAlY/Pt	100	0.56	The oxide formed was predominantly Al_2O_3, which was largely adherent. Corners and edges were more severely attacked.
NiCrAlY/Al	100	-2.6	The oxide formed was predominantly Al_2O_3, which spalled to a considerable extent.
CoNiCrAlY	20	1.27	The oxide was mainly Al_2O_3 which spalled in localized areas. The test was terminated due to incipient melting of the coating.
CoCrAlTaY	40	-8.7	The oxide formed was a dark blue spinel, which spalled excessively.
NiCrAlSiY	100	-8.2	The oxide formed was a mixture of a green-grey spinel and Al_2O_3. Oxide spalling was more restrained than on the CoCrAlTaY coated specimen.

TABLE IX

1422°K (2100°F) FURNACE CYCLIC OXIDATION BEHAVIOR OF COATED $\gamma/\gamma'-\delta$ EUTECTIC ALLOYS

Coating Designation	Cycles	Total Wt. Change ($mg\ cm^{-2}$)	Comments
W/NiCrAlY*	100	---	Weight changes were not recorded since the coating became detached extensively. Some oxide spalling occurred on unaffected portions of coating.
NiCrAlY	100	-4.4	The oxide formed was a mixture of Al_2O_3 and spinel. Considerable spalling was observed.
NiCrAlY/Pt	40	3.1	The oxide formed appeared to be Ni-rich (NiO or a spinel) and was not typical. This result cannot be explained.
NiCrAlY/Pt*	100	-1.27	Selective spalling is the reason for the weight losses recorded. The oxide formed on the specimen was primarily Al_2O_3.
NiCrAlY/Al	100	-2.6	The Al_2O_3 formed on this specimen was generally non-adherent.
CoNiCrAlY	100	-3.5	The performance of this specimen was compromised by a massive crack, exposing the base metal. The Al_2O_3 formed on this specimen was generally non-adherent.
CoCrAlTaY	100	-10.3	The oxide formed was a mixture of Al_2O_3 and spinel which was generally non-adherent.
NiCrAlSiY	100	0.21	The oxide formed was a mixture of Al_2O_3 and spinel which spalled to a modest extent.

*These specimens had previously been exposed for 260 hours at 1600°F in the laboratory hot corrosion test.

The initial NiCrAlY/Pt specimen tested at 1422°K (2100°F) behaved in an unusual and unexplained manner. The oxide formed on this specimen appeared to be nickel-rich and was not typical of previous results obtained with the NiCrAlY/Pt specimens evaluated in other tests. This specimen was removed from test after 40 hours and one of the NiCrAlY/Pt specimens previously exposed for 260 hours in the 1144°K (1600°F) hot corrosion test was thoroughly washed to remove any Na_2SO_4 residue, placed in the 1422°K (2100°F) cyclic oxidation test and exposed for 100 hours. While selective spalling was observed with this specimen, the oxide formed was primarily Al_2O_3. A review of the records pertaining to the processing of the initial specimen tested indicated no abnormalities which could account for the anomalous behavior observed. In view of the excellent behavior of the NiCrAlY/Pt specimen evaluated at 1478°K (2200°F) and the behavior of the second specimen evaluated at 1422°K (2100°F), the results for the initial specimen evaluated at 1422°K (2100°F) must be considered non-representative.

The specimen coated with W/NiCrAlY and CoNiCrAlY had large portions of uncoated base metal exposed to the 1422°K (2100°F) oxidizing atmosphere. Due to specimen availability, the W/NiCrAlY specimen used in the 1422°K (2100°F) test had also been previously exposed for 260 hours in the 1144°K (1600°F) hot corrosion furnace test. It should be recalled that the W/NiCrAlY specimens experienced edge chipping during processing and were locally repaired with a slurry coating. Failure initiated early in the 1422°K (2100°F) test in these areas, resulting in some coating delamination and base metal exposure. A machining crack in the eutectic alloy substrate was the source of exposed base metal on the CoNiCrAlY coated specimen. Thus, the 1422°K (2100°F) weight change data for these systems is inconclusive. Microstructures of the W/NiCrAlY and CoNiCrAlY coated specimens in areas removed from the localized failures are shown in Figures 22a and 26a, respectively. In addition, metallographic examination revealed no evidence of incipient melting in the interdiffusion zone of the CoNiCrAlY coated specimen.

It should be noted that in the 1422°K (2100°F) test, as in the 1478°K (2200°F) test, the plasma sprayed NiCrAlSiY coating performed significantly better than the plasma sprayed CoCrAlTaY coating.

Photomicrographs of the specimens described in Tables VIII and IX are presented in Figures 21 through 28. The phases present in the 1422°K (2100°F) and 1478°K (2200°F) specimen photomicrographs are comparable despite the difference in contrast. While the same etching solutions were used, the 1422°K (2100°F) specimens were under-etched. The testing of a Ni/CoCrAlY coated specimen at 1422°K (2100°F) was deleted because of specimen availability.

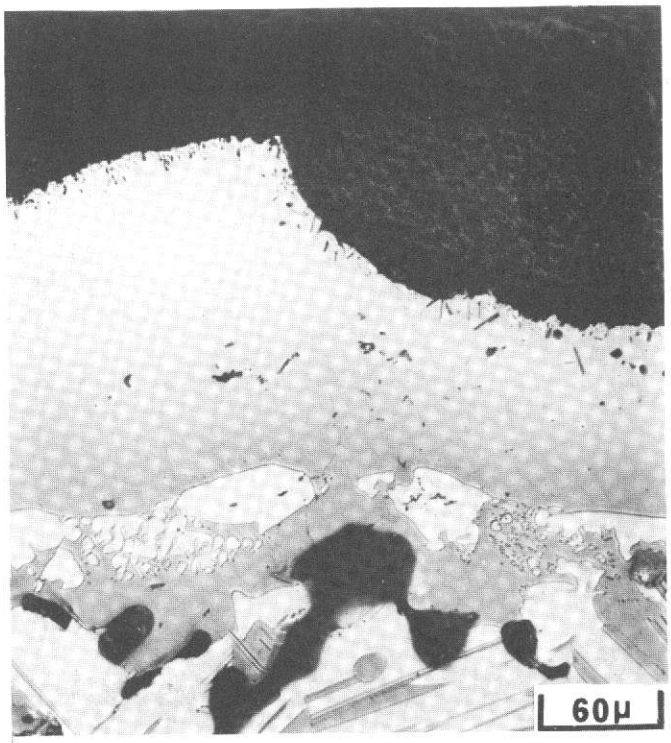

Figure 21 Representative Microstructure of Ni/CoCrAlY Coated $\gamma/\gamma' - \delta$ Eutectic Alloy After 40 Hours of Cyclic Oxidation at 1478°K (2200°F)

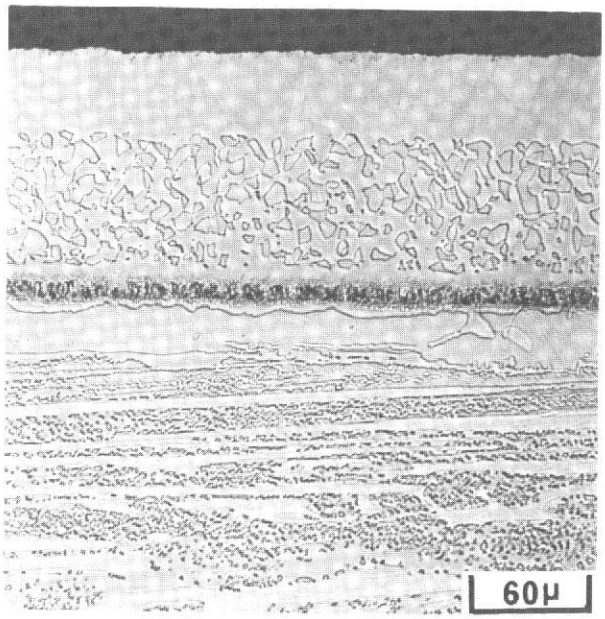

A

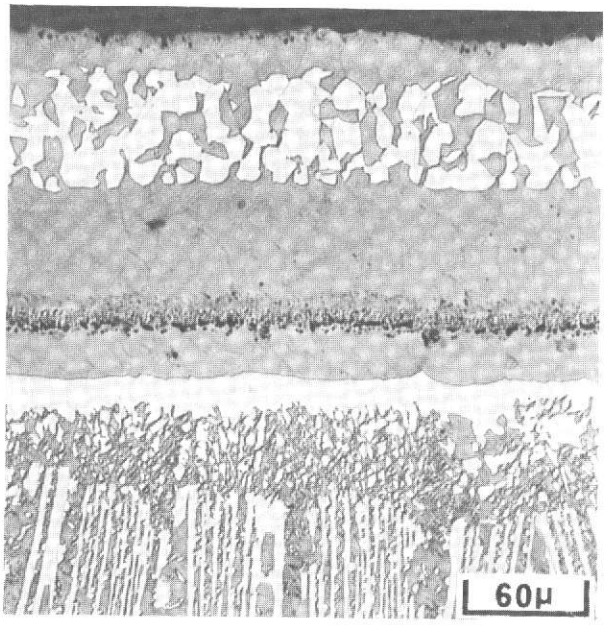

B

Figure 22 Representative Microstructures of W/NiCrAlY Coated $\gamma/\gamma' - \delta$ Eutectic Alloy After (A) 100 Hours Cyclic Oxidation at 1422°K (2100°F) and (b) 100 Hours Cyclic Oxidation at 1478°K (2200°F)

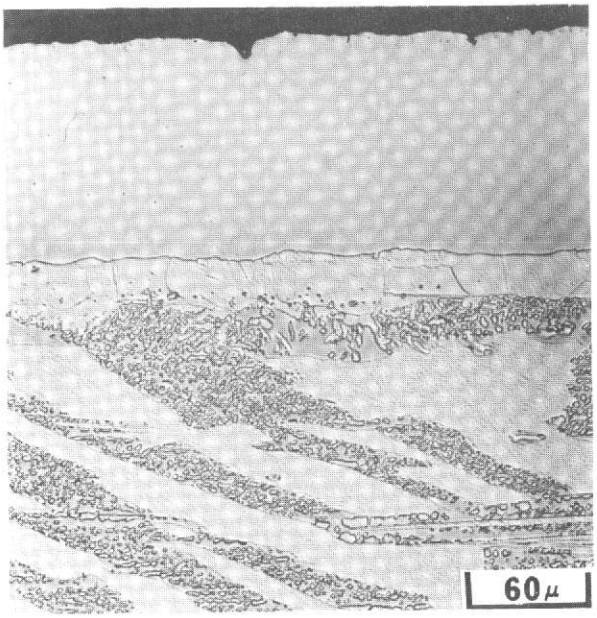

A

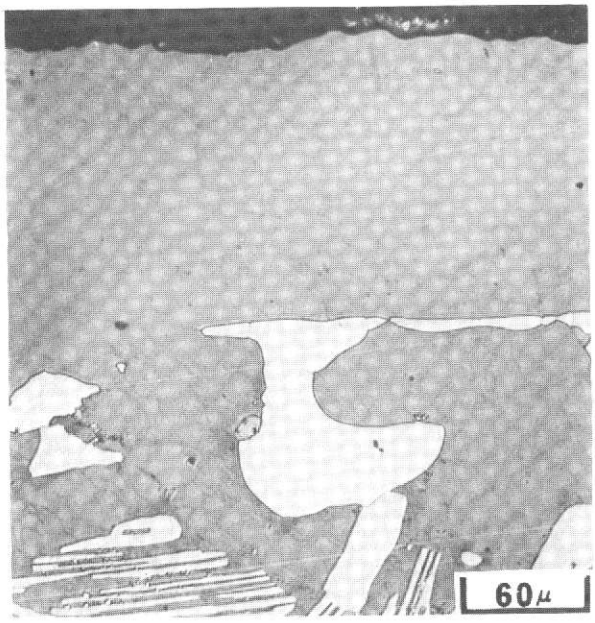

B

Figure 23 Representative Microstructures of NiCrAlY Coated $\gamma/\gamma' - \delta$ Eutectic Alloy After (A) 100 Hours Cyclic Oxidation at 1422°K (2100°F) and (B) 100 Hours Cyclic Oxidation at 1478°K (2200°F)

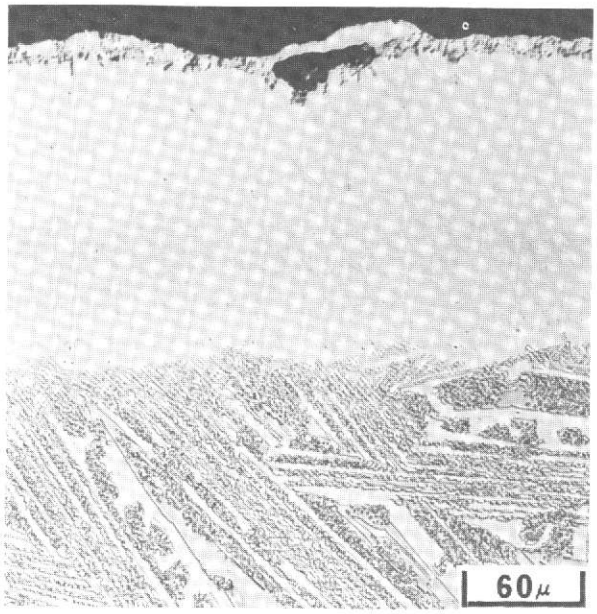

A

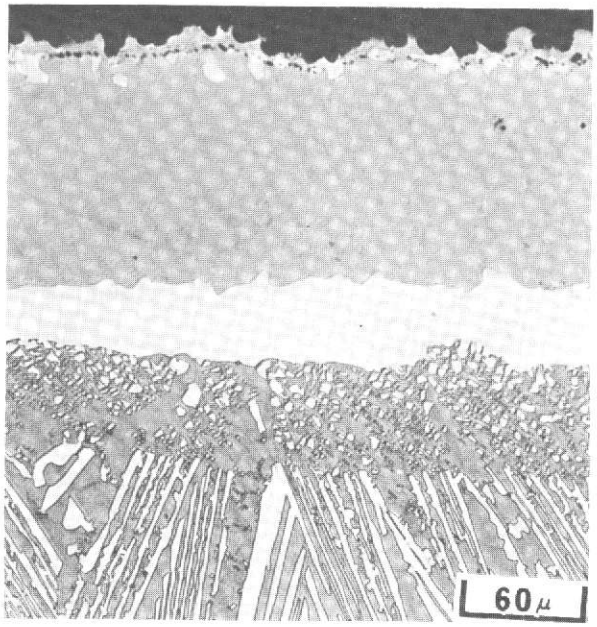

B

Figure 24 Representative Microstructures of NiCrAlY/Pt coated $\gamma/\gamma' - \delta$ Eutectic Alloy After (A) 100 Hours Cyclic Oxidation at 1422°K (2100°F) and (B) 100 Hours Cyclic Oxidation at 1478°K (2200°F)

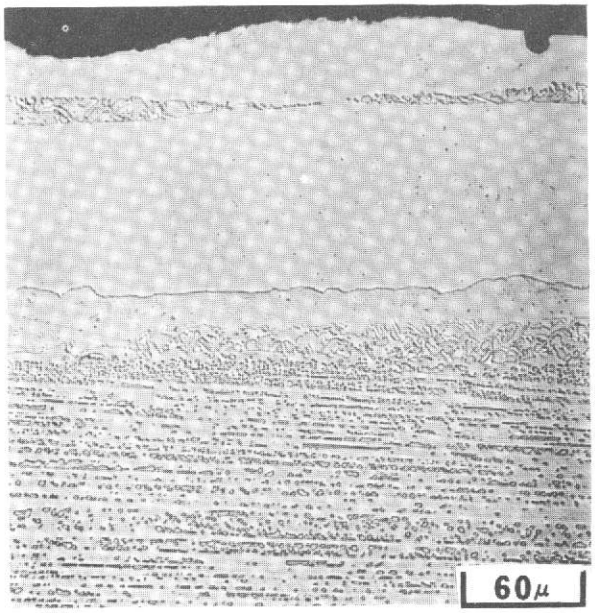

A

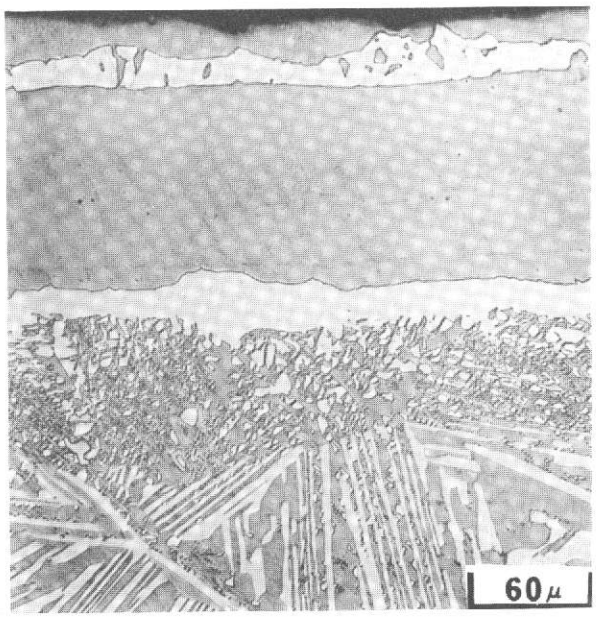

B

Figure 25 Representative Microstructures of NiCrAlY/Al Coated $\gamma/\gamma' - \delta$ Eutectic Alloy After (A) 100 Hours of Cyclic Oxidation at 1422°K (2100°F) and (B) 100 Hours Cyclic Oxidation at 1478°K (2200°F)

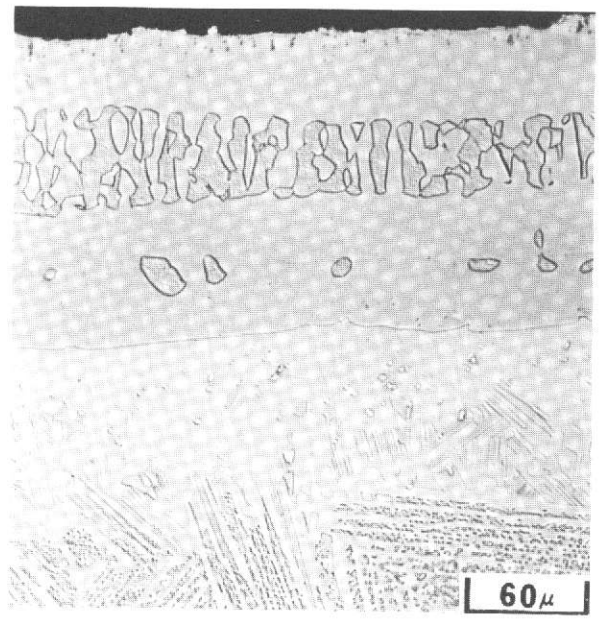

A

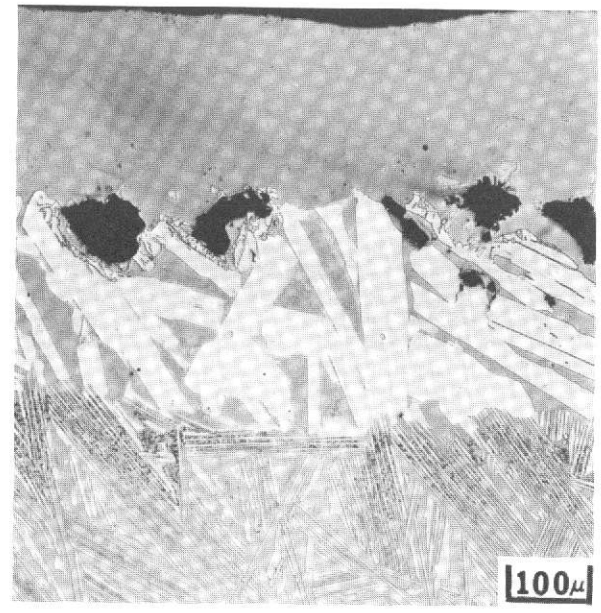

B

Figure 26 Representative Microstructures of CoNiCrAlY Coated $\gamma/\gamma' - \delta$ Eutectic Alloy After (A) 100 Hours of Cyclic Oxidation at 1422°K (2100°F) and (B) 20 Hours Cyclic Oxidation at 1478°K (2200°F)

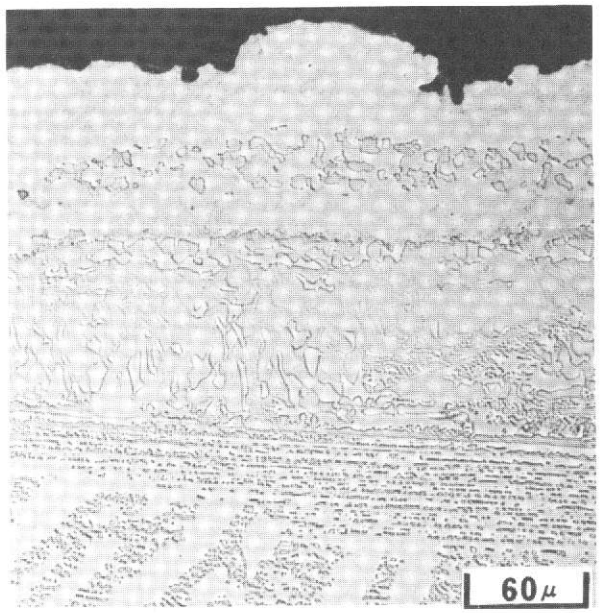

A

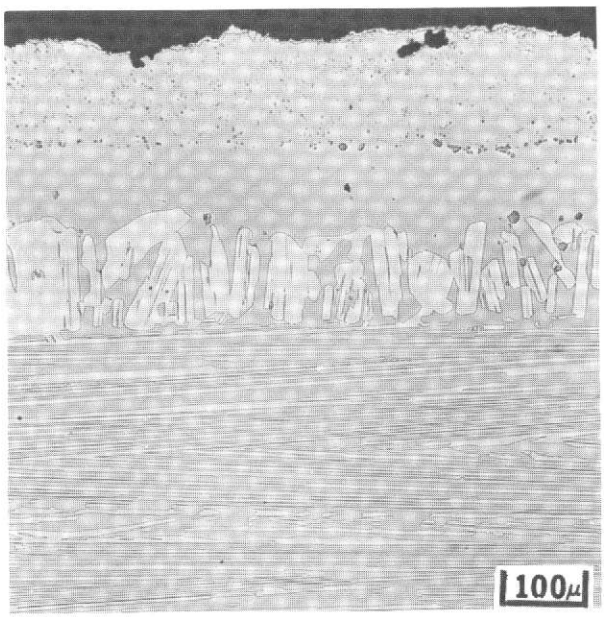

B

Figure 27 Representative Microstructures of CoCrAlTaY Coated $\gamma/\gamma' - \delta$ Eutectic Alloy After (A) 100 Hours Cyclic Oxidation at 1422°K (2100°F) and (B) 40 Hours Cyclic Oxidation at 1478°K (2200°F)

E. MICROPROBE ANALYSIS

At the conclusion of the furnace oxidation tests, the following three coatings were selected for microprobe analysis:

1. NiCrAlY
2. W/NiCrAlY
3. NiCrAlY/Pt

Two D.S. eutectic alloy coupons which were electron beam vapor deposited with about 127μ (5 mils) of a Ni-18Cr-12Al-0.3Y coating and which had been oxidized for 100 one-hour cycles at 1478°K (2200°F) were examined by electron microprobe spectroscopy. Prior to the application of the NiCrAlY, one of the specimens had been sputter coated with about 12.7μ (0.5 mils) of tungsten while the other had not. The purpose of the investigation was to examine the relative stabilities of the two coatings after an extended time at an elevated temperature and to evaluate the effectiveness of the tungsten layer as a diffusion barrier.

Electron backscatter photomicrographs of the two coatings after oxidation at 1478°K (2200°F) are presented in Figure 29. It appears that the NiCrAlY coating without a tungsten barrier consists of a single phase, presumably γ-nickel solid solution. There are two phases in the outer portion of the coating which had the tungsten barrier, i.e. γ -nickel solid solution and γ'-Ni_3Al. The very bright layer separating the alloy from the coating proper is the tungsten diffusion barrier, which remained intact despite the severe exposure conditions.

Relative intensities of the characteristic x-radiations for Ni, Al, Cr and Cb were obtained for both specimens and are presented in Figures 30 and 31. The intensities show the changes in elemental composition from the alloy through the coating but not their absolute concentrations.

As seen in Figure 30, the intensity gradients of the NiCrAlY coated specimen can be divided into two regions, (1) the coating, including a diffusion zone and (2) the base metal. The large particles within the diffusion zone (see Figure 29) are rich in columbium. Within the coating the Ni, Al and Cb contents increase linearly and the Cr content decreases linearly proceeding from the exterior edge of the coating to the base metal. The thickness of the coating plus the diffusion affected substrate zone after 100 hours at 1478°K (2200°F) was about 305μ (12 mils) (initial coating thickness approximately 127μ (5 mils)).

The microstructure of the W/NiCrAlY coated specimen was somewhat more complex and has been divided into five regions, namely:

- the external oxide layer (1) which is rich in aluminum;
- the bulk of the coating (2) which can be seen to consist of two

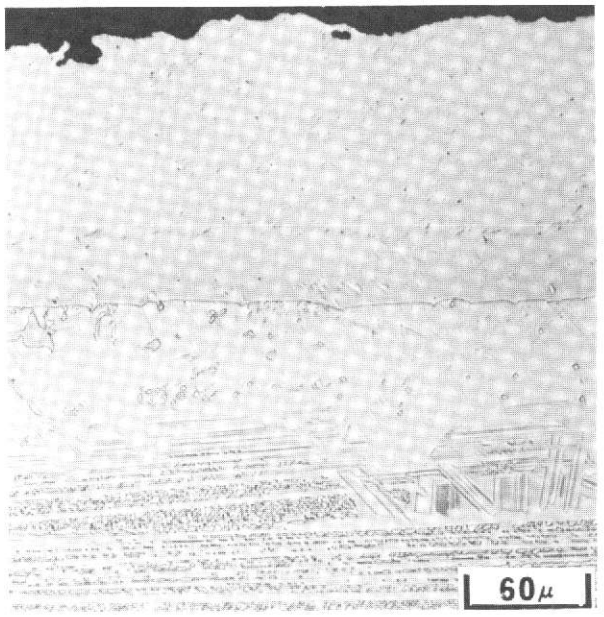

A

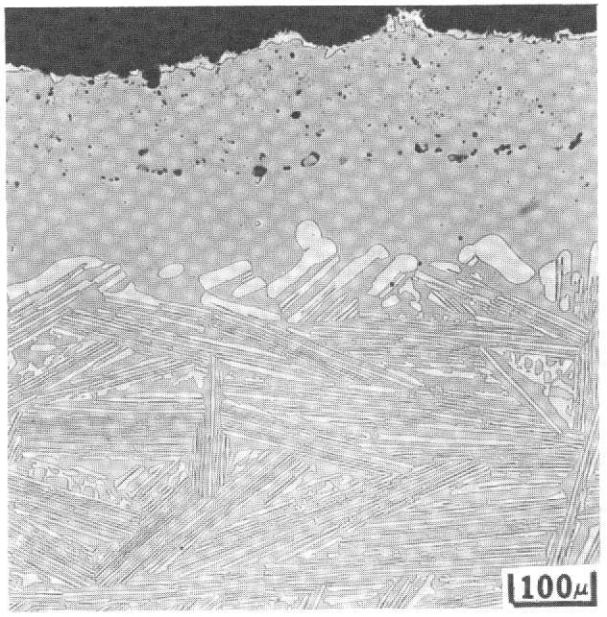

B

Figure 28 Representative Microstructures of NiCrAlSiY Coated $\gamma/\gamma'-\delta$ Eutectic Alloy After (A) 100 Hours Cyclic Oxidation at 1422°K (2100°F) and (B) 100 Hours Cyclic Oxidation at 1478°K (2200°F).

phases; the γ -nickel solid solution is rich in chromium while the γ'-Ni_3Al phase contains only a relatively small amount of chromium;

- the concentrations of Ni, Al, Cr and Cb are virtually nil at the site of the tungsten diffusion barrier (3);
- a small diffusion zone (4) exists below the tungsten diffusion barrier which is very similar in composition to the inner portion of region (2);
- the base metal (5).

The coating plus diffusion zone thickness after 100 one-hour cycles at 1478°K (2200°F) was 203μ (8 mils), while that of the NiCrAlY specimen without the tungsten layer was 305μ (12 mils).

Three D.S. eutectic alloy coupons, which were electron beam vapor deposited with about 127μ (5 mils) of Ni-18Cr-12Al-0.3Y and then sputter coated with about 6.3μ (0.25 mils) of platinum, were examined by electron microprobe spectroscopy. Specimens evaluated included the as-coated coupon as well as coupons which had been oxidized for 500 one-hour cycles at 1366°K (2000°F) and 100 one-hour cycles at 1478°K (2200°F). Electron backscatter photomicrographs and characteristic x-ray images were obtained from each specimen. The pertinent photomicrographs are presented in Figures 32 to 34. In addition, elemental traces to determine the relative amounts of all the elements of the coating or alloy were obtained and this information will be referred to in the discussion below.

The electron microprobe photomicrographs obtained for the as-coated specimen are shown in Figure 32. The original γ/γ'- δ /NiCrAlY and NiCrAlY/Pt interfaces are apparent in Figure 32a. The NiCrAlY/Pt interface is decorated by a line of discrete Al_2O_3 particles which was possibly produced by residual oxygen in the sputtering apparatus. It can be seen from the Pt x-ray photograph that a significant amount of Pt diffusion occurred during the sputtering operation. This was verified by the Pt concentration profile. Surprisingly, the concentration profile for Cb indicated that substantial amounts of this element were present in the coating, particularly just below the line of Al_2O_3 particles.

The electron microprobe photomicrographs obtained for the specimen oxidized for 500 one-hour cycles at 1366°K (2000°F) are shown in Figure 33. The platinum present is uniformly distributed throughout the coating (Figure 33b). The external oxide is rich in Al as well as the inner portion of the coating (Figure 33c). The distribution of Cr is shown in Figure 33d. The particles just below the external surface in Figure 33a were determined to be yttrium-rich and are presumably Y_2O_3.

The electron microprobe photomicrographs obtained for the specimen oxidized for 100 one-hour cycles at 1478°K (2200°F) are shown in Figure 34. Similar trends were observed in this specimen as were noted for the 1366°K (2000°F) specimen. In this specimen, however, the particles just below the external surface were found to be Al-rich and are presumably Al_2O_3.

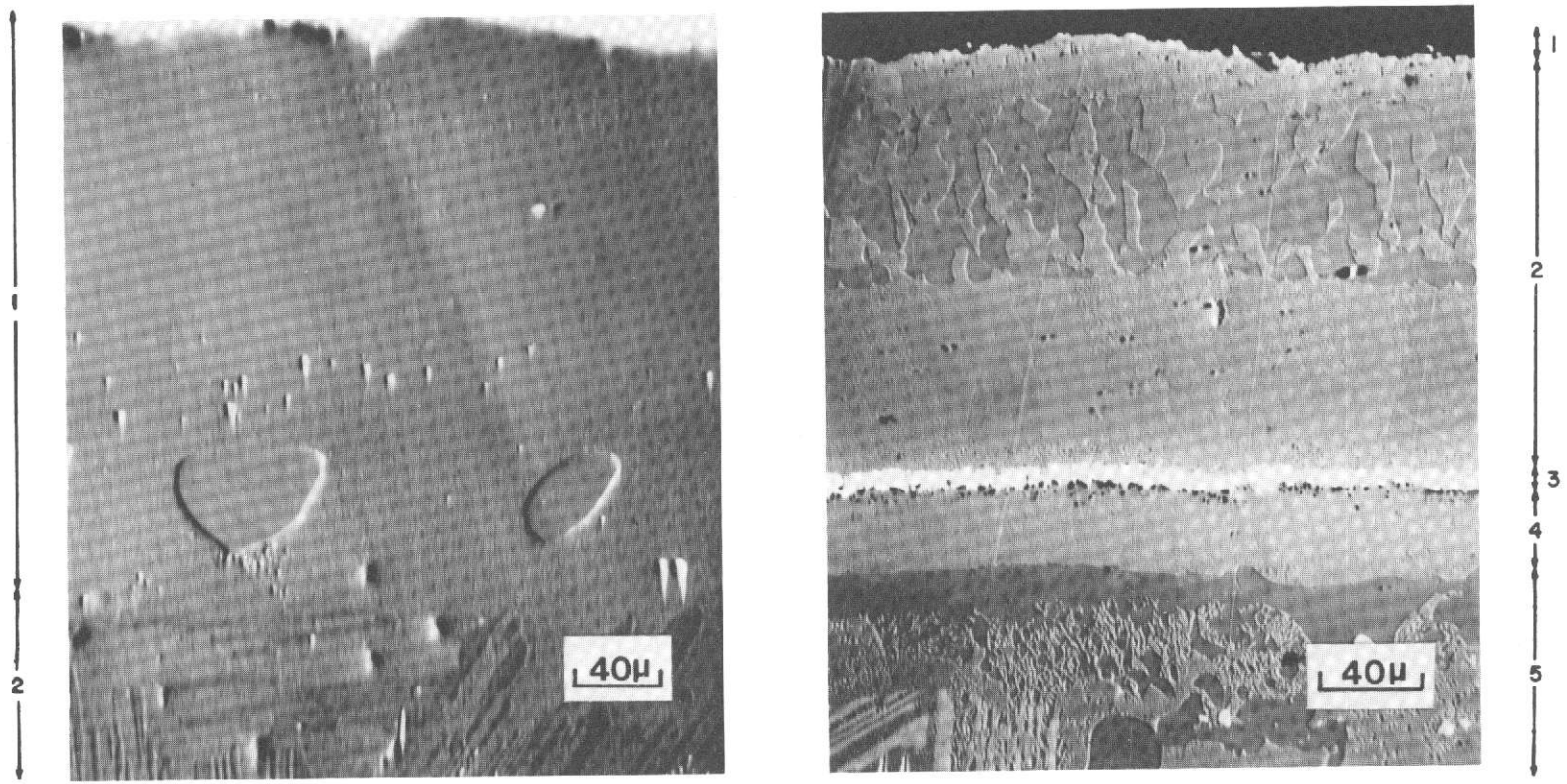

Figure 29 Electron Backscatter Microphotographs of D.S. $\gamma/\gamma' - \delta$ Alloy Electron Beam Vapor Deposited with 127μ (0.005 inches) Ni-17Cr-12Al-0.3Y (Left) and 12.7μ (0.0005 inches) W Plus 127μ (0.005 Inches) Ni-17Cr-12Al-0.3Y (Right) After 100 One Hour Cycles at 1478°K (2200°F) in Air.

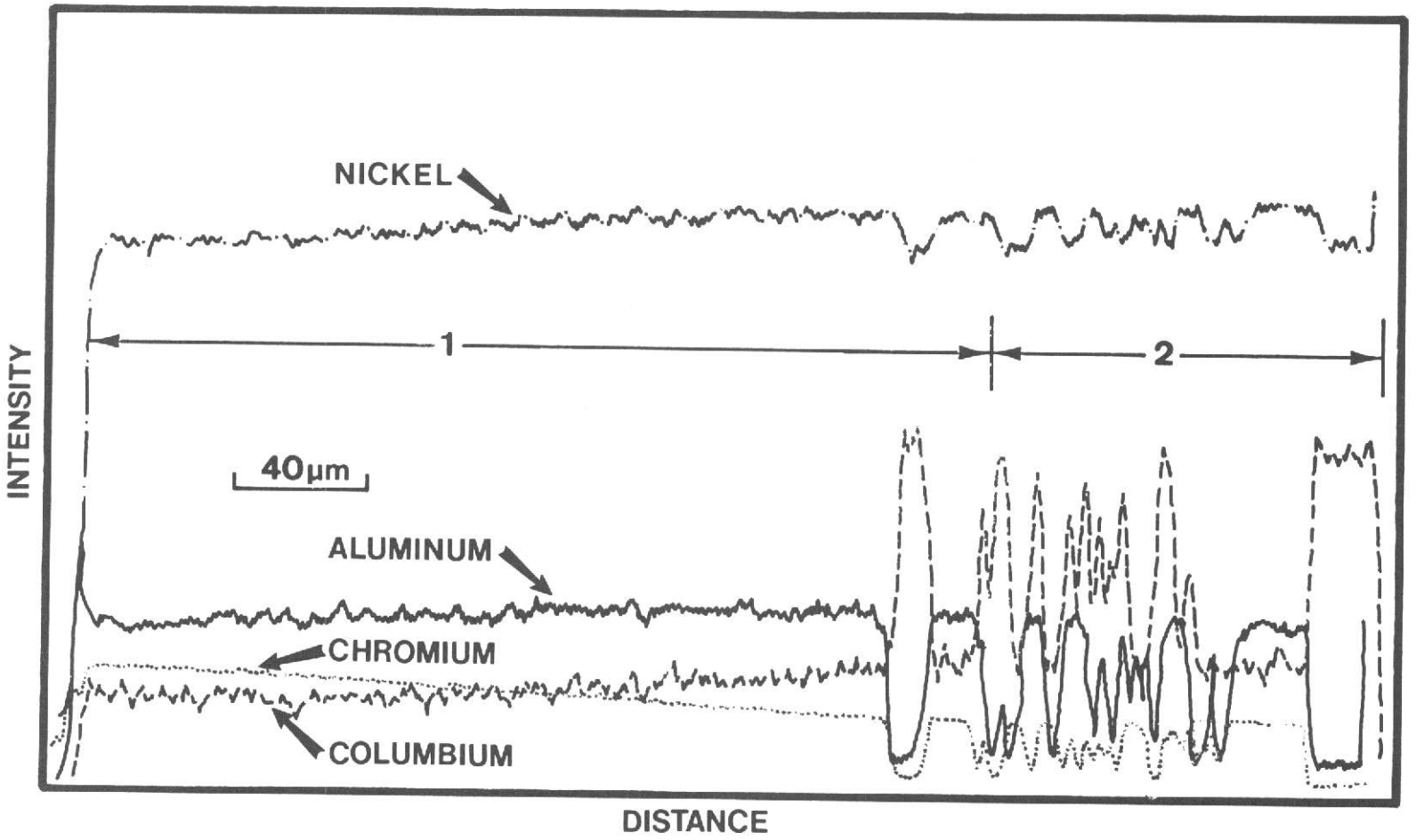

Figure 30 Relative Ni, Al, Cr and Cb X-Radiation Intensities for D.S. $\gamma/\gamma'-\delta$ Alloy Electron Beam Vapor Deposited With 127μ (0.005 Inches) Ni-17Cr-12Al-0.3Y After 100 One Hour Cycles at 1478°K (2200°F) in Air.

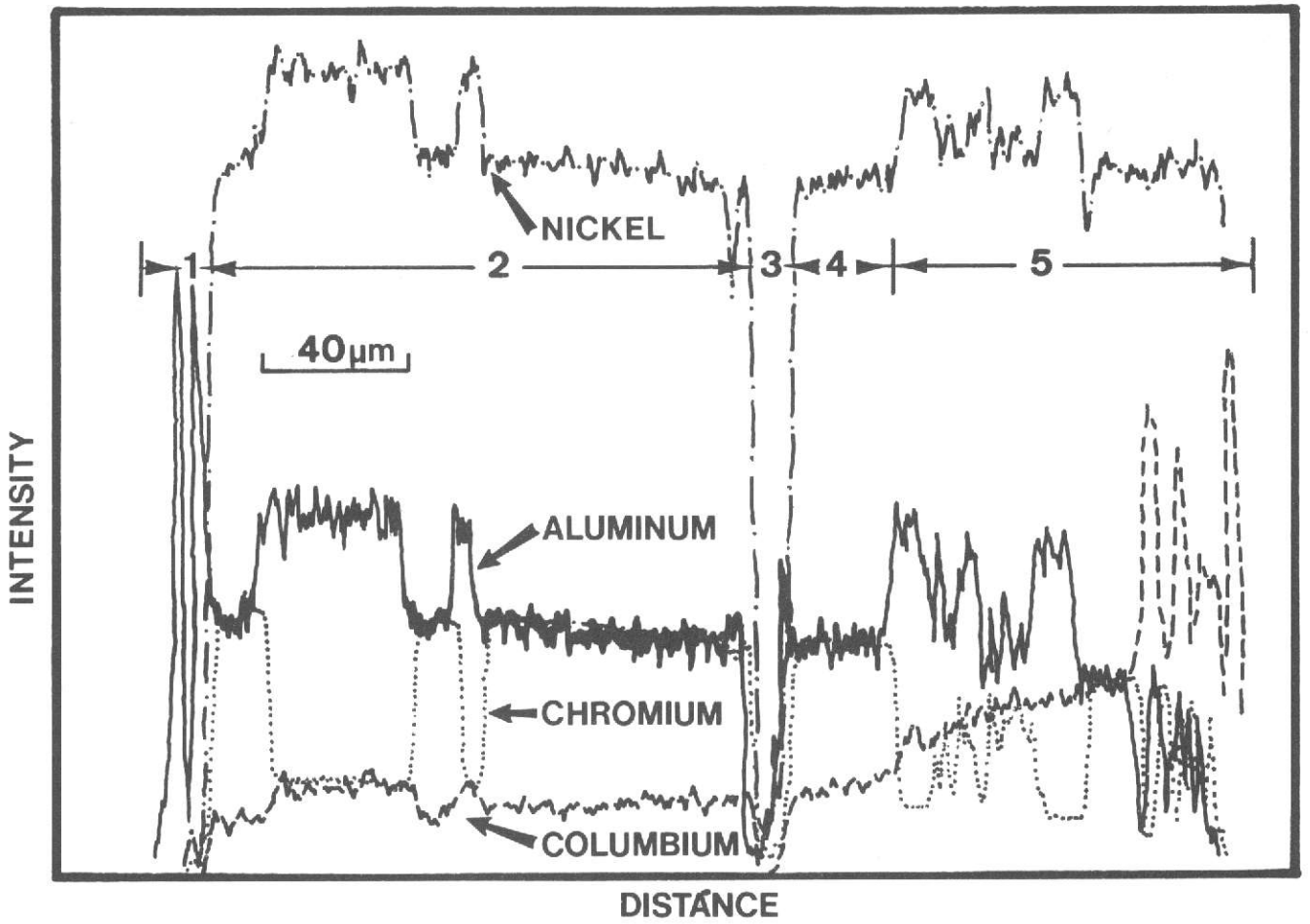

Figure 31 Relative Ni, Al, Cr and Cb X-Radiation Intensities for D.S. $\gamma/\gamma'-\delta$ Alloy Sputter Coated With 12.7μ (0.0005 Inches) W and Electron Beam Vapor Deposited with 127μ (0.005 Inches) Ni-17Cr-12Al-0.3Y After 100 One Hour Cycles at 1478°K (2200°F) in Air.

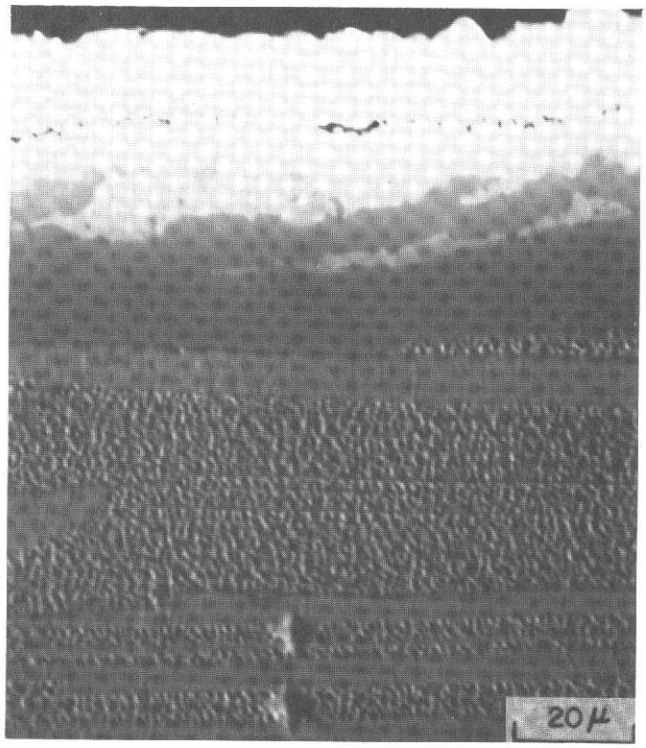

A. Electron Backscatter

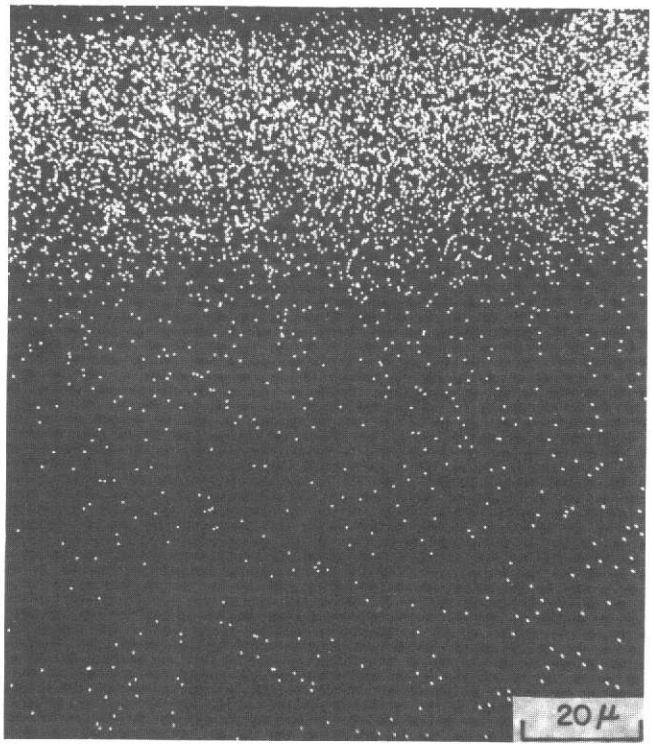

B. Pt X-ray

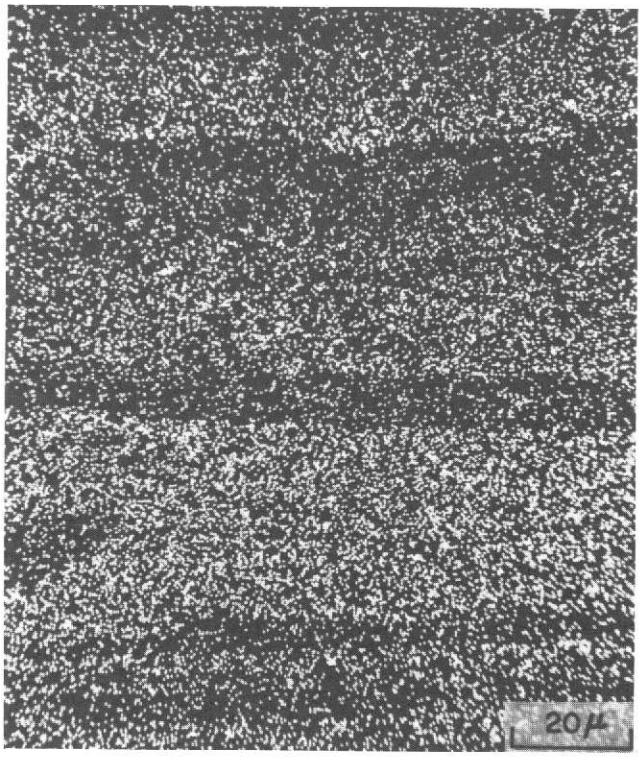

C. Al X-ray

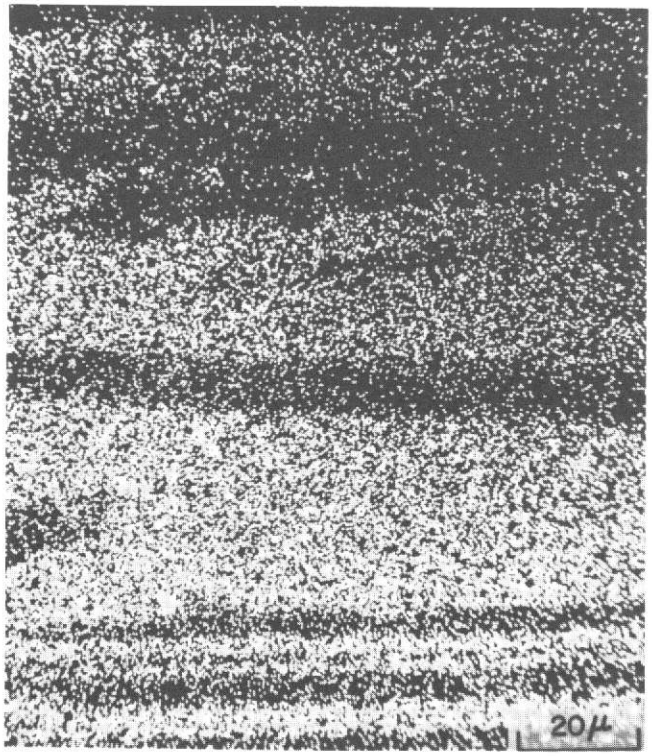

D. Cr X-ray

Figure 32 Electron Microprobe Photomicrographs of a D.S. Eutectic Alloy-NiCrAlY/Pt Coated Specimen in the As-Coated Condition.

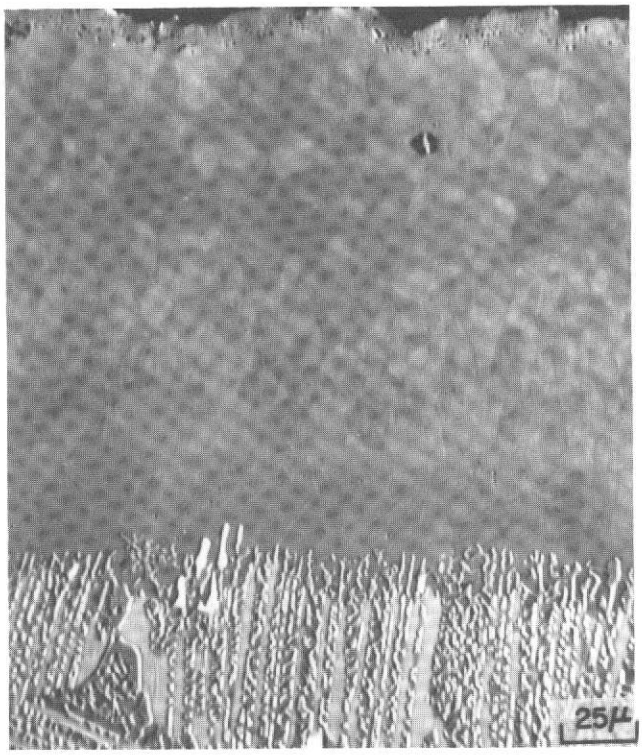

A. Electron Backscatter

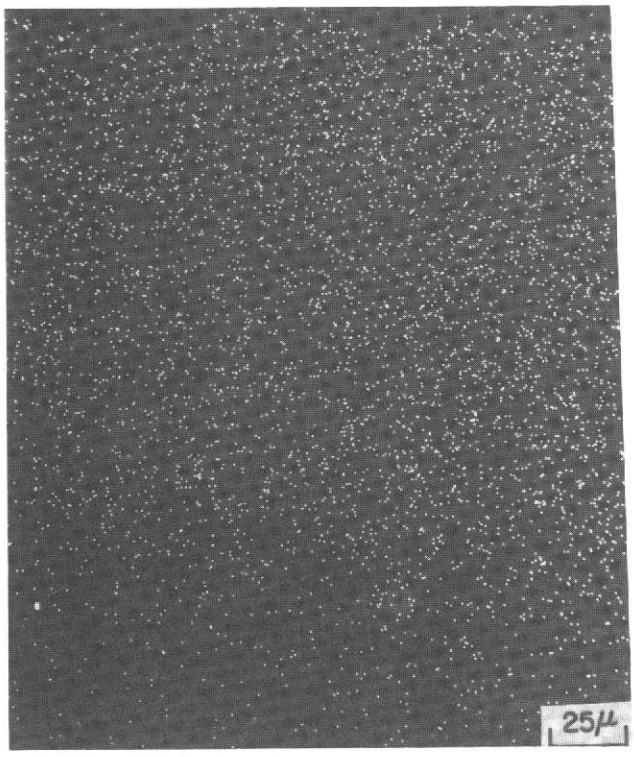

B. Pt X-ray

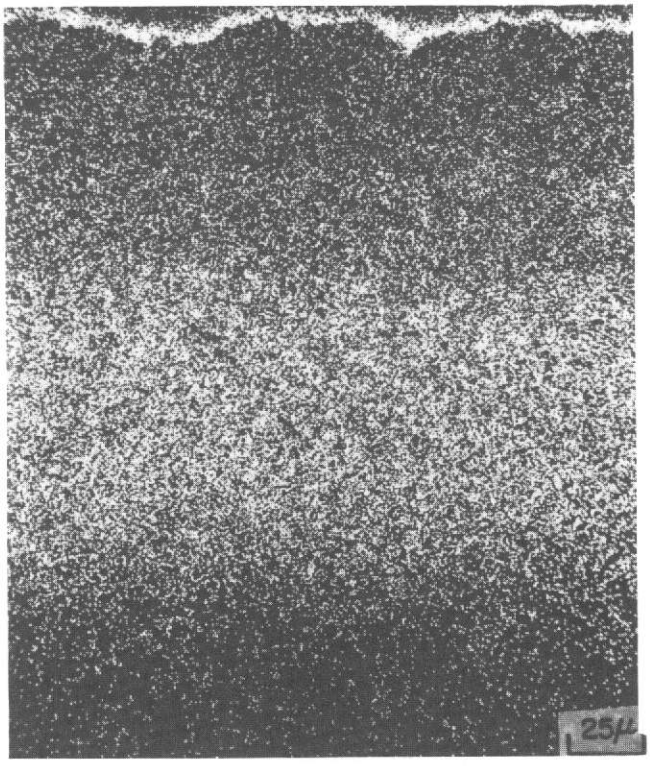

C. Al X-ray

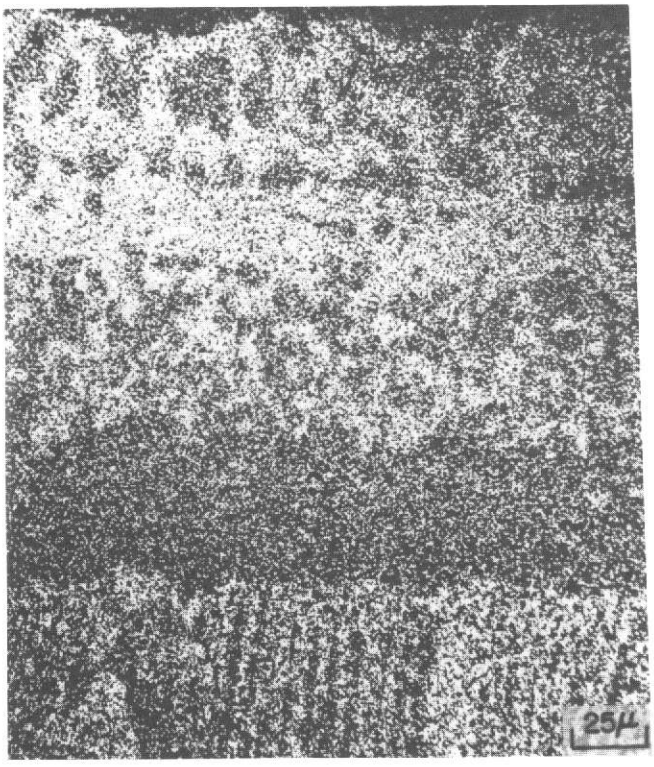

D. Cr X-ray

Figure 33 Electron Microprobe Photomicrographs of a D. S. Eutectic Alloy – NiCrAlY/Pt Coated Specimen After 500 – 1 Hour Cycles at 1366°K (2000°F).

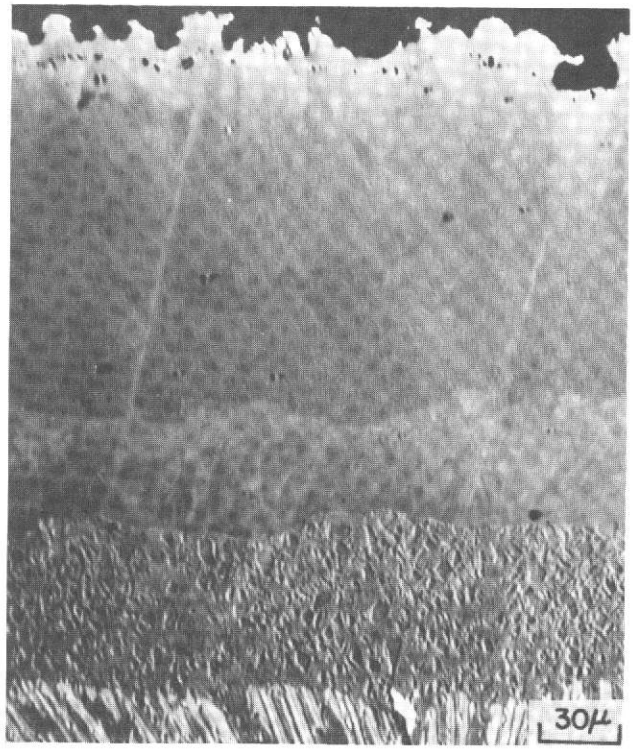

A. Electron Backscatter

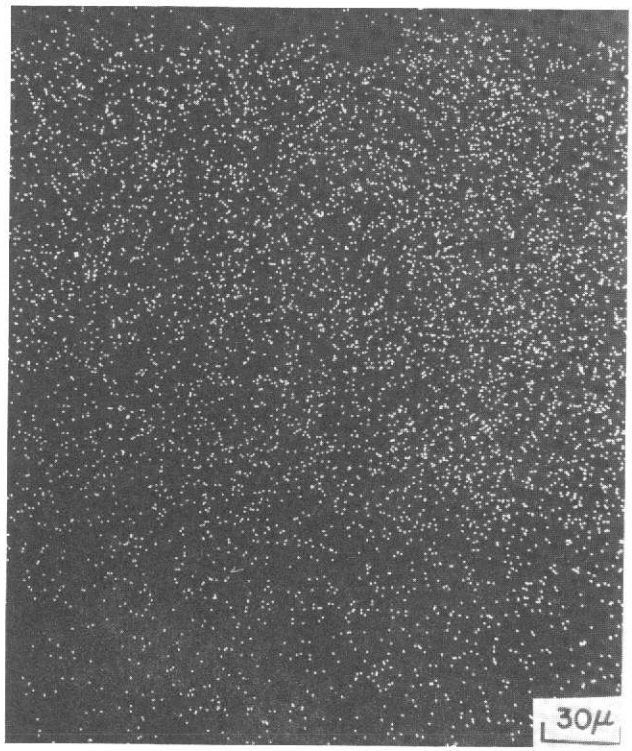

B. Pt X-ray

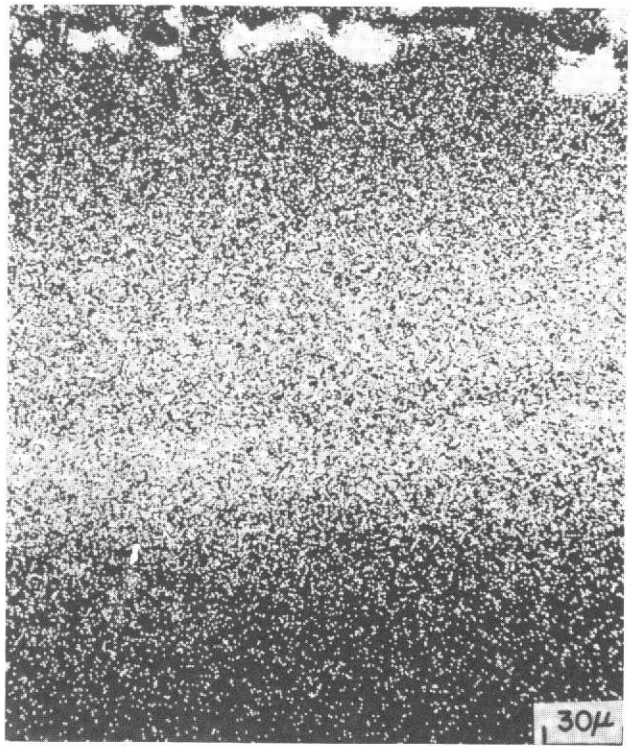

C. Al X-ray

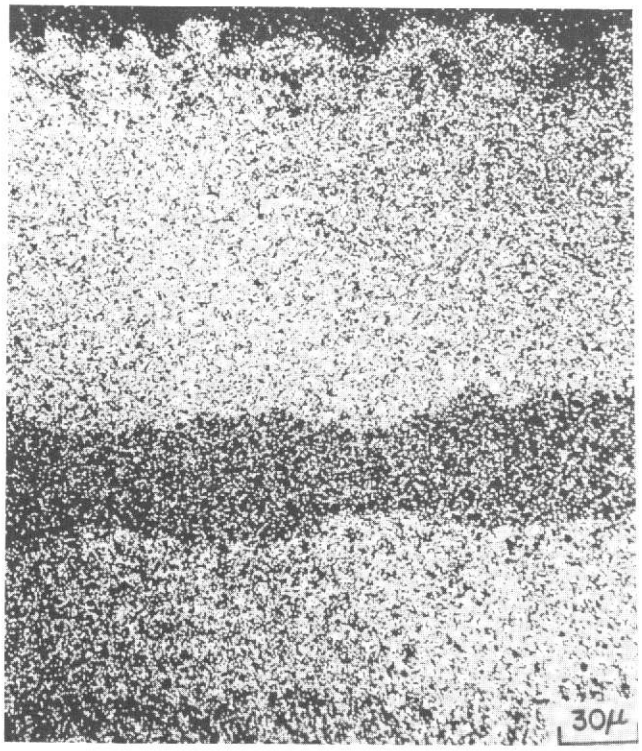

D. Cr X-ray

Figure 34 Electron Microprobe Photomicrographs of a D.S. Eutectic Alloy – NiCrAlY/Pt Coated Specimen After 100 – 1 Hour Cycles at 1478°K (2200°F).

F. DISCUSSION OF FURNACE TEST RESULTS

From the results of the laboratory oxidation and hot corrosion evaluation of these overlay and diffusion aluminide coatings on the directionally solidified $\gamma/\gamma'-\delta$ eutectic alloy, the following conclusions were derived:

- In all tests in which they were compared, overlay coatings were superior to diffusion aluminide coatings.
- Diffusion aluminide coatings should provide adequate protection at 1144°K (1600°F) in the absence of Na_2SO_4. Pitting type failures were observed when Na_2SO_4 was applied to the surfaces of these coatings. Exactly to what extent these localized failures would affect the useful life of a coating is difficult to determine. It should be noted, however, that the diffusion aluminide coatings would be applied to internal surfaces of airfoils where salt deposits would be minimal.
- All of the e.b. vapor deposited overlay coatings provided a significant amount of protection in cyclic oxidation tests. The coatings were still protective after 100 one-hour cycles at 1144°K (1600°F), 500 one-hour cycles at 1366°K (2000°F) and 100 one-hour cycles at 1422°K (2100°F).
- The oxidation behavior of the plasma sprayed overlay coatings was inferior to that of the e.b. vapor deposited overlay coatings (compare Figure 12 and 13 for example) but superior to that of the diffusion aluminide coatings (Figure 14). The plasma sprayed overlay coatings on the $\gamma/\gamma'-\delta$ alloy were still protective after 100 one-hour cycles at 1144°K (1600°F), 500 one-hour cycles at 1366°K (2000°F) as seen in Figure 17, and for 100 one-hour cycles at 1422°K (2100°F).
- The diffusion aluminide coatings on the $\gamma/\gamma'-\delta$ deteriorated rapidly at 1366°K (2000°F) due to excessive oxide spallation as reflected in the weight change - time relationship obtained, Figure 14. Specimens were removed from test within 140 one-hour cycles at 1366°K (2000°F).
- In tests performed at 1478°K (2200°F), the overlay coatings of the NiCrAlY type provided protection for up to 100 one-hour cycles (see Figure 19). Overlay coatings of the CoCrAlY type experienced incipient melting at this temperature.
- The plasma sprayed coatings were more severely degraded after 100 one-hour cycles at 1478°K (2200°F) than were the e.b. vapor deposited coatings (compare Figure 19 and 20, for example). The plasma sprayed CoCrAlTaY and NiCrAlSiY coatings (Figures 27 and 28) were much less diffusionally stable than their e.b. vapor deposited counter parts (Figures 21 and 23b). It is worth noting, however, that the plasma sprayed CoCrAlTaY coating showed no evidence of incipient melting during 100 one-hour cycles at 1478°K (2200°F) while incipient melting was clearly evident on the Ni/CoCrAlY coating after only 20 one-hour cycles.
- The coatings based on NiCrAlY tended to be more diffusionally stable than those based on CoCrAlY. In particular, the NiCrAlY coatings modified with tungsten or platinum, and the low aluminum NiCrAlY coating which was subsequently aluminized, appear to offer additional improvements in diffusional stability.

Additional comment on the W/NiCrAlY coating system is in order. While the tungsten layer definitely retards interdiffusion, it is not considered to constitute a viable coating system. Microprobe analysis of this system following 100 hours of 1478°K (2200°F) exposure indicated that minimal interaction between the coating -- tungsten or alloy -- tungsten regions occurs. Indeed, this effect may account for the coating chipping tendency which was observed during post-coating processing. Because of the chipped edges, a repair coating was applied locally to these areas prior to test. Failure initiated in the repair coated areas causing rapid demise of the NiCrAlY coating due to selective attack of the tungsten rich layer (for example, see Figure 15b). Thus, while the tungsten may appear to offer potential for increased coating performance, practical considerations of reliability indicate that it is not desirable to employ a discrete tungsten layer.

It is quite clear that the test results show that overlay coatings are mandatory for the protection of external surfaces at high temperatures. It is also clear that diffusion aluminide coatings must be used for internal cooling passages since overlay coatings are limited by line-of-sight restrictions. Further development, to obtain added protection from the diffusion aluminide coatings, is desirable.

While a number of the vapor deposited overlay coatings exhibited excellent high temperature properties, the NiCrAlY/Pt coating provided the best protection in the furnace tests conducted. The performance of this coating in the 100 hour 1478°K (2200°F) cyclic oxidation test was particularly impressive.

The plasma sprayed coatings did not perform as well as might be expected. The increased surface area due to the surface finish of these coatings may have contributed to spinel formation instead of, or in addition to, Al_2O_3. The excessive spalling noted may reflect the non-homogeneity of these coatings, particularly as it may influence the yttrium distribution and activity. Despite these reservations, the use of plasma sprayed alloy powders allows for the introduction of modifying elements, such as tantalum and silicon, into the coatings. The coating compositions tested cannot be duplicated by vapor deposition techniques at this time. Further evaluation of plasma sprayed coatings should be considered in the future as processing capabilities are improved.

It would appear, therefore, at least for the external surfaces of the directionally solidified $\gamma/\gamma'-\delta$ eutectic alloy, that a variety of overlay coatings are available for protection at temperatures up to 1478°K (2200°F). For protection of the internal passages of airfoils, currently developed diffusion aluminide coatings should prove adequate. It would be prudent, however, to develop more oxidation resistant coatings of this type.

IV. COATING DUCTILITY EVALUATION

A. SELECTION OF COATING SYSTEMS AND TEST TECHNIQUE

Based on the results from furnace oxidation and hot corrosion evaluations discussed in the preceeding section, the coating systems listed in Table X were selected for coating ductility determination. While overlay type coatings exhibited the most potential for protection of airfoil surfaces, an apparent need for total surface protection for this alloy cannot be neglected. Therefore, the two diffusion aluminide coatings were included because of their potential as internal, or possibly as root coatings, for the $\gamma/\gamma'-\delta$ alloy.

Fourteen, nominal 1.27 cm (0.5 inch) diameter by approximately 15.2 cm (6 inch) long, D.S. eutectic bars were prepared by United Aircraft Research Laboratories according to the procedure previously described. These castings were machined to produce the specimen configuration shown in Figure 35. Rough grinding of specimens was accomplished with conventional aluminum oxide grinding wheels and flood coolant; finish grinding was done electrochemically with a contoured wheel. Conventional machining techniques were employed to machine the threads and extensometery attachments. Duplicate specimens were prepared for each of the coating systems given in Table X. In addition, for two of the overlay coating systems (NiCoCrAlY and NiCrAlY/Pt), one additional specimen of each was coated. Coatings were applied to the gage area of each specimen using the techniques previously described.

Coating ductility determinations were made by running an interrupted tensile test. The coated specimen was heated to the specified temperature and then loaded in tension to a predetermined level of strain. The specimen was then unloaded and cooled to room temperature so that plastic surface replicas could be taken. Testing was continued in an incremental fashion, with replicas being taken after each strain increase, until cracking of the coating was detected. Duplicate specimens for each of these coating systems were tested at 578°K (600°F) and for two overlay systems, single data points at 811°K (1000°F) were also obtained. In addition, the failure strains for all the coated specimens were also determined.

B. COATING DUCTILITY TESTING

For the NiCrAlY and CoNiCrAlY coated specimens the results indicated that coating cracking and specimen failure occurred concurrently on 4 of 5 specimens. Those specimens which showed coating cracking without concurrent specimen failure were subsequently tested to determine the coating specimen failure strain. These data are tabulated in Table XI, along with 578°K (600°F) failure strain data for uncoated $\gamma/\gamma'-\delta$ specimens which were generated in a separate P&WA program.

TABLE X

COATING SYSTEMS SELECTED FOR COATING
DUCTILITY DETERMINATION

Ni-18Cr-12Al-0.3Y	overlay
Ni-18Cr-12Al-0.3Y plus Pt	overlay
Ni-18Cr-5Al-0.3Y plus pack aluminide	overlay/pack
Co-33Ni-18Cr-15Al-0.6Y	overlay
"Ductile" aluminide	pack
Nickel/chromize/aluminize	pack

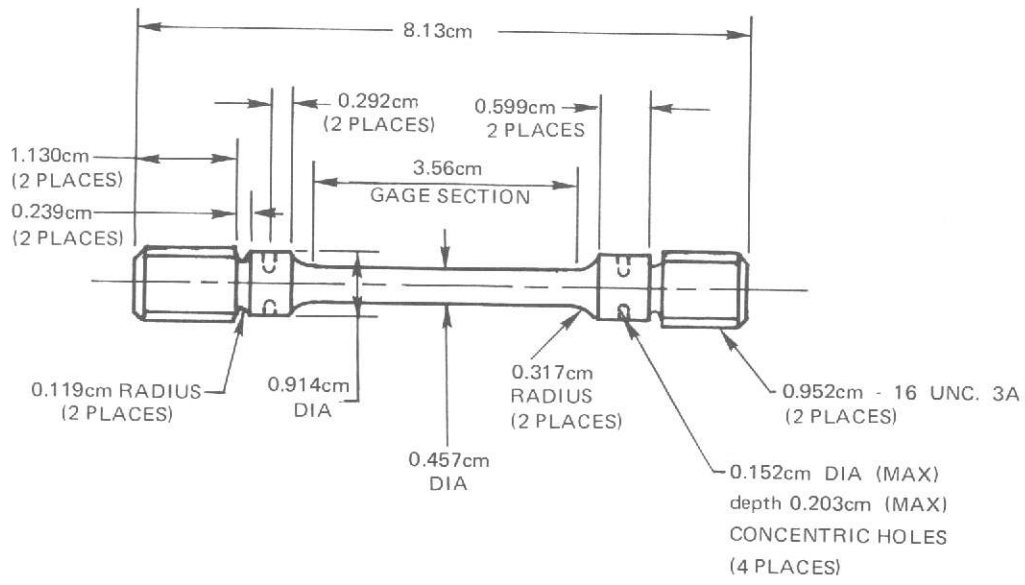

Figure 35 Coating Ductility Specimen

TABLE XI

COATING FRACTURE AND γ/γ'- δ FAILURE STRAIN

Coating System	Coating Fracture Strain (%)	Specimen Failure Strain (%)	Temperature (°K)	Coating Microstructure (Figure No.)
Ni-15.2Cr-12.8Al-0.31Y	0.60-0.70	0.70	578	
Ni-17.8Cr-12.6Al-0.31Y	0.40-0.49	0.74	578	36
Ni-29.4Co-19.1Cr-15.6Al-0.35Y	0.40-0.47	0.47	578	37
Ni-29.4Co-19.1Cr-15.6Al-0.35Y	0.40-0.48	0.48	578	
Ni-30.0Co-17.4Cr-14.6Al-0.80Y	0.61-0.77	0.77	811	
Ni-17.6Cr-12.7Al-0.33Y + Pt*	0.60-0.80	1.24	578	38
Ni-15.2Cr-12.8Al-0.31Y + Pt	0.61-0.81	1.97	578	39
Ni-17.8Cr-12.6Al-0.31Y + Pt*	Not Measured	0.92	811	
Ni-15.3Cr-7.1Al-0.34Y + Pack Aluminide	0.41-0.51	> 7.15	578	40
Ni-15.3Cr-7.1Al-0.34Y + Pack Aluminide	0.40-0.52	6.1	578	
Ductile Aluminide	0.51-0.67	4.04	578	41
Ductile Aluminide	0.79-1.02	2.28	578	
Nickel/Chromize/Aluminize	0.40-0.50	6.04	578	42
Nickel/Chromize/Aluminize	0.41-0.51	4.83	578	
Uncoated		3.56	578	
Uncoated		3.40	578	

*Incipient melting in coating/alloy interdiffusion zone. This condition was related to an apparent overtemperature condition which occurred during the platinum coating process.

Specimens representing each of the above coating systems tested at 578°K (600°F) were metallographically examined and typical post-test microstructures are shown in Figures 36 through 42.

Post-test visual examination of the surfaces of one of the NiCrAlY and both of the CoNiCrAlY coated eutectic alloy specimens revealed that small pit defects provided sites for coating crack initiation. A single crack in one of the NiCrAlY coated specimens is believed to have initiated at a coating pit, between 0.40% and 0.49% strain. This coating crack spiraled up and down the specimen and initiated numerous secondary cracks in the $\gamma/\gamma'-\delta$ substrate before specimen failure occurred at 0.74% strain (Figure 36). In a couple of instances, it was observed that the coating crack did not sever the relatively ductile diffusion affected coating layer before penetrating into the substrate as shown in Figure 36.

Metallographic examination of a CoNiCrAlY coated specimen (Figure 37) revealed that a secondary crack, which may also have initiated at a coating pit, had propagated through the porous region in the interdiffusion zone and continued into the substrate. (An explanation of the presence of the porous layer is presently not available. Such a condition was not observed for this system during furnace testing.)

Formation of the platinum rich outer layer of the NiCrAlY + Pt coating appears to withdraw aluminum from the underlying NiCrAlY coating, thereby creating a relatively ductile NiCrAlY zone which may retard crack propagation. In the specimen which had incipient melting in the interdiffusion zone between the NiCrAlY and the $\gamma/\gamma'-\delta$, the aluminum content of the entire thickness of the NiCrAlY layer was significantly decreased, and cracks in the outer platinum rich layer did not penetrate to the substrate (Figure 38). Incipient melting is believed to have been contributory to the failure of this specimen. (It appears that the overtemperature condition which produced incipient melting occurred during the sputter deposition of the platinum layer.) Melting of the coating-substrate interdiffusion zone did not occur during formation of the platinum rich layer in the second NiCrAlY + Pt coated specimen. Development of the Pt-rich surface layer consumed less aluminum from the NiCrAlY coating, and the thickness and relative ductility of the adjacent NiCrAlY layer was less. As a result, it is thought that cracks, which initiated between 0.61% and 0.81% strain in the platinum rich layer, propagated slowly through the partially "ductilized" NiCrAlY coating and finally caused specimen failure at 1.97% strain. Secondary coating cracks are shown in Figure 39; in this case, the crack path in the coating appears to be predominately along phase boundaries.

In addition, CoNiCrAlY and NiCrAlY + Pt coated $\gamma/\gamma'-\delta$ specimens were tested at 811°K (1000°F); failure strains of these specimens were 0.77% and 0.92%, respectively. (This NiCrAlY + Pt specimen showed visual indications of incipient melting prior to test.) The 811°K (1000°F) data is considered to be consistent with the 578°K (600°F) data.

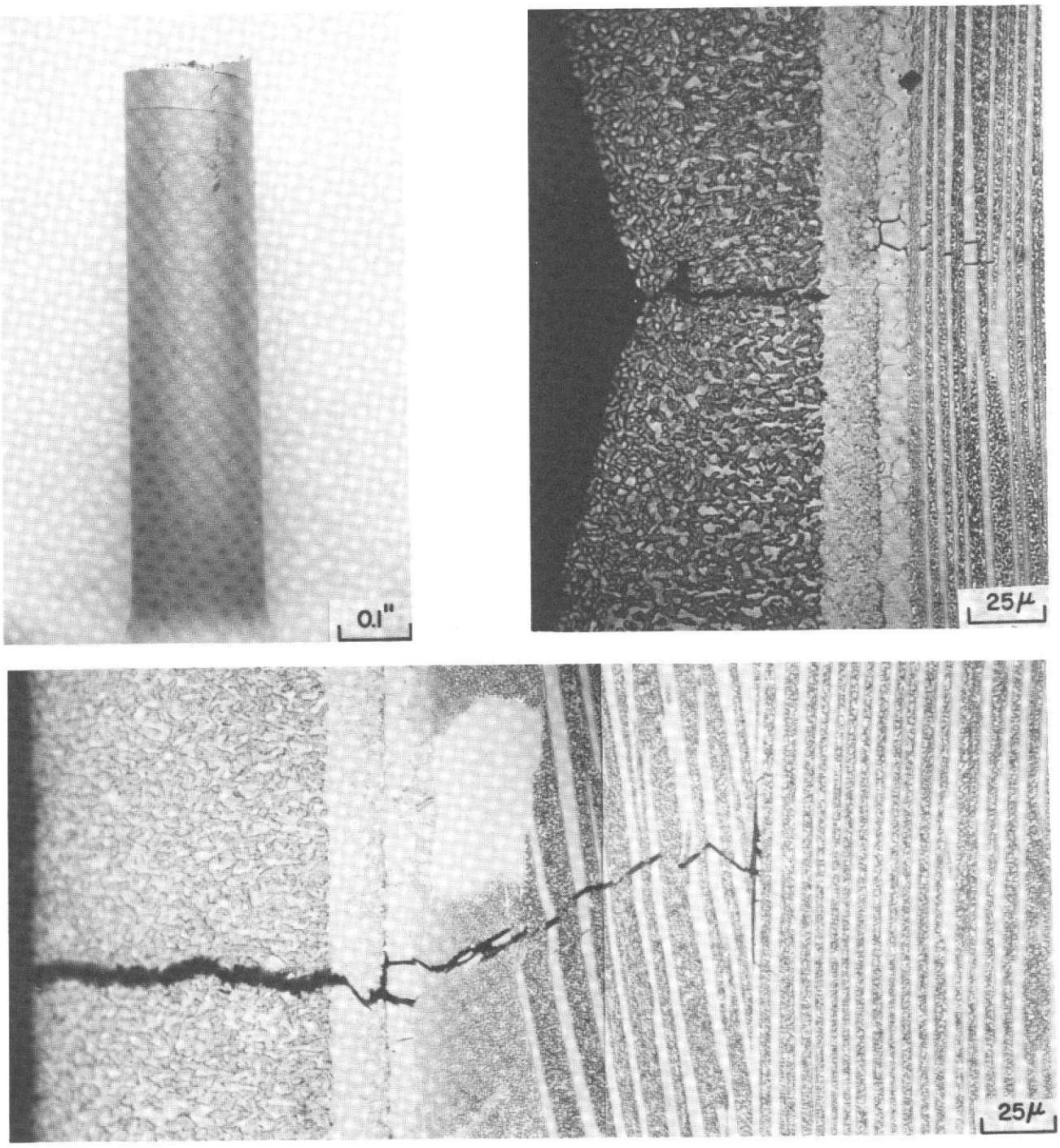

Figure 36 Post-Test Surface and Microstructural Condition of a Ni-17.8Cr-12.6Al-0.31Y Coated $\gamma/\gamma' - \delta$ Coating Ductility Specimen. A Single Coating Crack Which Spiraled Up and Down the Specimen Surface (Top-Left). Planar Sections Showing Secondary Substrate Cracks Associated With the Spiraling Coating Crack (Top-Right and Bottom).

Coating Fracture Strain – 0.40-0.49%
Substrate Failure Strain – 0.74%
Test Temperature – 578°K (600°F)

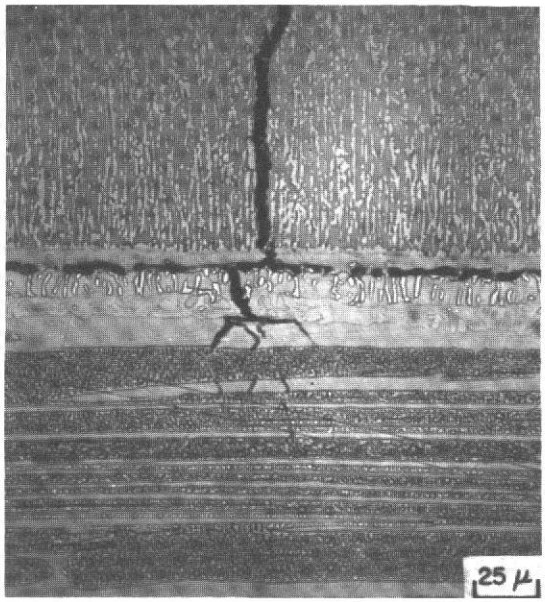

Figure 37 Planar Section of a Ni-29.4Co-19.1Cr-15.6Al-0.35Y Coated $\gamma/\gamma' - \delta$ Coating Ductility Specimen Showing a Secondary Coating Crack. The Presence of the Porous Layer Within the Interdiffusion Zone is Presently Unexplained.
Coating Fracture Strain – 0.4-0.47%
Substrate Failure Strain – 0.47%
Test Temperature – 578°K (600°F)

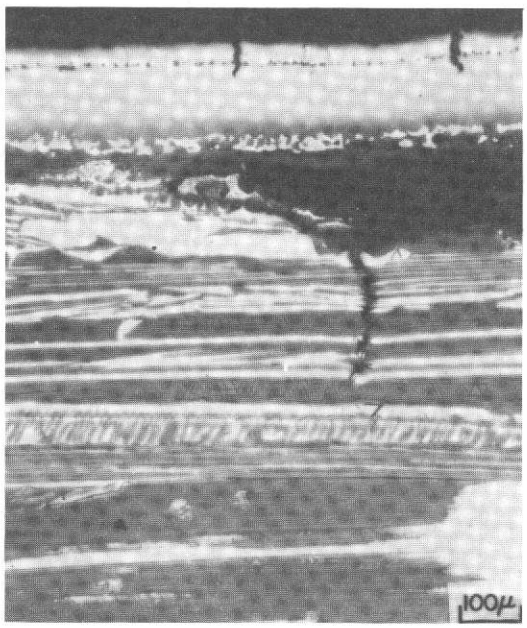

Figure 38 Planar Section of a Ni-17.6Cr-12.7Al-0.33Y + Pt Coated $\gamma/\gamma' - \delta$ Coating Ductility Specimen Showing Interdiffusion Zone Incipient Melting Which Contributed to the Initiation of a Secondary Substrate Crack. The Melting is Believed Due to an Overtemperature Condition During Application of the Sputtered Platinum Surface Layer. Also Note That Cracks in the Platinum-Rich Surface Layer Did Not Propagate to the $\gamma/\gamma' - \delta$ Substrate.

Coating Fracture Strain – 0.6-0.8%
Substrate Failure Strain – 1.24%
Test Temperature – 578°K (600°F)

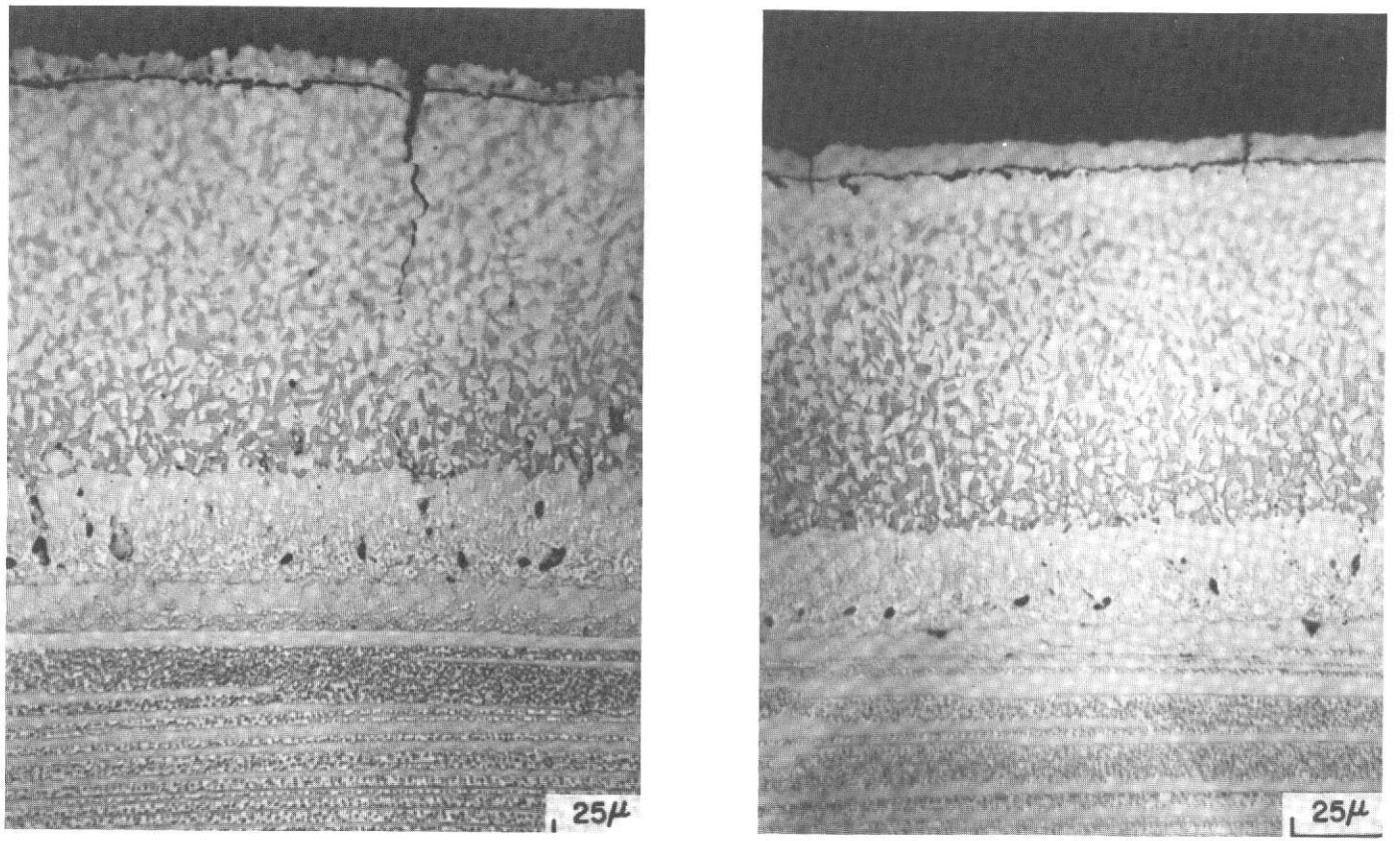

Figure 39 Planar Sections of a Ni-15.2Cr-12.8Al-0.31Y + Pt Coated $\gamma/\gamma' - \delta$ Coating Ductility Specimen Showing Secondary Coating Cracks. Note that the Amount of the Aluminum Rich β (NiAl) Phase (Dark Etching) in the Outer Portion of the NiCrAlY Coating was Reduced During the Formation of the Platinum Rich Surface Layer (Right).

Coating Fracture Strain – 0.61-0.81%
Substrate Failure Strain – 1.97%
Test Temperature – 578°K (600°F)

Specimens coated with the two diffusion aluminide type coatings and the low aluminum NiCrAlY overlay which was subsequently aluminized, had failure strains comparable to those for the uncoated $\gamma/\gamma'-\delta$ alloy. Although the surfaces of the coatings on these specimens were extensively cracked (see Figures 40 through 42), post-test metallography indicated that most of these cracks failed to propagate into the $\gamma/\gamma'-\delta$ substrate. It is assumed that the lower aluminum, more ductile, inner zones associated with these coatings inhibited crack penetration into the substrate. Formation of numerous cracks in the outer higher aluminum content zones of these coatings also tended to reduce the magnitidue of the elastic strain in these coatings; consequently, the driving force for crack penetration into the substrate was probably somewhat lower than if isolated cracks were present.

Microhardness measurements were obtained for each of the coating systems after 578°K (600°F) ductility testing. The interdiffusion zones formed between the alloy and the NiCrAlY and NiCoCrAlY coatings are relatively soft (Rc 28.5 and 39, respectively) in comparison with the coatings (Rc 47 to 52 and Rc 47.5 to 53, respectively) and the substrate (Rc 47.5 to 52). Microhardness for the inner coating zones and interdiffusion zones of the other overlay and diffusion coatings are generally higher, Rc 38.5 to 54. A complete tabulation of the hardness data for these systems is given in Table XII.

C. DISCUSSION OF TEST RESULTS

In order to interpret the above results, it is useful to consider additional coating and substrate fracture strain data on $\gamma/\gamma'-\delta$ which were generated in support of a U.S. Air Force program to develop a eutectic turbine vane ("Applied High Temperature Technology Program," AF Contract F 33657-71-C-0789). These data were obtained in a manner equivalent to the ductility tests performed for the NASA program. Based on prior results, two thicknesses, 63.5 and 127 μ (2.5 and 5 mils) of PWA 270 (Nominal Ni-23Co-18Cr-12.5Al-0.45Y) coatings and two layered coatings consisting of 25.4μ (1 mil) and 63.5μ (2.5 mils) inner layers of Ni-18Cr-5Al-0.3Y and 101.6μ (4 mils) and 63.5μ (2.5 mils) outer layers of PWA 270, respectively, were selected for evaluation. In addition, a nominal 50.8μ (2 mil) thick diffusion aluminide coating, as well as uncoated $\gamma/\gamma'-\delta$ specimens, were tested at 578°K (600°F). The coating and substrate fracture strains obtained in these tests are given in Table XIII.

TABLE XII

DUCTILITY SPECIMEN COATING MICROHARDNESS

	Microhardness (Rc)			
		Interdiffusion Zone		
	Coating	Affected Coating	Affected Substrate	γ/γ'-δ Substrate
NiCrAlY	47-52	28.5	47.5	48-49
CoNiCrAlY	47.5-53	39	52	49
NiCrAlY + Pt				
Pt-Rich Layer	50.5-57			
Low Al Zone Adjacent to Pt	39.5-45			
Inner NiCrAlY Zone	37.5	44	48	
NiCrAlY/Al				
Outer Al-Enriched Layer	57-61			
Intermediate Al-Enriched Layer	52-54			
Low Al NiCrAlY Layer	45.5	42		53
Ductile Aluminide				
Outer Al-Rich Layer	47-59.5			
Inner Layer	52.5			53-57
Ni/Cr/Al				
Outer Al-Enriched Layer	50.5-56			
Intermediate Al-Enriched Layer	47.5-48			
Inner Most Layer	38.5-48			52.5-54

TABLE XIII

578°K (600°F) COATING AND Y/Y'-S SUBSTRATE FRACTURE STRAINS
(AF CONTRACT F33657-71-C-0789)

Coating(s)	Coating Fracture Strain (%)	Specimen Failure Strain (%)
PWA 270 [127μ (5 mils)]	1.10-1.18	1.18
PWA 270 [127μ (5 mils)]	> 2.00	2.21
PWA 270 [63.5μ (2.5 mils)]	> 2.00	2.47
PWA 270 [63.5μ (2.5 mils)]	> 2.00	2.58
Low Al NiCrAlY [25.4μ (1 mil)] + PWA 270 [101.6μ (4 mils)]	0.50-0.67	0.67
Low Al NiCrAlY [25.4μ (1 mil)] + PWA 270 [101.6μ (4 mils)]	0.0-0.49	0.50
Low Al NiCrAlY [63.5μ (2.5 mils)] + PWA 270 [63.5μ (2.5 mils)]	> 2.01%	2.64
Low Al NiCrAlY [63.5μ (2.5 mils)] + PWA 270 [63.5μ (2.5 mils)]	1.35-1.68	2.68
Aluminide [50.8μ (2 mils)]	0.5-0.6	3.95
Aluminide [50.8μ (2 mils)]	0.6-0.8	2.37
Uncoated	---	3.86
Uncoated	---	2.68

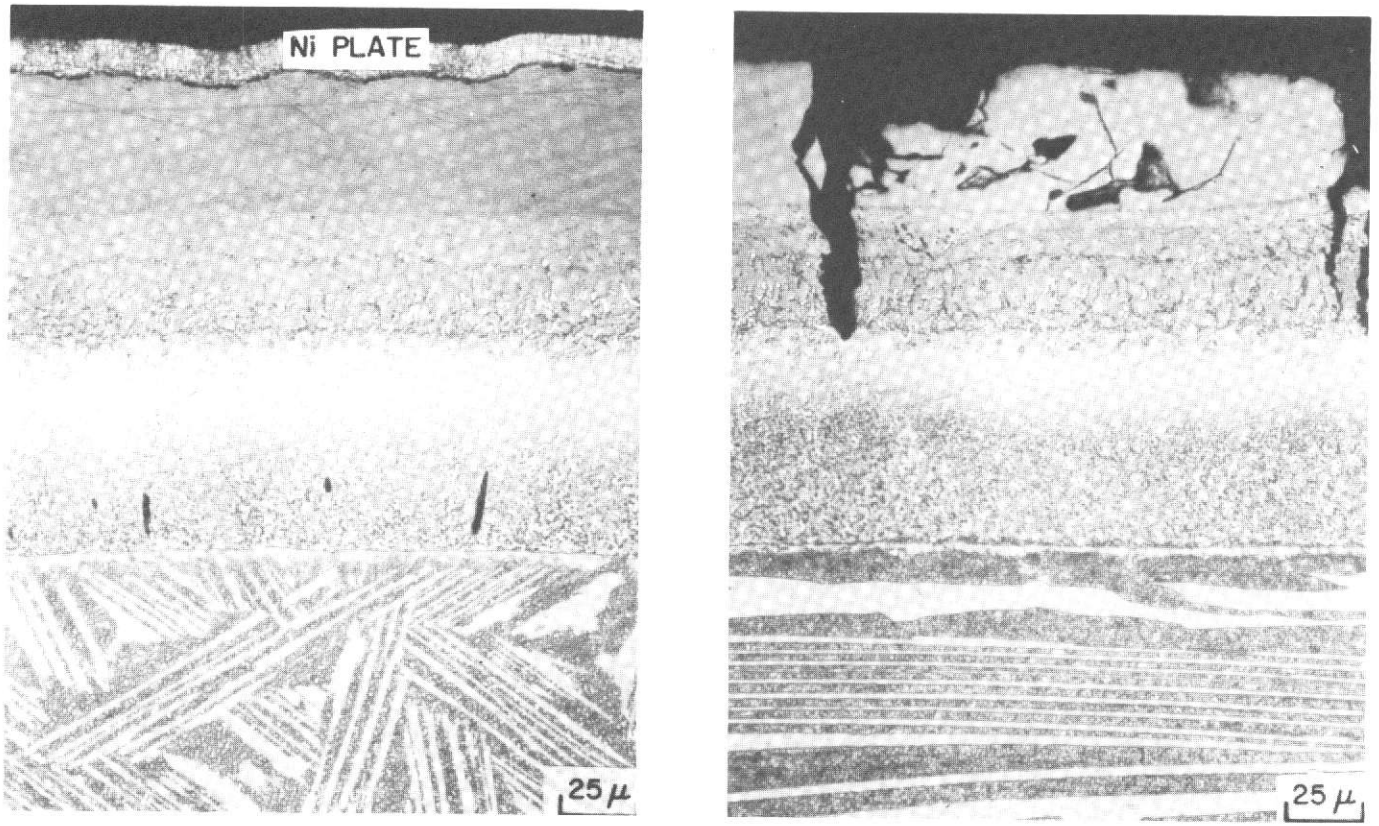

Figure 40 Transverse (Left) and Longitudinal (Right) Sections of a Ni-15.3Cr-7.1Al-0.34Y + Diffusion Aluminized Coated $\gamma/\gamma' - \delta$ Coating Ductility Specimen. Note that Coating Cracks are Confined to the Outer Portion of the Coating.

Coating Fracture Strain – 0.41 – 0.51%
Substrate Failure Strain – > 7.15%
Test Temperature – 578°K (600°F)

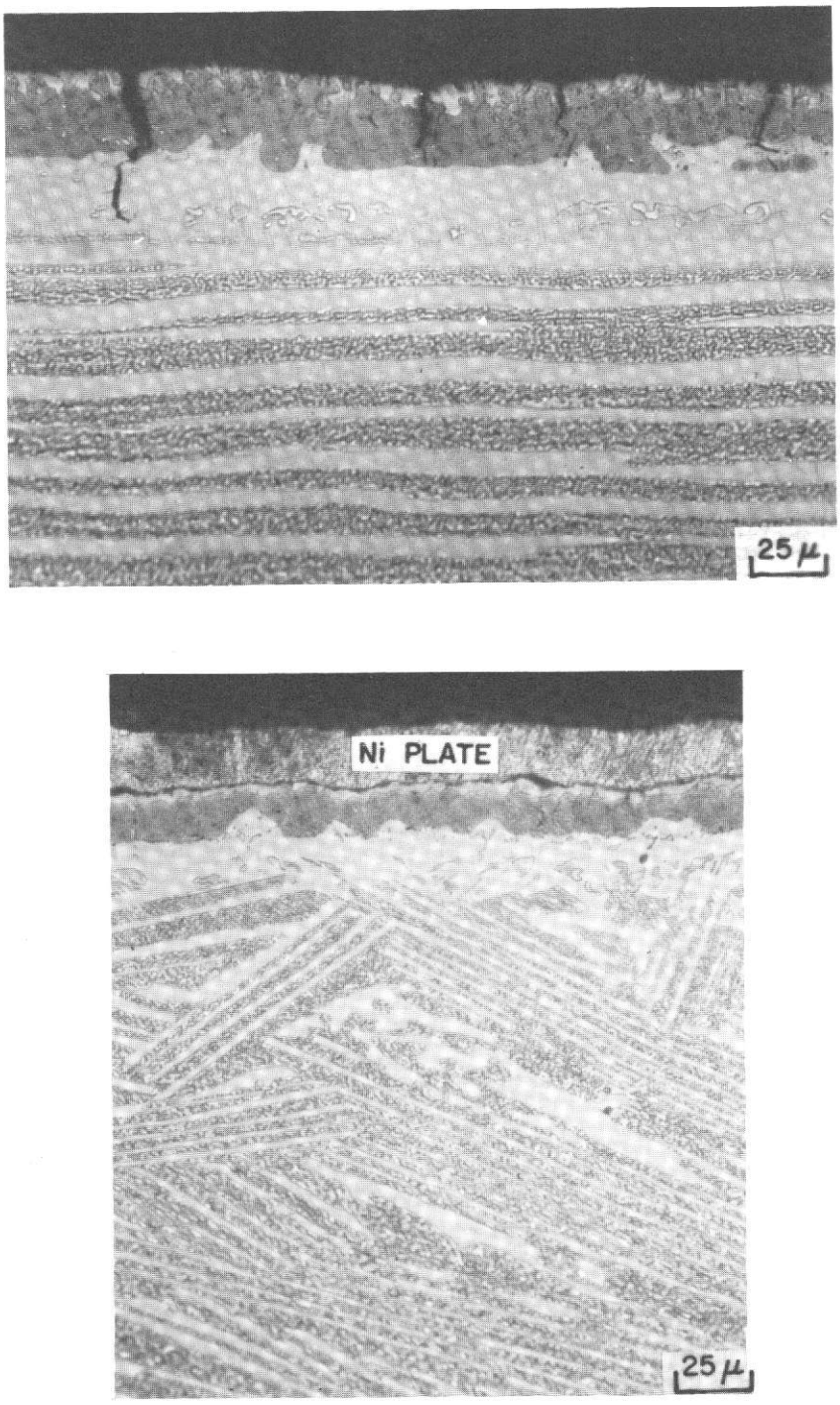

Figure 41 Longitudinal (Upper) and Transverse (Lower) Sections of the Ductile Aluminide (Cr/Al) Coated $\gamma/\gamma' - \delta$ Coating Ductility Specimen.
Coating Fracture Strain – 0.51-0.67%
Substrate Failure Strain – 4.04%
Test Temperature – 578°K (600°F)

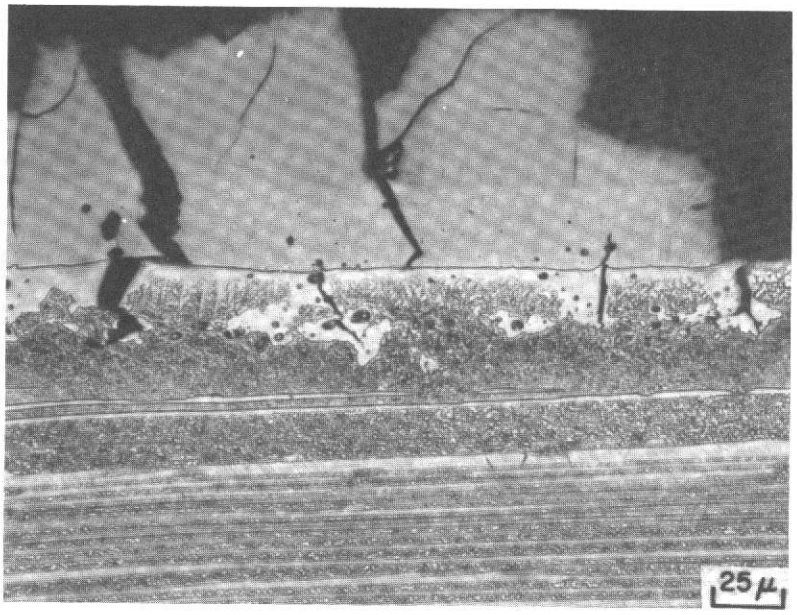

Figure 42 Longitudinal Section of the Nickel Plate/Chromized/Aluminized Coated $\gamma/\gamma' - \delta$ Coating Ductility Specimen.
Coating Fracture Strain – 0.4-0.5%
Substrate Failure Strain – 6.04%
Test Temperature – 578°K (600°F)

These results indicate that for the PWA 270 overlay, with or without an inner lower aluminum layer, coating thickness had a significant influence upon the coated specimen failure strain. Thus at 63.5μ (2.5 mils), the anticipated PWA 270 coating fracture strain ($>$ 2% strain) was attained in 3 out of 4 instances and substrate failure strains comparable to the uncoated alloy were realized in all instances. The behavior of the aluminide coating in this test was consistent with the results obtained for the aluminides evaluated in the NASA program. (This behavior of the aluminide coating indicates that for the $\gamma/\gamma'-\delta$, unlike the $\gamma'-\delta$ alloy, a simple aluminide coating, i.e. no pre-aluminizing step, such as chromizing, is necessary to achieve metallurgical compatibility. Apparently, the chromium content of the $\gamma/\gamma'-\delta$ alloy is sufficient to suppress η, $CbNi_2Al$, phase formation, which was observed[10] for the $\gamma'-\delta$ alloy, when aluminized.)

The relatively good failure strains which have been obtained with $\gamma/\gamma'-\delta$ specimens coated with the thin PWA 270 (63.5μ thick) and the low Al NiCrAlY (63.5μ) + PWA 270 (63.5μ) indicated that the critical interaction between the substrate and the coating is probably mechanical and not coating-substrate interdiffusion dependent; i.e. the elastic properties and the thickness of the "strong" layers in the coating are probably the significant factors affecting system behavior.

This explanation is also compatible with the good failure strains noted for pack aluminized $\gamma/\gamma'-\delta$ specimens which had numerous cracks. Because of the very high density of coating cracks, the effective elastic modulus of the cracked coatings was very low. If this hypothesis is correct, an individual crack in a highly cracked coating would not represent a large stress raiser. The thin coating thickness would also be beneficial from a stress raiser standpoint.

Fracture mechanics concepts are also helpful in explaining the behavior observed. If the coating is cracked to the substrate, the elastic modulus and the thickness of the coating will affect the magnitude of the crack's stress intensity factor, i.e. a crack in a strong, thick coating should be more deleterious than a crack in a strong, thin coating.

In summary, the available test results indicate that the low strain, low temperature (578°K) failures of some coated $\gamma/\gamma'-\delta$ specimens are probably the result of a mechanical interaction between the coating and the substrate. Reducing the thickness of the "strong" coating layer may provide an acceptable engineering solution for alleviating low strain substrate failures. For example, NiCoCrAlY coatings with a thickness of 63.5μ have resulted in specimen failure strains which are similar to those obtained with uncoated $\gamma/\gamma'-\delta$ substrates.

V. SELECTION OF COATING SYSTEMS FOR BURNER RIG EVALUATION

Collectively, the furnace exposure and coating ductility data discussed in the preceeding sections (internal P&WA and AF program ductility data were not available at the time) were used to select three overlay coating systems for the 1366°K (2000°F) cyclic oxidation burner rig test. The systems selected for evaluation were as follows:

- 127μ (5 mils) Ni-18Cr-12Al-0.3Y (electron beam) plus 6.3μ (0.25 mils) platinum (sputter)
- 127μ (5 mils) Ni-20Co-18Cr-13Al-0.3Y (electron beam)
- 127μ (5 mils) Ni-18Cr-5Al-0.3Y (electron beam) plus 63.5μ (2.5 mils) diffusion aluminide (pack)

Based on the furnace data, each of these systems appeared to provide significant potential for protecting the D.S. eutectic alloy in a high-temperature turbine environment. While the CoNiCrAlY coating (Item C - Table I) may have a somewhat lower overtemperature capability than the other two coatings, each is capable of exposure to 1422°K (2100°F) without experiencing incipient melting of the coating/alloy interdiffusion zone. However, in order to provide increased coating ductility, the initial CoNiCrAlY composition was modified (lower cobalt and aluminum). In addition, this compositional change, particularly lower cobalt, was also expected to contribute to a higher incipient melting temperature. The platinum modified and aluminized NiCrAlY coatings had exhibited behavior in the ductility tests which appeared to qualify them for evaluation in the burner rig.

As discussed previously, relatively ductile overlay coatings of about 63.5μ (2.5 mils) thickness have demonstrated fracture strains ($>2\%$) for the coated γ/γ'- δ eutectic alloy which are quite similar to those for the uncoated alloy (at 578°K). Significantly lower failure strains ($<1\%$) were obtained when the same coatings were thicker. While a complete explanation of this behavior is not presently available, current data indicates that a mechanical interaction between the coating (normal thickness 127μ) and substrate is the most likely cause. When sufficient component design data is available, if the 578°K (600°F) coated substrate tensile behavior is determined to be critical, coating thickness for the overlay systems could be decreased. Obviously, decreased coating thickness will reduce the oxidation resistance (lifetime) for any given system. However, the burner rig results which will be discussed subsequently suggest that some of the systems under evaluation may still provide satisfactory protection at reduced thickness.

VI. 1000 HOUR - CYCLIC OXIDATION BURNER RIG EVALUATION

A. PREPARATION OF TEST SPECIMENS

Eutectic alloy erosion bar specimens (Figure 43) were directionally solidified by the Casting Development Section of the Materials Engineering and Research Laboratory using a multiple cavity shell mold. The bars were solidified at the rate of 1.27 cm (0.5 inch)/hour in a modified Bridgman furnace. Since the erosion bar configuration is cast to size, the only pre-coating surface preparation employed was a light abrasive belting to radius edges and improve surface finish. The three coating systems selected for evaluation were as follows:

- Approximately 127μ (5 mils) Ni-18Cr-12Al-0.3Y (electron beam) plus approximately 6.3μ (0.25 mil) platinum (sputter)
- Approximately 127μ (5 mils) Ni-20Co-18Cr-13Al-0.3Y (electron beam)
- Approximately 127μ (5 mils) Ni-18Cr-5Al-0.3Y (electron beam) plus approximately 63.5μ (2.5 mils) diffusion aluminide (pack)

Coating procedures employed were identical to those described previously for preparation of the furnace coupon and coating ductility specimens. Actual chemistries for the electron beam coatings on the erosion bar specimens are given in Table XIV.

B. BURNER RIG TEST PROCEDURE AND RESULTS

These coating systems were evaluated for times up to 1016 hours in a 1366°K (2000°F) cyclic oxidation burner rig test (cycle: 55 minutes hot - 5 minutes forced air cool) which simulates a gas turbine engine environment. The burner rig is shown in Figure 44. Twelve erosion bars were simultaneously exposed to the exhaust gases (combustion products of Jet A fuel and air) of the burner which had a gas velocity of Mach 0.37. The specimens were rotated at 1750 RPM in the burner exhaust gases to provide as uniform temperature conditions from specimen to specimen as possible. Specimen temperature was continuously monitored with an optical pyrometer and the fuel pressure automatically regulated to maintain the designated temperature. Cycling was accomplished by automatically moving the burner away from the specimens at designated intervals. During the cooling portion of the cycle, a compressed air blast was directed on the rotating specimens. Testing was interrupted every 16 to 20 hours to permit visual examination and weighing of each specimen.

The initial complement of specimens consisted of nine D.S. eutectic specimens (three with each coating) and three D.S. MarM-200 + Hf (PWA 1422) erosion bars (one with each coating) which were evaluated for comparative purposes. After 493 hours of testing, three D.S. eutectic erosion bars (one with each coating) were removed from test for metallographic evaluation; at this time, three additional PWA 1422 specimens (one with each coating) were inserted. Thus, at the conclusion of this test, both 500 and 1000 hour exposed PWA 1422 and γ/γ'- δ specimens with each of the three coating systems were available for metallographic examination.

C - 2

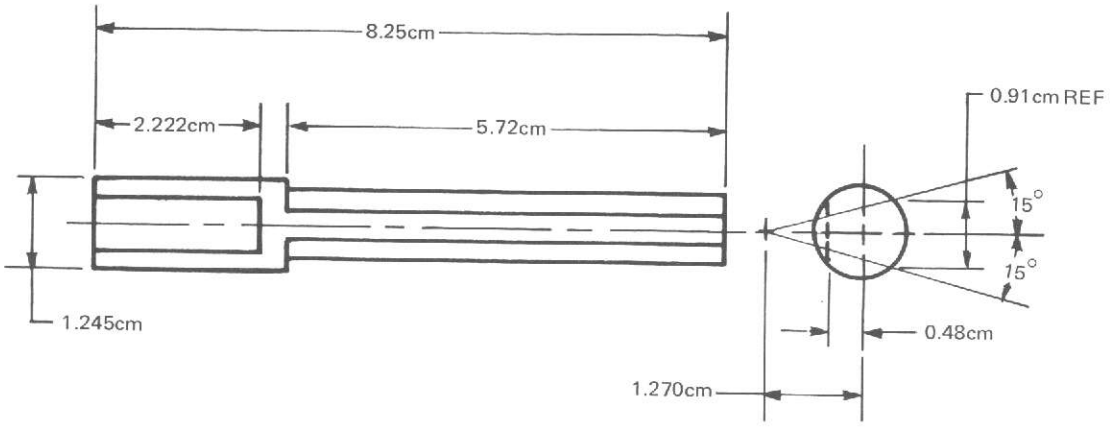

Figure 43 Burner Rig Oxidation – Erosion Bar

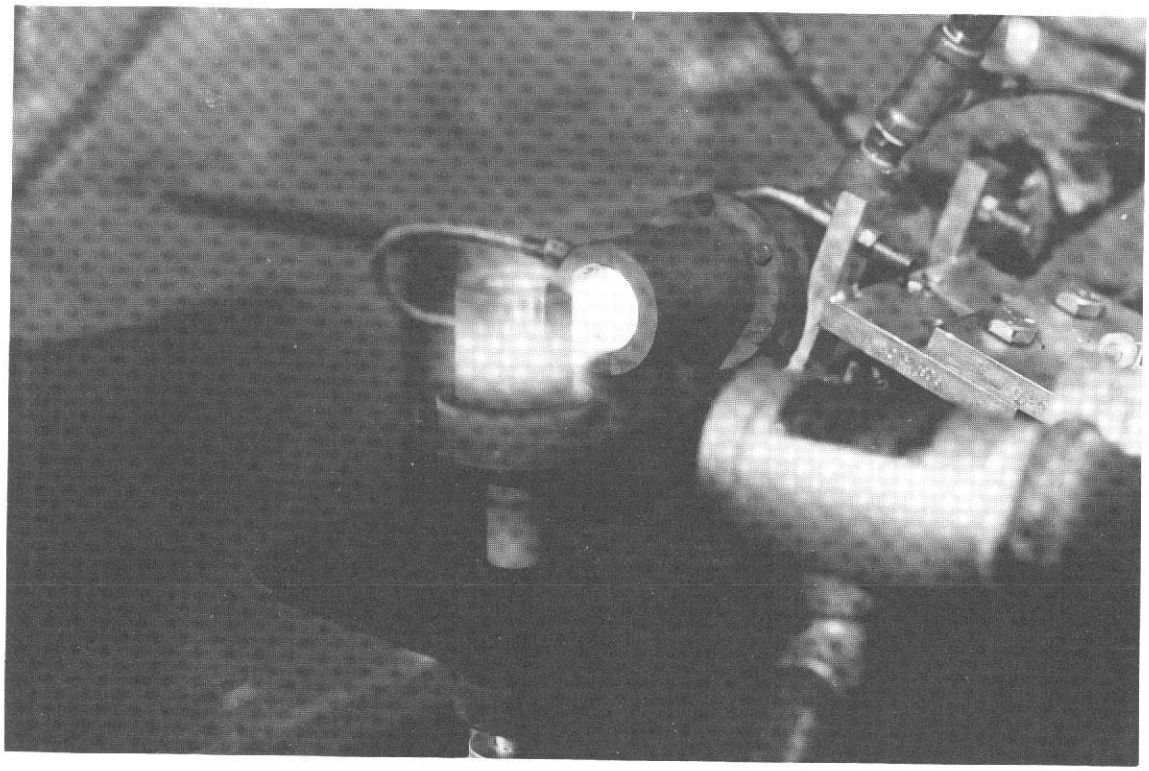

Figure 44 Oxidation Burner Rig

TABLE XIV

OVERLAY COATING CHEMISTRIES ON EROSION BAR SPECIMENS

Identification	Substrate	Coating(s)
R-7404	$\gamma/\gamma'-\delta$	Ni-16.4Cr-5.9Al-0.72Y + Al (pack)
R-7405	$\gamma/\gamma'-\delta$	Ni-17.2Cr-6.2Al-0.58Y + Al (pack)
R-7406	$\gamma/\gamma'-\delta$	Ni-17.2Cr-6.2Al-0.58Y + Al (pack)
R-7407	PWA 1422	Ni-16.4Cr-5.9Al-0.72Y + Al (pack)
R-7418	PWA 1422	Ni-17.7Cr-5.8Al-1.05Y + Al (pack)
R-7408	$\gamma/\gamma'-\delta$	Ni-21.5Co-19.3Cr-12.4Al-0.14Y
R-7409	$\gamma/\gamma'-\delta$	Ni-21.7Co-18.5Cr-12.2Al-0.20Y
R-7410	$\gamma/\gamma'-\delta$	Ni-21.7Co-18.5Cr-12.2Al-0.20Y
R-7411	PWA 1422	Ni-22.5Co-19.7Cr-12.1Al-0.10Y
R-7419	PWA 1422	Ni-22.5Co-19.7Cr-12.1Al-0.10Y
R-7412	$\gamma/\gamma'-\delta$	Ni-18.2Cr-11.8Al-0.30Y + Pt (sputter)
R-7413	$\gamma/\gamma'-\delta$	Ni-19.2Cr-11.8Al-0.35Y + Pt (sputter)
R-7414	$\gamma/\gamma'-\delta$	Ni-17.4Cr-11.9Al-0.32Y + Pt (sputter)
R-7415	PWA 1422	Ni-18.2Cr-11.8Al-0.30Y + Pt (sputter)
R-7420	PWA 1422	Ni-19.2Cr-11.8Al-0.35Y + Pt (sputter)

Weight change data and a summary of the visual conditions of the specimens after 493 and 1016 hours (523 hours for the additional PWA 1422 specimens) of accumulated test time are given in Table XV. The appearances of the coated $\gamma/\gamma'-\delta$ and PWA 1422 erosion bars which were metallographically evaluated are shown in Figure 45.

NiCrAlY/Al

During visual inspection of the NiCrAlY/Al coated $\gamma/\gamma'-\delta$ specimens, repeated spallation of the alumina scales and rather extensive thermal fatigue cracking of the coating were observed. These cracks were oriented primarily axially (parallel to the solidification direction of the erosion bar). The most severe thermal fatigue cracks in the NiCrAlY/Al coated erosion bars were in the leading surface (surface of smallest arc) of specimen R-7406. Isolated cracks were detected as early as 89 hours. Progressive development of these cracks is shown in Figure 46. Cracking was also extensive in the trailing surface (surface of largest arc) of this specimen as shown in Figure 47. Metallographic examination of these specimens showed that the thermal fatigue cracks had propagated a short distance into the substrate (see Figures 46 and 48).

Metallographic examination of the NiCrAlY/Al coated $\gamma/\gamma'-\delta$ specimen (R-7404) which was removed from test after 493 hours revealed that, in addition to those cracks which were visually detectable, numerous microcracks were also present (Figure 49); alumina particles from the pack, which were incorporated into the coating, may have contributed to the initiation of some coating cracks. However, since the NiCrAlY/Al coatings on PWA 1422 also contained embedded alumina particles, the existence of this condition is apparently not sufficient to account for the severity of cracking in this coating when on $\gamma/\gamma'-\delta$.

In addition to relatively severe coating cracking, the aluminum-rich β (NiAl) phase had been consumed in the hot zone of specimen R-7404 during the 493 hours of testing. As a result of aluminum depletion, the hot zone coating consisted of $\gamma'(Ni_3Al)$ and γ(Ni solid solution) at the time of removal from this test (Figure 49). The thickness of the diffusion affected substrate layer in the hot zone was approximately 73.7μ (2.9 mils). In the hot zone of specimen R-7406, which was tested for 1016 hours, the coating was predominately γ phase with some surface connected oxide stringers (Figure 48). Failure of the hot zone coating shown in Figure 48 is imminent. The thickness of the diffusion affected substrate layer in the hot zone was approximately 119.4μ (4.7 mils).

NiCrAlY/Al coated PWA 1422 specimens, R-7418 and R-7407, were evaluated in the burner rig 1366°K (2000°F) cyclic oxidation test for 523 and 1016 hours, respectively. Although thermal fatigue cracks were not visually observed, post-test metallographic examination revealed regions of intergranular oxidation which could also be regarded as microcracks in these coatings. Oxide blisters formed in the hot zones of both NiCrAlY/Al coated PWA 1422 specimens and initiated a localized failure in the specimen tested for 1016 hours as shown in Figure 45.

TABLE XV

VISUAL CONDITION OF COATED EROSION BARS IN 2000°F CYCLIC OXIDATION BURNER RIG TEST
(CYCLE: 55 MINUTES HOT - 5 MINUTES FORCED AIR COOL)

Coating System	Specimen Identification	Substrate	Time In Test (Hours)	Change in Erosion Bar Weight (Grams)	Comments
NiCrAlY/Al	R-7404	$\gamma/\gamma'-\delta$	493	0.03	Repeated spallation of alumina and extensive coating cracking; specimen removed for metallographic examination.
NiCrAlY/Al	R-7405	$\gamma/\gamma'-\delta$	1016	-0.05	Repeated spallation of alumina and fewer coating cracks.
NiCrAlY/Al	R-7406	$\gamma/\gamma'-\delta$	1016	-0.03	Repeated spallation of alumina and other oxides which formed in hot zone. Cracking was extensive; cracks in hot zone became oxide-filled.
NiCrAlY/Al	R-7407	PWA 1422	1016	-0.08	Initially alumina spallation was less than that of the $\gamma/\gamma'-\delta$ bars coated with NiCrAlY/Al. Oxide blisters started forming and eventually localized coating failure occurred in the blistered region. Coating cracks were not visually observed.
NiCrAlY/Al	R-7418	PWA 1422	523	0.01	Moderate alumina spallation and some oxide blisters in the hot zone. Coating cracks were not visually observed.
NiCoCrAlY	R-7408	$\gamma/\gamma'-\delta$	1016	-0.04	Coating degradation mode in the hot zone changed from moderate alumina spallation to spinel formation. Thermal fatigue cracks are associated with coating defects.
NiCoCrAlY	R-7409	$\gamma/\gamma'-\delta$	1016	-0.15	Coating degradation mode in the hot zone changed from moderate alumina spallation to spinel formation. Thermal fatigue cracks were initially

TABLE XV (CONTINUED)

Coating System	Specimen Identification	Substrate	Time In Test (Hours)	Change in Erosion Bar Weight (Grams)	Comments
					associated with coating defects; eventually thermal fatigue cracks were initiated in nominally defect free coating. Localized oxidation failures were eventually initiated at thermal fatigue cracks.
NiCoCrAlY	R-7410	$\gamma/\gamma'-\delta$	493	0.03	Moderate spallation of alumina and some cracking associated with coating defects; specimen removed for metallographic examination.
NiCoCrAlY	R-7411	PWA 1422	1016	0.04	Generally adherent alumina scale and one coating crack associated with coating defect.
NiCoCrAlY	R-7419	PWA 1422	523	0.02	Generally adherent alumina scale and no coating cracking associated with coating defects.
NiCrAlY/Pt	R-7412	$\gamma/\gamma'-\delta$	1016	0.04	Generally adherent alumina scale with only minor spallation. Minor cracking associated with coating defects.
NiCrAlY/Pt	R-7413	$\gamma/\gamma'-\delta$	493	0.03	Generally adherent alumina scale and minor cracking associated with coating defects; specimen removed for metallographic examination.
NiCrAlY/Pt	R-7414	$\gamma/\gamma'-\delta$	1016	0.03	Moderate alumina spallation and minor cracking associated with coating defects.

TABLE XV (CONTINUED)

Coating System	Specimen Identification	Substrate	Time In Test (Hours)	Change in Erosion Bar Weight (Grams)	Comments
NiCrAlY/Pt	R-7415	PWA 1422	1016	0.06	Generally adherent alumina scale with only minor spallation and no cracking associated with coating defects. Very small oxide eruptions are now forming in the hot zone.
NiCrAlY/Pt	R-7420	PWA 1422	523	0.01	Moderate alumina spallation and no cracking associated with coating defects. Green oxide eruptions are now present in the hot zone.

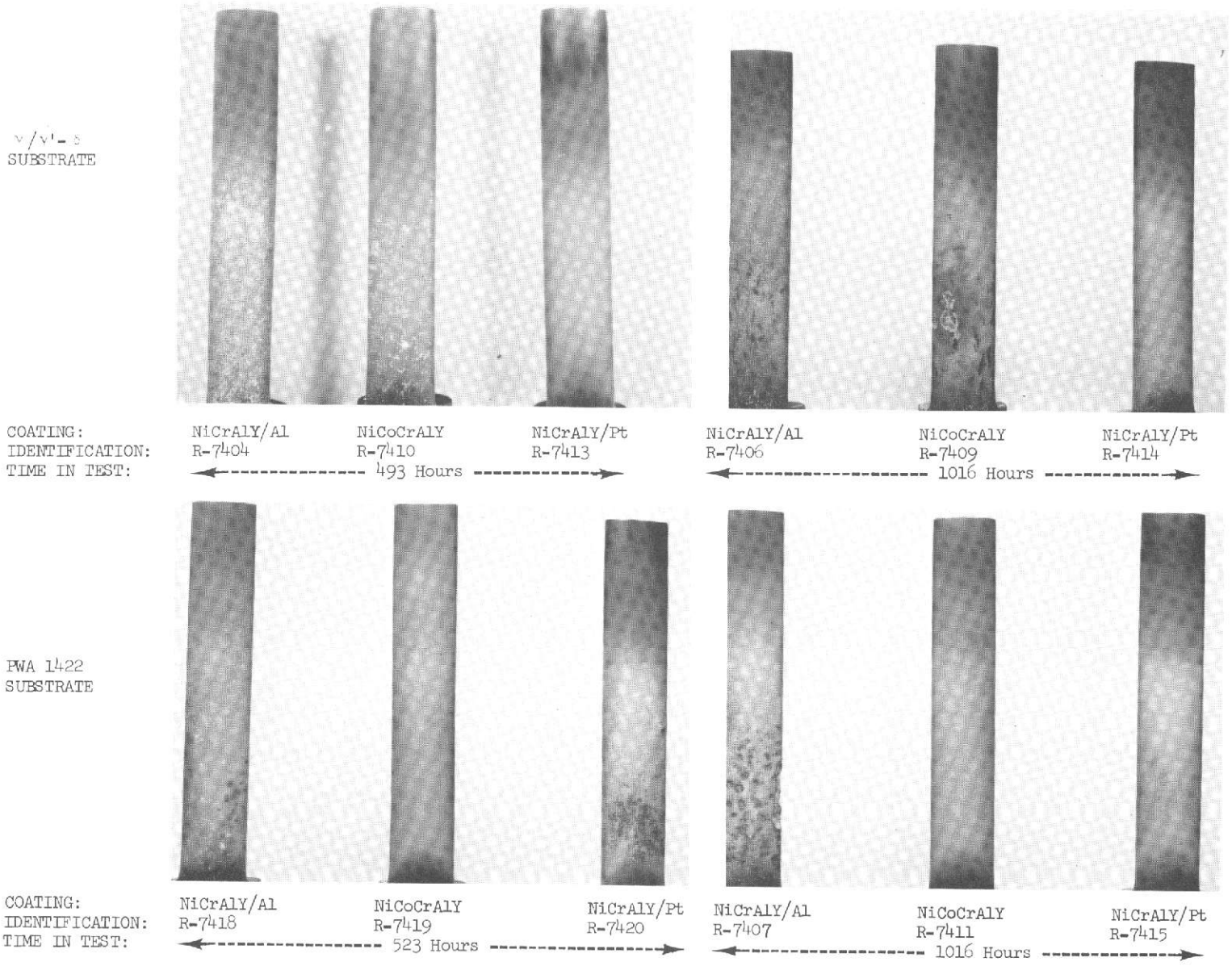

Figure 45 Appearance of Coated $\gamma/\gamma' - \delta$ (Top) and PWA 1422 (Bottom) Erosion Bars Which Were Metallographically Examined After Evaluation in the 1366°K (2000°F) Cyclic Oxidation Burner Rig Test for the Indicated Exposures. Note Excellent Condition of the NiCrAlY/Pt Coated $\gamma/\gamma' - \delta$ Specimen After 1016 Hours of Testing (Top, Right).

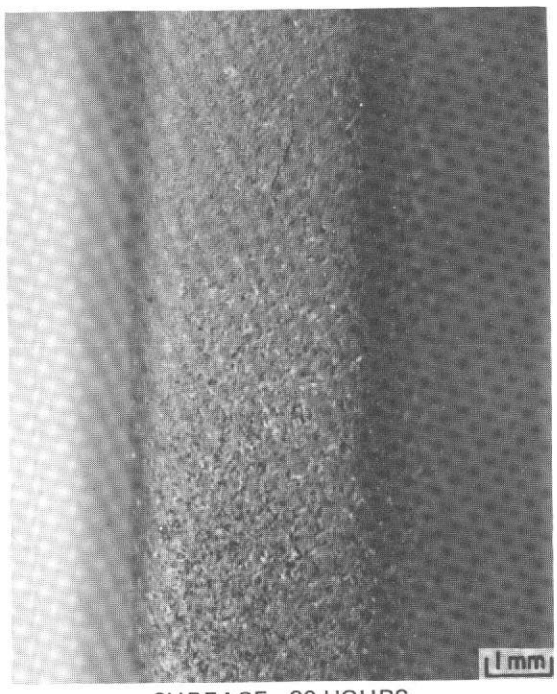

SURFACE, 89 HOURS

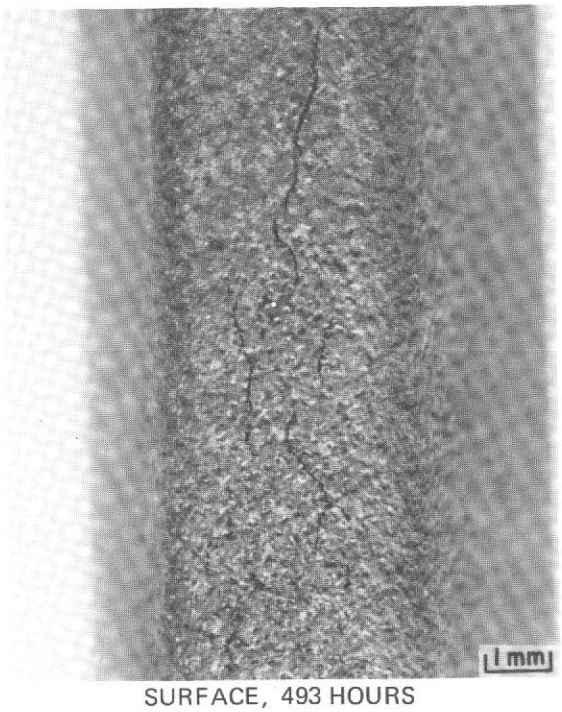

SURFACE, 493 HOURS

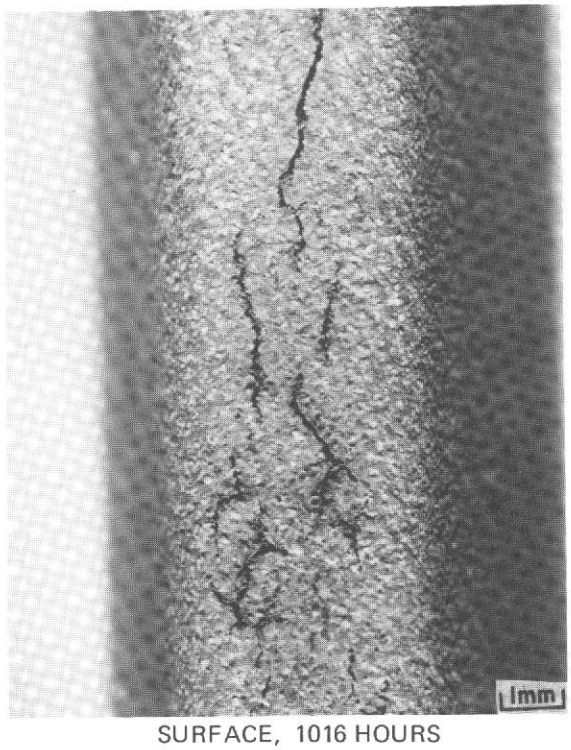

SURFACE, 1016 HOURS

CROSS SECTION, 1016 HOURS

Figure 46 Surface Appearance of Thermal Fatigue Cracks in the Leading Surface of NiCrAlY/Al Coated $\gamma/\gamma' - \delta$ Erosion Bar (R-7406) After 89, 493 and 1016 Hours of Testing in the Burner Rig 1366°K (2000°F) Cyclic Oxidation Test. Post-Test Examination of This Region Shows Crack Propagation into the $\gamma/\gamma' - \delta$ Substrate.

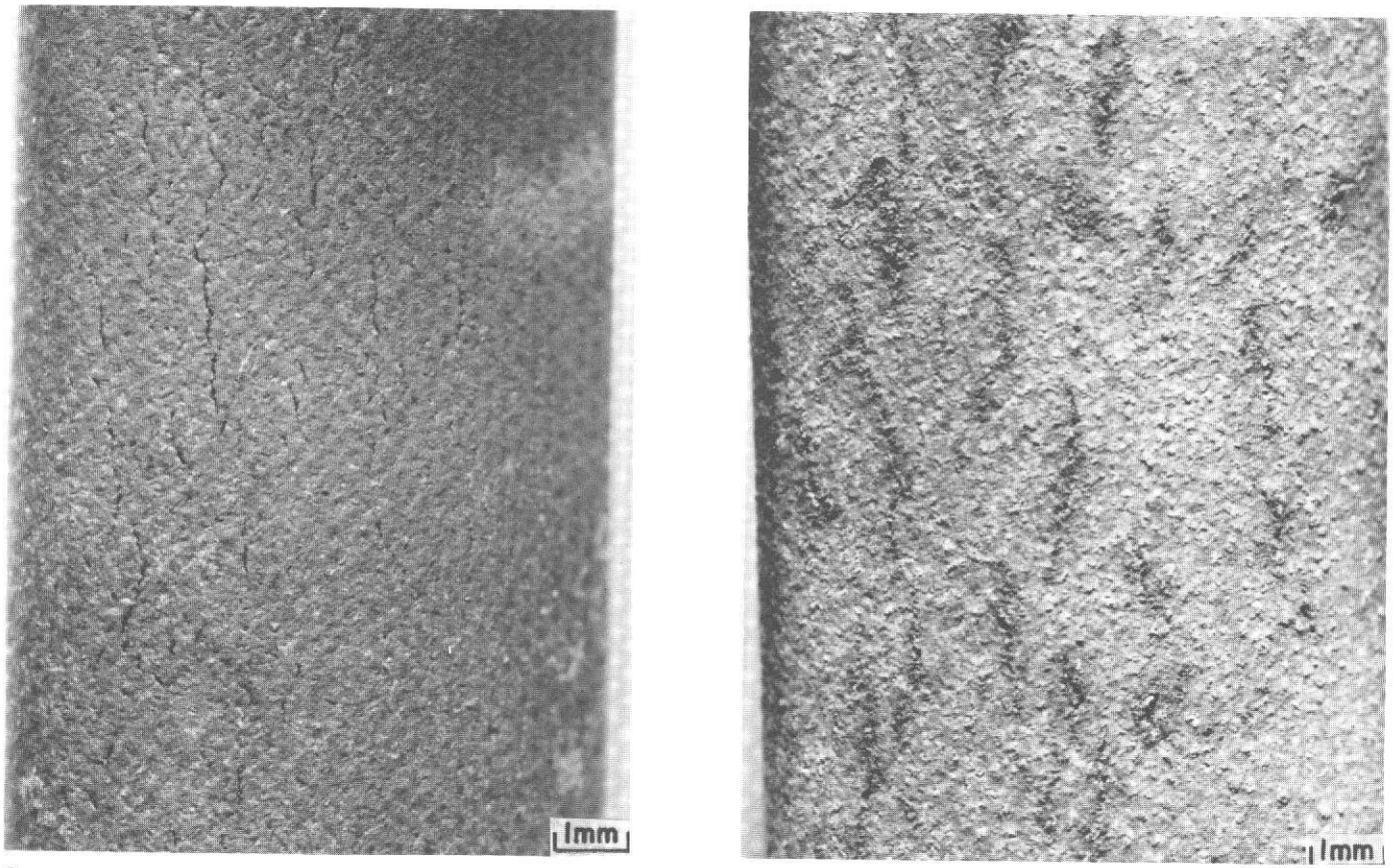

818 HOURS

1016 HOURS

Figure 47 Surface Appearance of Thermal Fatigue Cracks in the Trailing Surface of NiCrAlY/Al Coated $\gamma/\gamma' - \delta$ Erosion Bar (R-7406) After 818 (Left) and 1016 Hours (Right) of Testing in the Burner Rig 1366°K (2000°F) Cyclic Oxidation Test. Cracks Appear to be Developing into Localized Oxidation Failures. Post-Test Metallographic Examination of this Area (Figure 48) Indicated that the Coating Cracks Propagated into the $\gamma/\gamma' - \delta$ Substrate.

PRE-TEST

POST-TEST, "COLD" ZONE

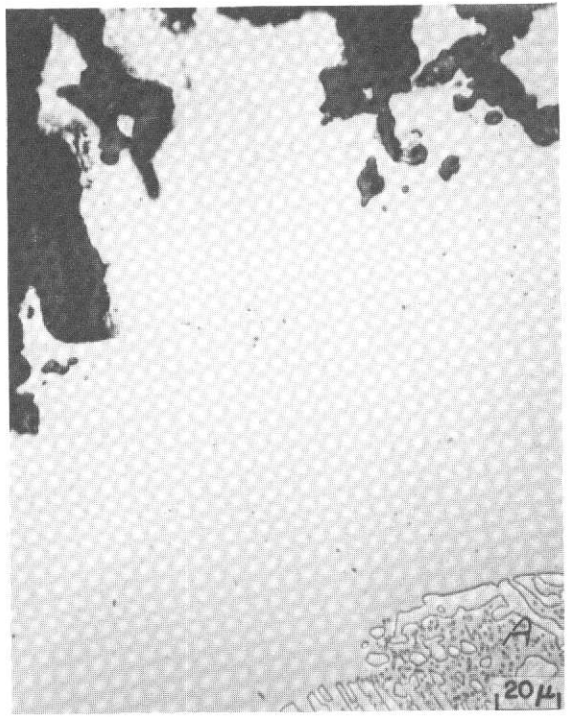

POST-TEST, HOT ZONE

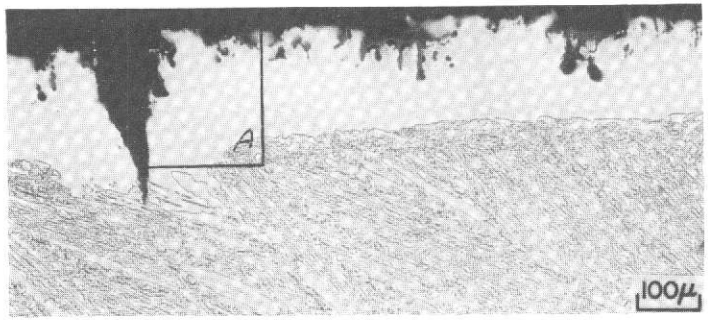

POST-TEST, HOT ZONE

Figure 48 Pre-Test and Post-Test Microstructures of Ni-17.2Cr-6.2Al-0.58Y (Overlay) + Al (Pack) Coated $\gamma/\gamma' - \delta$ Specimen (R-7406) Which was Tested for 1016 Hours in the Burner Rig 1366°K (2000°F) Cyclic Oxidation Test (Cycle: 55 Minutes Hot – 5 Minutes Forced Air Cool). Surface Appearance of Hot Zone Coating Cracks is Provided in Figure 47.

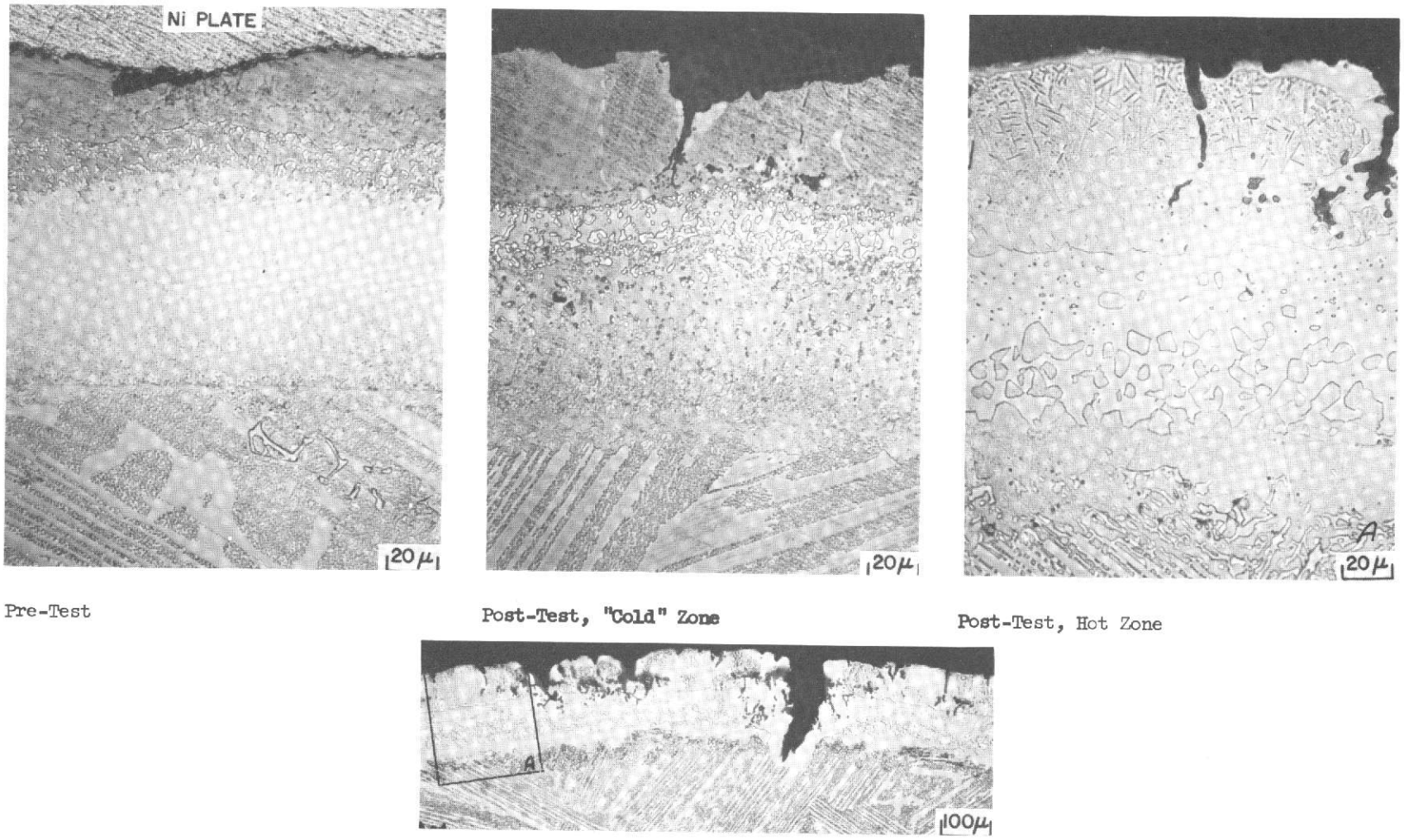

Pre-Test

Post-Test, "Cold" Zone

Post-Test, Hot Zone

Post-Test, Hot Zone

Figure 49 Pre-Test and Post-Test Microstructures of Ni-16.4Cr-5.9Al-0.72Y (Overlay) + Al (Pack) Coated $\gamma/\gamma' - \delta$ Specimen (R-7404) Which was Tested for 493 Hours in the Burner Rig 1366°K (2000°F) Cyclic Oxidation Test (Cycle:55 Minutes Hot – 5 Minutes Forced Air Cool). Alumina Particles from the Pack Which Were Incorporated Into the Coating During Aluminizing May Have Been Contributory to Crack Initiation.

Post-test examination showed that the hot zone blisters were associated with a depleted γ phase coating which contained extensive amounts of intergranular oxidation. The thicknesses of the diffusion affected PWA 1422 substrate layers in the NiCrAlY/Al coated specimens after 523 and 1016 hours of testing were 101.6 and 152.4μ (4.0 and 6.0 mils) respectively.

NiCoCrAlY

Visual inspection of the NiCoCrAlY coated $\gamma / \gamma' - \delta$ specimens indicated that the alumina scales repeatedly spalled and reformed during the initial portion of the burner rig 1366°K (2000°F) cyclic oxidation test. It can be seen in Figure 45 that the comparative spallation rate after 493 hours of testing was moderate relative to the NiCrAlY/Al system. Eventually, the hot zones of the NiCoCrAlY coated $\gamma/\gamma' - \delta$ specimens exhibited localized areas of spinel formation which was first observed after approximately 400 hours. In contrast, visual appearances of the NiCoCrAlY coatings on the PWA 1422 specimens were excellent after 523 and 1016 hours (see Figure 45). Alumina scale adherence was significantly better than on $\gamma/\gamma'-\delta$ and significant amounts of spinel formation were not observed.

Thermal fatigue cracks were also observed for the NiCoCrAlY coatings on $\gamma/\gamma' - \delta$. These cracks initially originated predominately at coating imperfections. However, some cracks were initiated in defect-free coating after approximately 658 hours. Relatively severe cracking was present in the hot zone of specimen R-7409 which was tested for 1016 hours; examples of thermal fatigue cracking in the leading surface (Figure 50) and trailing surface (Figures 51 and 52) are shown. The crack shown in cross-section in Figure 50 had propagated a distance of several hundred microns into the substrate. Some of the thermal fatigue cracks in the trailing surface eventually developed into localized oxidation failures (Figures 51 and 52). In contrast, thermal fatigue cracking in the NiCoCrAlY coated PWA 1422 specimen (R-7411) which was evaluated for 1016 hours was minimal. Post-test metallographic examination indicated that PWA 1422 substrate porosity may have contributed to initiation of the only crack which was observed.

Metallographic examination of the NiCoCrAlY coated $\gamma/\gamma'-\delta$ specimen (R-7410) which was removed from test after 493 hours revealed that the hot zone still contained a significant amount of the aluminum rich β phase (Figure 53). In addition, moderate amounts of γ' were also observed. While $\gamma'(Ni_3Al)$ is not a principal phase in the virgin coating, this phase is formed at the expense of the β phase as aluminum is depleted from the coating. The thickness of the diffusion-affected substrate layer in the hot zone was approximately 96.5μ (3.8 mils).

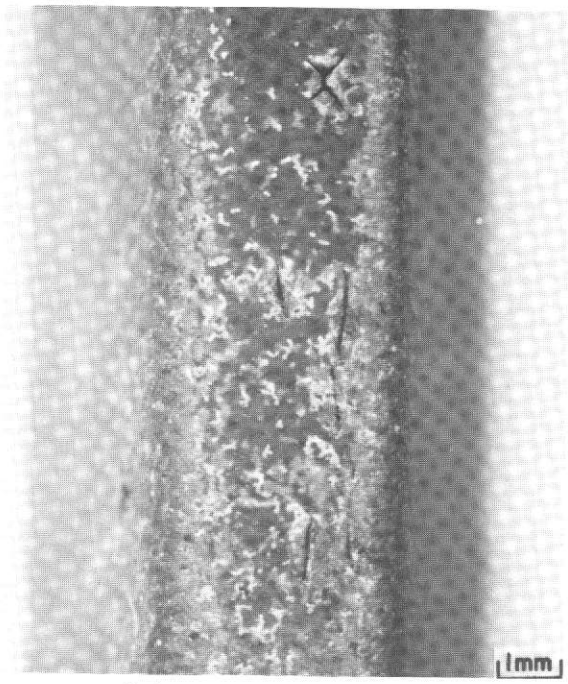

SURFACE, 818 HOURS

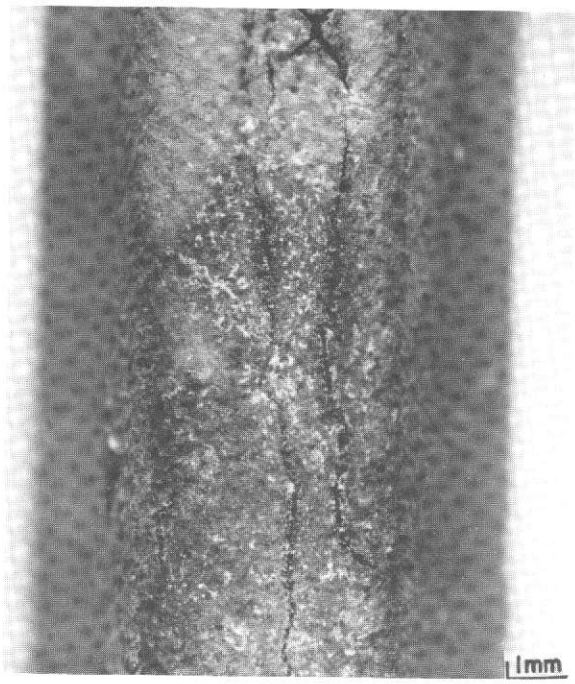

SURFACE, 1016 HOURS

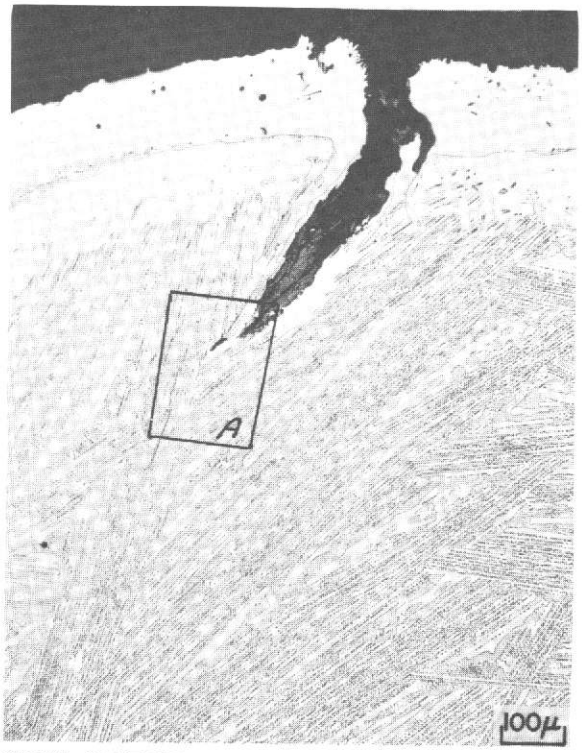

CROSS SECTION

Figure 50 Surface Appearance of Thermal Fatigue Cracks in the Leading Surface of NiCoCrAlY Coated $\gamma/\gamma' - \delta$ Erosion Bar (R-7409) After 818 and 1016 Hours (Top) of Testing in the Burner Rig 1366°K (2000°F) Cyclic Oxidation Test. Post-Test Examination of this Region Shows Crack Propagation into the $\gamma/\gamma' - \delta$ Substrate (Bottom).

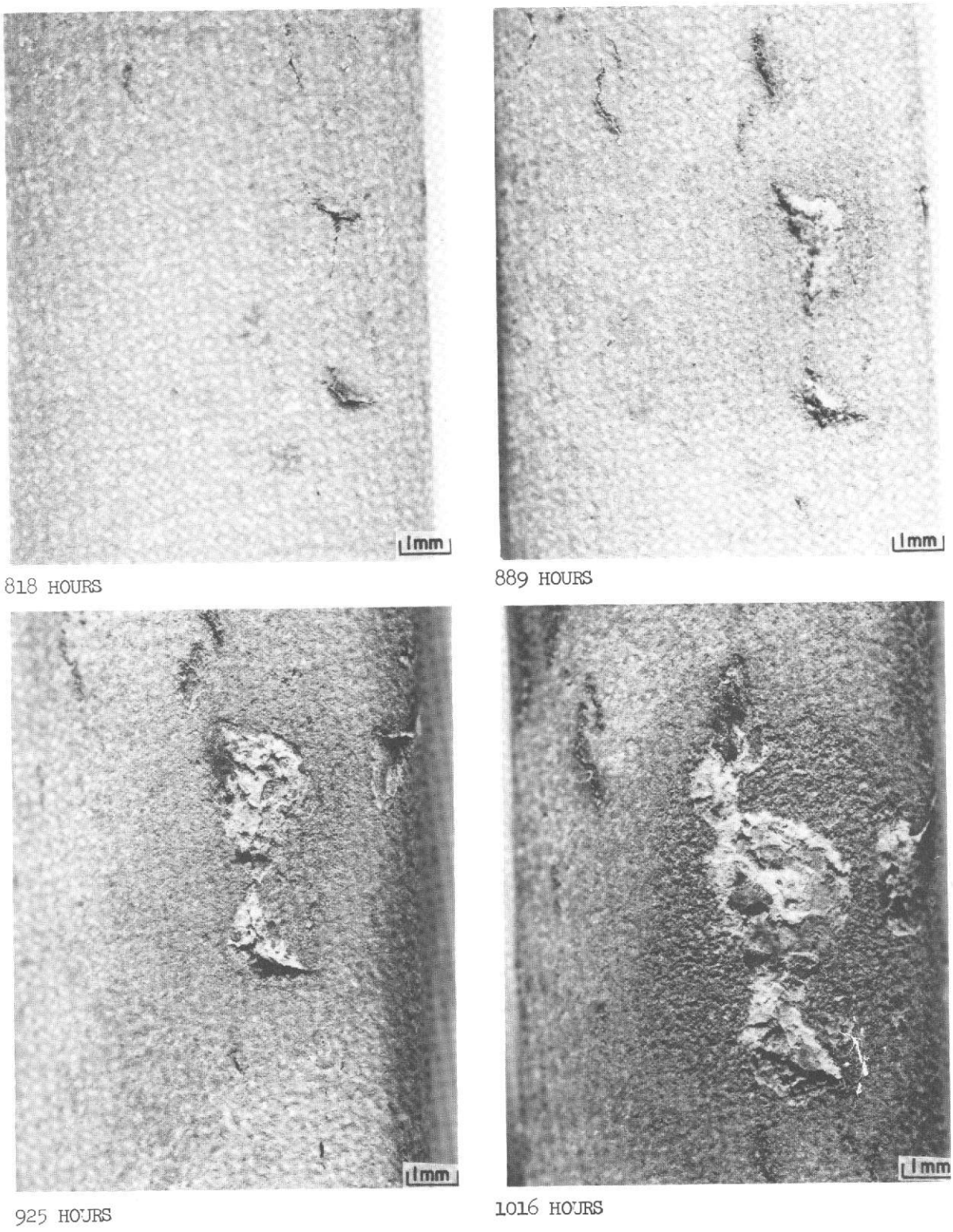

Figure 51 Surface Appearance of Thermal Fatigue Cracks in the Trailing Surface of NiCoCrAlY Coated $\gamma/\gamma' - \delta$ Erosion Bar (R-7409) After Indicated Time in the Burner Rig 1366°K (2000°F) Cyclic Oxidation Test. Localized Oxidation Failures of the Coating Were Initiated at the Thermal Fatigue Cracks.

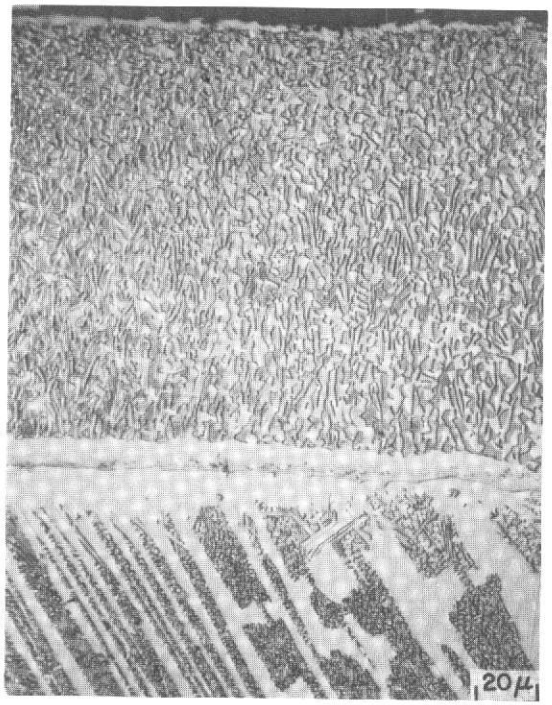

PRE-TEST

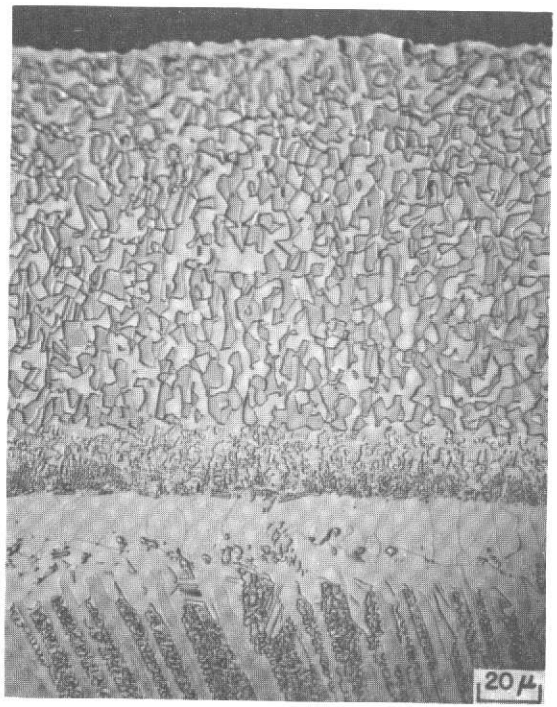

POST-TEST, "COLD" ZONE

POST-TEST, HOT ZONE

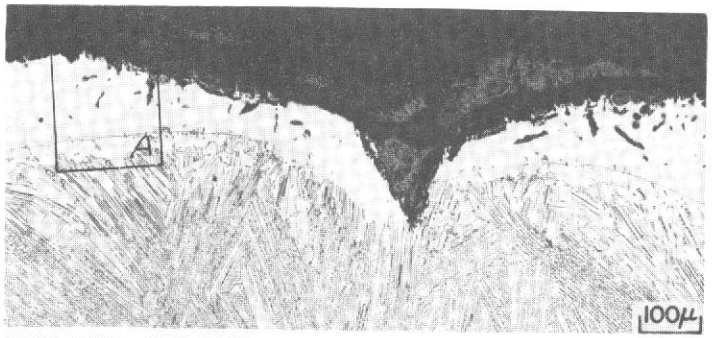

POST-TEST, HOT ZONE

Figure 52 Pre-Test and Post-Test Microstructures of Ni-21.7Co-18.5Cr-12.2Al-0.20Y Coated $\gamma/\gamma' - \delta$ Specimen (R-7409) Which Was Tested for 1016 Hours in the Burner Rig 1366°K (2000°F) Cyclic Oxidation Test (Cycle: 55 Minutes Hot – 5 Minutes Forced Air Cool). Thermal Fatigue Cracks in the Coating Contributed to the Local Oxidation Failure .

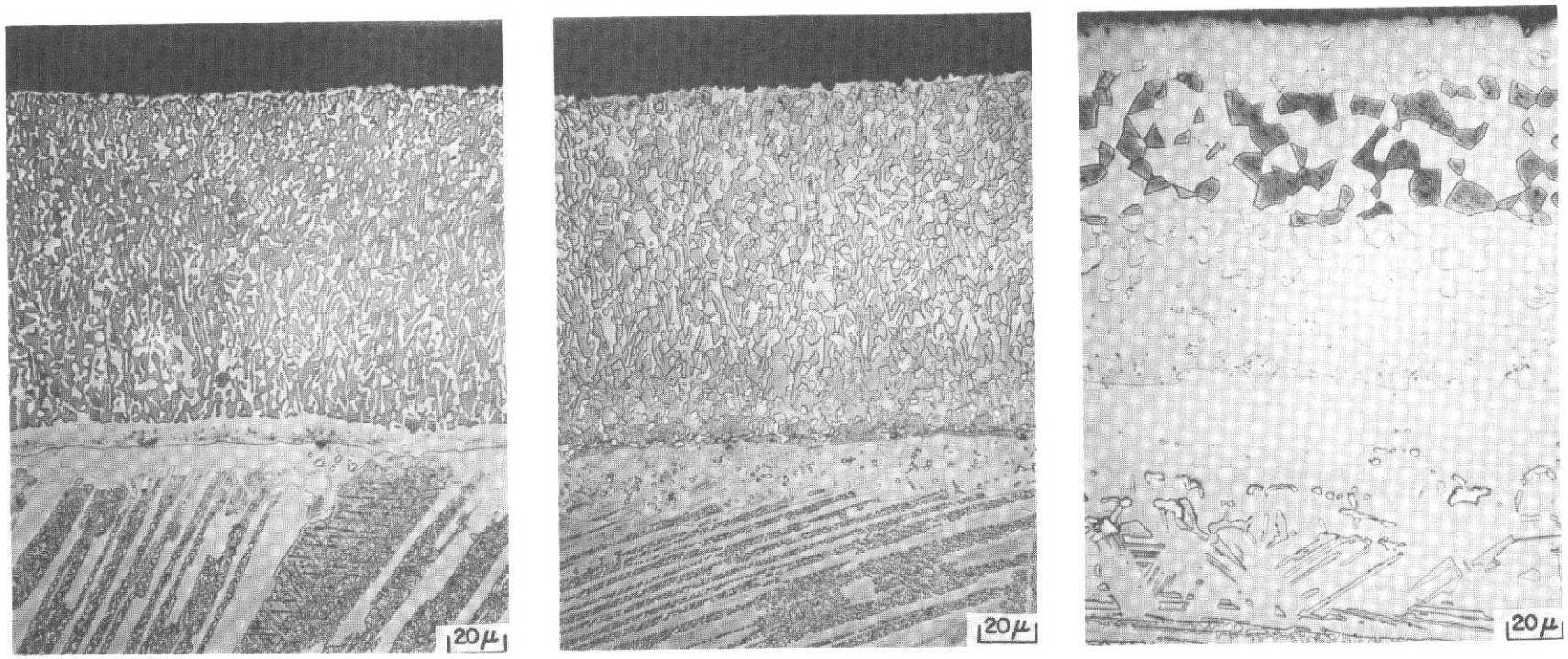

Pre-Test

Post-Test, "Cold" Zone

Post-Test, Hot Zone

Figure 53 Pre-Test and Post-Test Microstructures of Ni-21.7Co-18.5Cr-12.2Al-0.20Y Coated $\gamma/\gamma' - \delta$ Specimen (R-7410) Which Was Tested for 493 Hours in the Burner Rig 1366°K (2000°F) Cyclic Oxidation Test (Cycle: 55 Minutes Hot – 5 Minutes Forced Air Cool).

Examination of the NiCoCrAlY coating on γ/γ'- δ specimen (R-7410) also revealed that the β phase was locally depleted adjacent to thermal fatigue cracks (Figures 54 and 55). (Since lower aluminum contents tend to increase the ductility of NiCoCrAlY coatings, it is speculated that a slightly increased rate of localized coating degradation around a coating defect might deter crack initiation and/or propagation.) The thermal fatigue crack which is shown in Figure 55 is propagating intergranularly into the substrate. It appears that the highly cellular condition of the γ/γ'- δ microstructure and porosity which was associated with the cellular regions in these erosion bars may have contributed to a majority of the coating "defects" which were oriented parallel to the eutectic alloy solidification direction; this observation will be elaborated upon later. The hot zone microstructure of the NiCoCrAlY coated γ/γ'- δ specimen (R-7409) was γ (Ni solid solution) phase. A band of γ'(Ni_3Al) phase was present in the diffusion affected substrate region; however, in the vicinity of the local coating failure, the γ' layer had been consumed (see Figure 52). The average thickness of the diffusion affected substrate zone was approximately 152.4μ (6.0 mils).

Although the hot zone microstructures of the NiCoCrAlY coated PWA 1422 specimens were also predominantly γ phase, some differences were observed. An extensive network of oxide stringers was present in the outer portion of these coatings (see Figure 56); these oxide stringers appeared to be attached to the external alumina scale. It is speculated that this stringer network may have inhibited the spallation of the alumina scale. A layer of prosity is also present in the coating just above the original interface between the NiCoCrAlY and PWA 1422 substrate; the porosity is related to the presence of residual columnar defects which were present in the fully processed pre-test coating. In addition, the diffusion affected PWA 1422 did not contain a continuous band of the γ' phase. The average thicknesses of the diffusion affected substrate zones of specimens R-7419 (NiCoCrAlY/PWA 1422; 523 hours) and R-7411 (NiCoCrAlY/PWA 1422; 1016 hours) were approximately 71.1 and 88.9μ (2.8 and 3.5 mils), respectively.

NiCrAlY/Pt

It can be seen in Figure 45 that the NiCrAlY/Pt coating provided excellent protection for γ/γ'- δ and good protection for PWA 1422 specimens. Alumina scale spallation could be characterized as minor to moderate when compared with the NiCrAlY/Al and NiCoCrAlY coating systems. Small oxide blisters eventually formed in the hot zones of the PWA 1422 specimens. This effect was more pronounced on the specimen (R-7420) which was only tested for 523 hours; the high time (1016 hours) NiCrAlY/Pt coated PWA 1422 specimen showed less degradation. Comparison of the pre-test microstructures indicates no apparent reason for the difference in behavior for these two specimens.

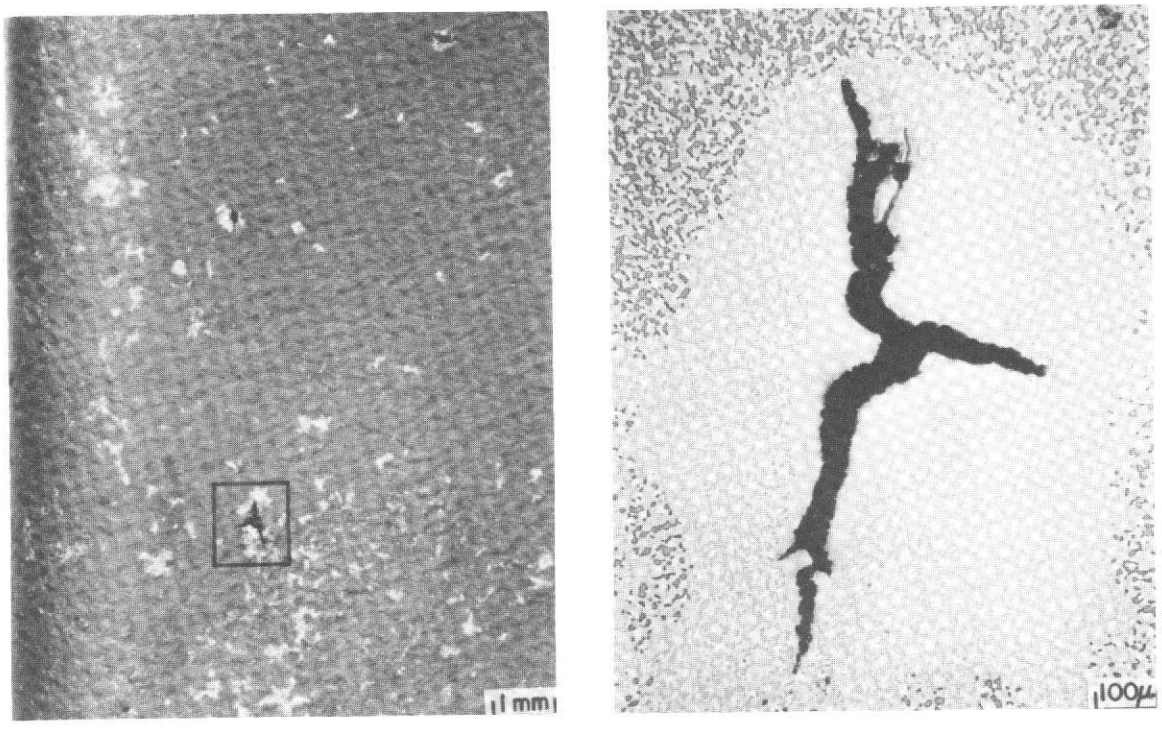

Figure 54 Surface Photograph (Left) and Planar Section (Right) Through Thermal Fatigue Crack Which Initiated at a Small Coating Pit. Note the Depletion Zone Which Surrounds the Crack. This Ni-21.7Co-18.5Cr-12.2Al-0.20Y Coated $\gamma/\gamma'-\delta$ Specimen (R-7410) was Evaluated for 493 Hours in the Burner Rig 1366°K (2000°F) Cyclic Oxidation Test (Cycle: 55 Minutes Hot - 5 Minutes Forced Air Cool).

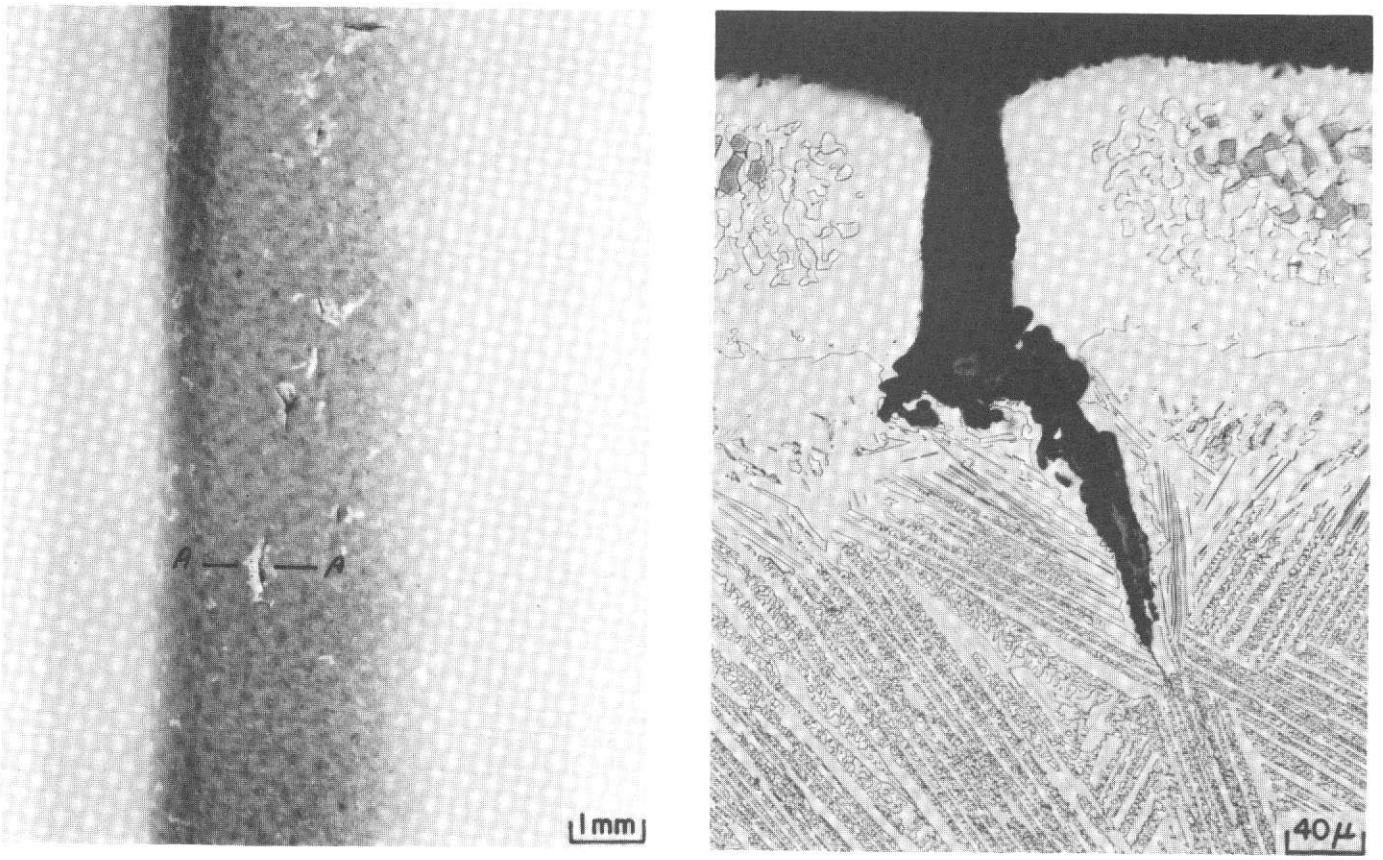

A-A

Figure 55 Surface Photograph (Left) and Cross-Section (Right) Through Thermal Fatigue Crack Which Initiated at a Small Depression in the Ni-21.7Co-18.5Cr-12.2Al-0.20Y Coated $\gamma/\gamma' - \delta$ Specimen (R-7410). Note That Crack Propagation Into the Substrate is Intergranular. This Specimen Was Evaluated for 493 Hours in the Burner Rig 1366°K (2000°F) Cyclic Oxidation Test (Cycle: 55 Minutes Hot - 5 Minutes Forced Air Cool).

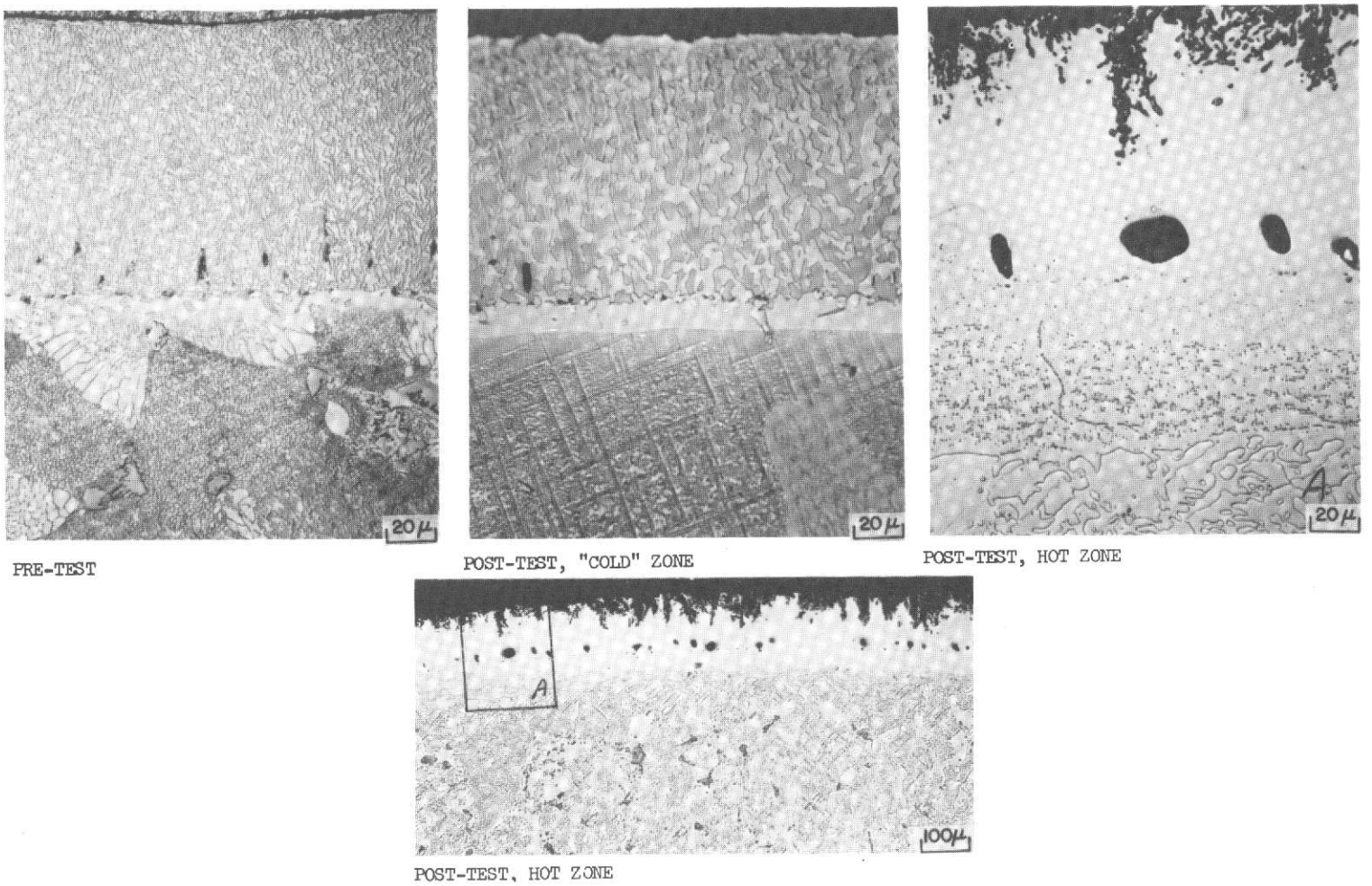

Figure 56 Pre-Test and Post-Test Microstructures of Ni-22.5Co-19.7Cr-12.1Al-0.10Y Coated PWA 1422 Specimen (R-7411) Which was Tested for 1016 Hours in the Burner Rig 1366°K (2000°F) Cyclic Oxidation Test (Cycle: 55 Minutes Hot - 5 Minutes Forced Air Cool). Oxide Stringers in Outer Portion of the Coating May Have Contributed to Good Oxide Adherence. Porosity in the Inner Portion of the Hot Zone Coating is Believed to Initiate From Residual Columnar Defects in the As-Deposited Coating Which Were Not Eliminated During Post-Coating Processing as Shown in the Pre-Test and Post-Test "Cold" Zone Microstructures.

Thermal fatigue cracking was minimal in the NiCrAlY/Pt coated γ/γ'-δ specimens and absent in the NiCrAlY/Pt coated PWA 1422 specimens. The largest thermal fatigue crack observed in a NiCrAlY/Pt coated γ/γ'-δ specimen (R-7414) is shown in Figure 57. Post-test metallography indiciated that the crack had not propagated through the diffusion affected substrate layer.

Metallographic examination of NiCrAlY/Pt coated γ/γ'-δ specimen R-7413 which was removed from test after 493 hours indicated that the NiCrAlY layer of the coating in the specimen hot zone had been depleted of the aluminum-rich β (NiAl) phase and consisted predominately of γ'(Ni_3Al) and γ (Ni solid solution) phases (Figure 58). The NiCrAlY layer of the coating in the relatively "cold" zone of the specimen appeared to have transformed from the high temperature β, γ', γ microstructure to the lower temperature γ', α (chromium) microstructure. The platinum-rich surface layer etches similar to the β(NiAl) phase of the NiCrAlY layer in the pre-test microstructure; post-test examination of the hot zone revealed that this layer etched similar to the γ' phase of the NiCrAlY layer after 493 hours of exposure.

Electron microprobe analysis was performed on the hot zone microstructures of NiCrAlY/Pt coated γ/γ'-δ specimens R-7413 and R-7414, which were evaluated in the burner rig 1366°K (2000°F) cyclic oxidation test for 493 and 1016 hours, respectively. Photomicrographs of the hot zones of these coatings are provided in Figure 59. Relative intensities of the characteristic x-rays for Ni, Cr, Al, Y, Pt and Cb were obtained for both specimens and are presented in Figures 60 and 61. The intensities show the changes in elemental composition from the alloy through the coating but not their absolute concentrations.

Examination of the photomicrograph and x-ray intensity data (Figures 59a and 60) for the NiCrAlY/Pt coated γ/γ'-δ specimen R-7413, which was tested for 493 hours, indicates that platinum from the sputtered surface layer is distributed throughout the coating and diffusion affected substrate zone. The outer portion of the coating, which was originally the platinum-rich surface layer, appears to be predominately γ' (Ni_3Al solid solution) phase and dispersed oxide particles. (Oxide particles were present in this layer in the virgin coating.) Adjacent to this layer, the aluminum content was somewhat lower and the coating was predominantly a γ(nickel solid solution) phase with some particles of the γ' phase. Near the original coating-substrate interface, which was marked by a fine line of oxide particles, the aluminum content increased and the γ' phase became continuous; the band of γ' includes the inner portion of the coating and the outer portion of the diffusion affected substrate zone. The composition (in weight percent) of the γ' band in the diffusion affected substrate zone was determined to be approximately 73.8Ni-4.4Cr-7.8Al-4.8Cb-9.2Pt. In the portion of the diffusion affected substrate which is adjacent to the unaffected substrate, the columbium-rich δ(Ni_3Cb) phase has dissolved. A new phase, which is columbium-rich, has formed and is assumed to be a carbide.

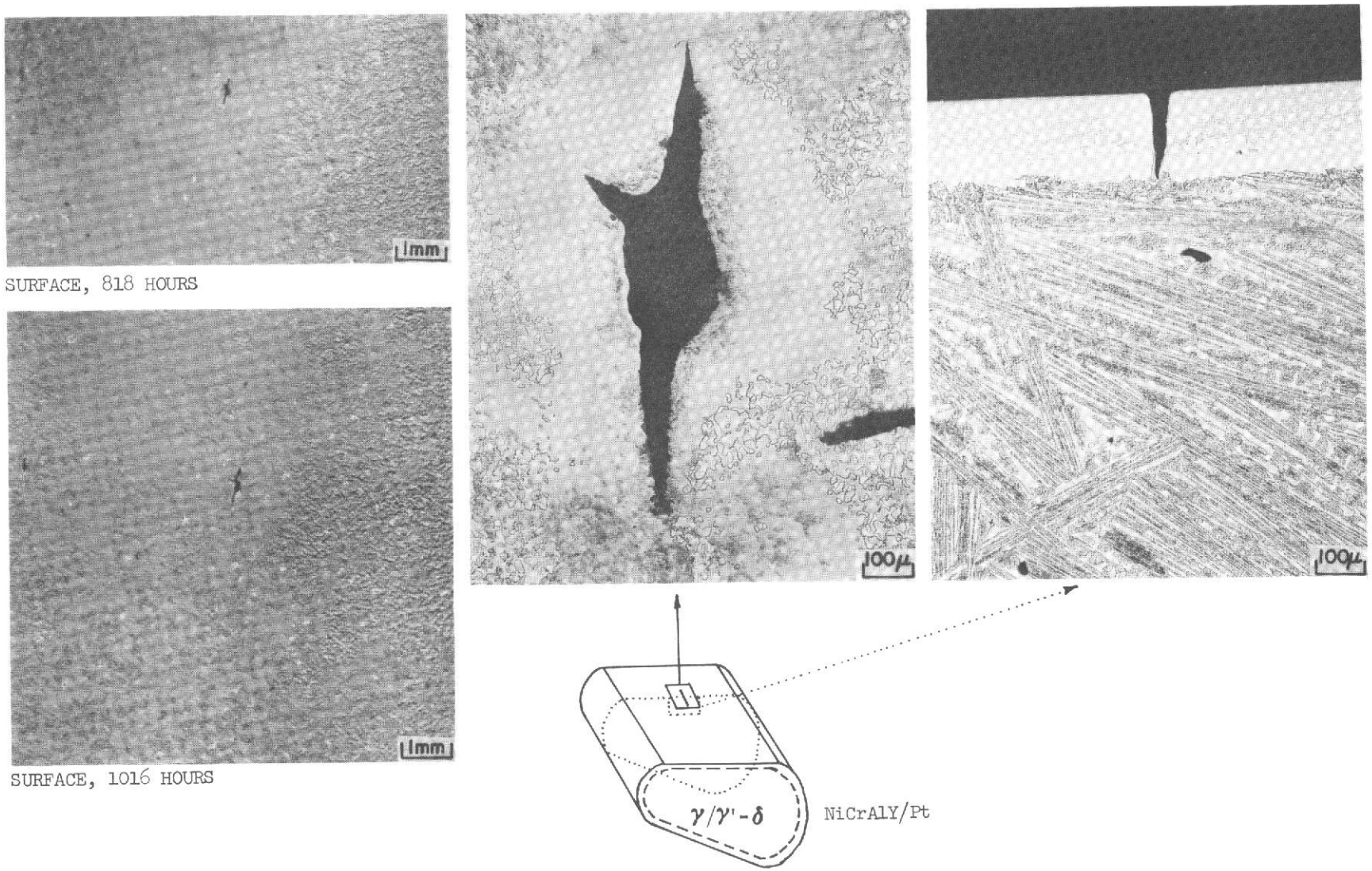

Figure 57 Surface Appearance (left) of the Largest Thermal Fatigue Crack (Which Initiated at a Coating Pit) in NiCrAlY/Pt Coated γ/γ'-δ Erosion Bar (R-7414) Which Was Evaluated for 1016 Hours in the Burner Rig 1366°K (2000°F) Cyclic Oxidation Test. Post-Test Planar (Center) and Cross Section (Right) Microstructures Indicate That the Coating is Locally depleted Adjacent to the Crack and That the Crack had not Propagated Through The Diffusion Affected Substrate Layer

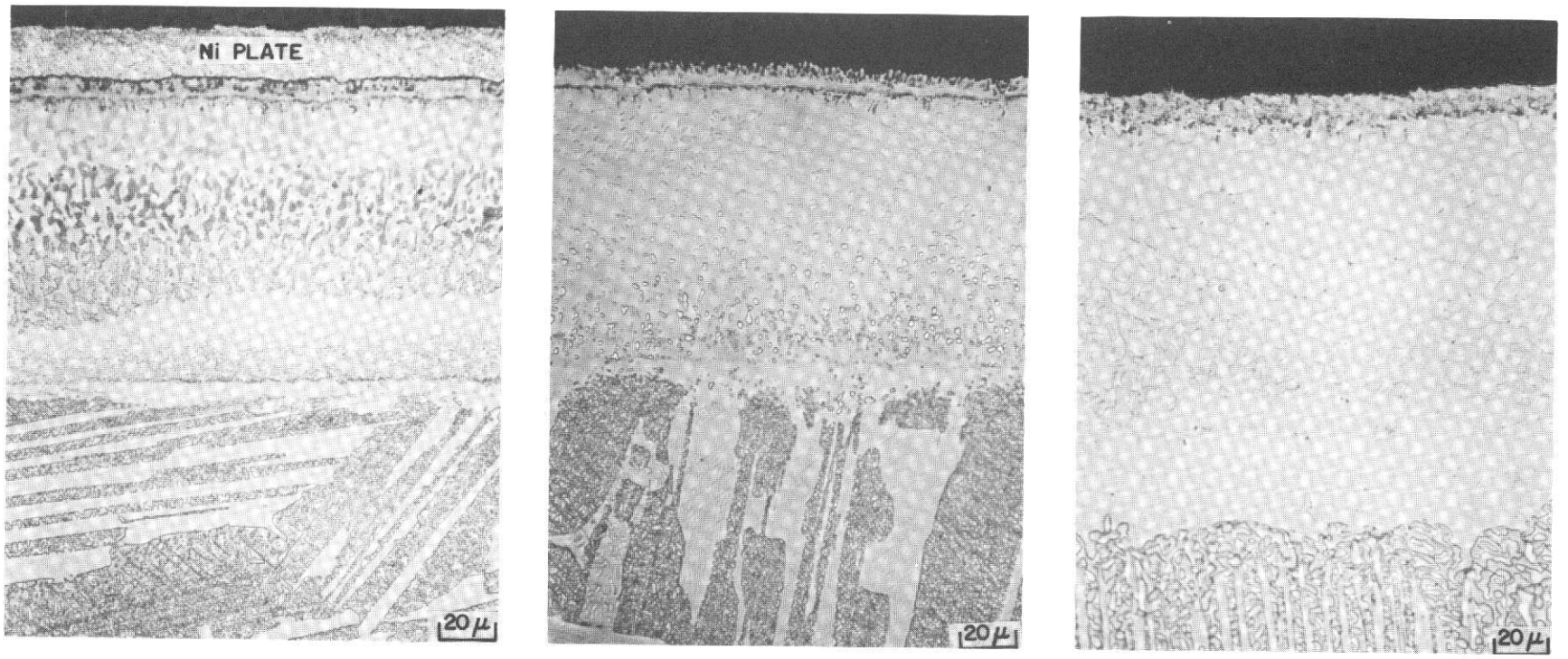

Pre-Test

Post-Test, "Cold" Zone

Post-Test, Hot Zone

Figure 58 Pre-test and Post-Test Microstructures of Ni-19.2Cr-11.8Al-0.35Y (Overlay) + Pt (Sputter) Coated γ/γ'-δ Specimen (R-7413) Which was Tested for 493 Hours in the Burner Rig 1366°K (2000°F) Cyclic Oxidation Test (Cycle: 55 Minutes hot - 5 Minutes forced air cool).

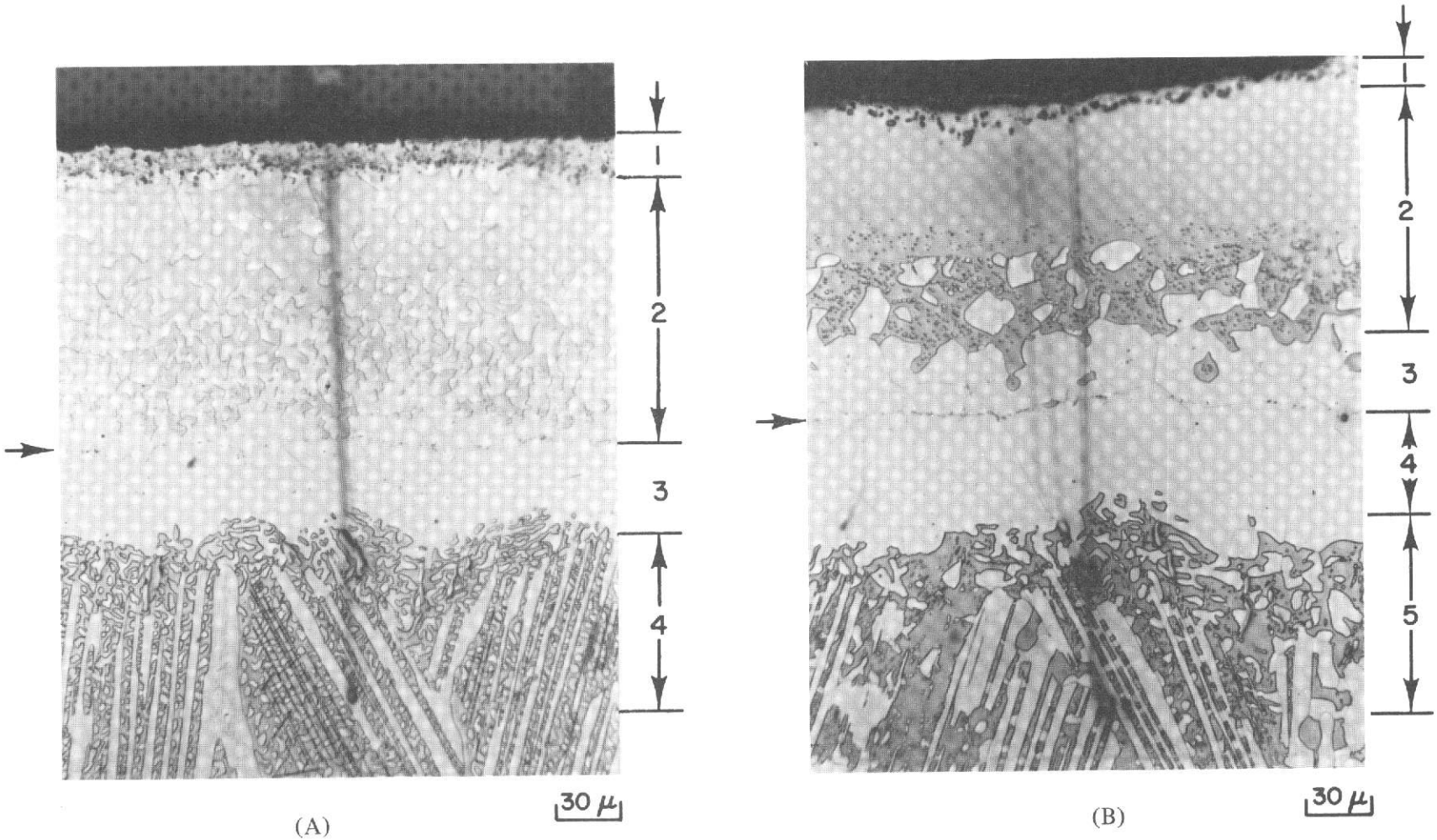

Figure 59 Hot Zone Microstructures of NiCrAlY/Pt Coated γ/γ'-δ Specimens R-7413 (a) and R-7414 (b) Which Were Evaluated in the Burner Rig 1366°K (2000°F) Cyclic Oxidation Test for 493 and 1016 Hours, Respectively. Arrows indicate locations of original coating-substrate interface.

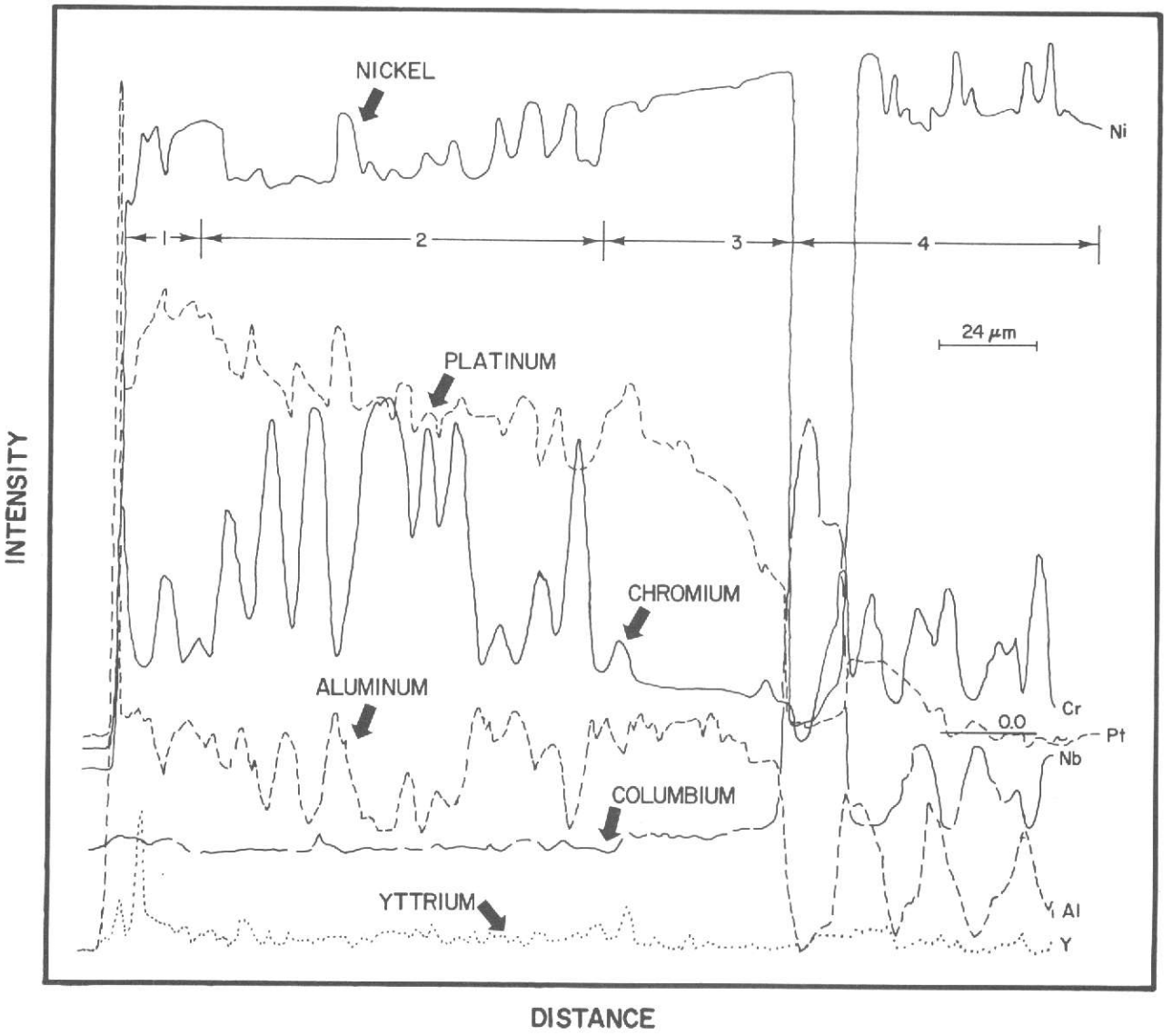

Figure 60 Relative Ni, Pt, Cr, Al, Cb and Y X-Ray Intensities for NiCrAlY/Pt Coated γ/γ'-δ Specimen R-7413 Which Was Evaluated for 493 Hours in the Burner Rig 1366°K (2000°F) Cyclic Oxidation Test. (See Figure 59a For Hot Zone Microstructure.)

The NiCrAlY/Pt coated $\gamma/\gamma'-\delta$ specimen, which was evaluated for 1016 hours in the 1366°K (2000°F) cyclic oxidation test, exhibited more depletion in the outer half of the coating; only the γ (nickel solid solution) phase was present in this layer (see Figure 59b). The composition (in weight percent) of this γ phase region was determined to be approximately 71.5Ni-15.1Cr-4.4Al-1.2Cb-7.8Pt. The platinum gradient was also relatively flat in the γ phase region (see Figure 61). Although the outer portion of the coating was more depleted, the band of γ' (Ni_3Al solid solution) phase, which includes the inner part of the coating and the outer portion of the diffusion affected substrate zone, was thicker. The thickness of the γ' layer suggests that aluminum diffusion into the substrate may be a primary coating degradation mechanism. The composition of the γ' region was determined to be approximately 75.8Ni-3.9Cr-7.6Al-6.3Cb-6.4Pt; the chemistry is not significantly different from that of the γ' layer in the specimen which was tested for 493 hours.

External surfaces of both samples were rich in aluminum which reflects the presence of an alumina scale. The region also had a relatively high yttrium content.

Post-test microstructures ofthe NiCrAlY/Pt coatings on PWA 1422 substrates were similar to those of NiCrAlY/Pt coatings on $\gamma/\gamma'-\delta$; however a few differences were noted. Oxide stringers (which have a similar morphology to those observed in the NiCoCrAlY coatings on PWA 1422) were present in the outer γ phase portion of the coating and oxide blisters were causing small localized coating failures. The average thicknesses of the diffusion affected substrate zones of specimens R-7413 (NiCrAlY/Pt coated $\gamma/\gamma'-\delta$; 493 hours), R-7414 (NiCrAlY/Pt coated $\gamma/\gamma'-\delta$; 1016 hours), R-7420 (NiCrAlY/Pt coated PWA 1422; 523 hours) and R-7415 (NiCrAlY/Pt coated PWA 1422; 1016 hours) were approximately 76.2, 139.7, 101.6 and 101.6 microns (3.0, 5.5, 4.0 and 4.0 mils), respectively.

C. DISCUSSION OF BURNER RIG RESULTS AND SELECTION OF COATING FOR MECHANICAL PROPERTY EVALUATION

Extensive prior experience in burner rig testing of numerous alloy/coating systems has not shown thermal fatigue cracking to be a significant factor in coating performance evaluations of this type. In this regard, the behavior of the $\gamma/\gamma'-\delta$ alloy in the burner rig evaluation was unique since the same coating systems on the PWA 1422 alloy exhibited very little or no thermal fatigue cracking. Consideration of several factors may be helpful in interpreting this behavior for the $\gamma/\gamma'-\delta$ alloy.

To determine if the pre-coating surface quality of the $\gamma/\gamma'-\delta$ substrate may have contributed to the formation of significantly more coating defects in overlay coatings on the $\gamma/\gamma'-\delta$ substrate compared with the PWA 1422 substrate, pre-test coating microstructures were reviewed. It was observed that exposed substrate porosity, which was associated with the highly cellular $\gamma/\gamma'-\delta$ microstructure, resulted in defects in the as-deposited overlay coating microstructures which were not eliminated by post-coating processing; examples are shown in Figure 62. Since the porosity tends to be somewhat elongated parallel to the solidification direction, it is speculated that most of the cracks oriented

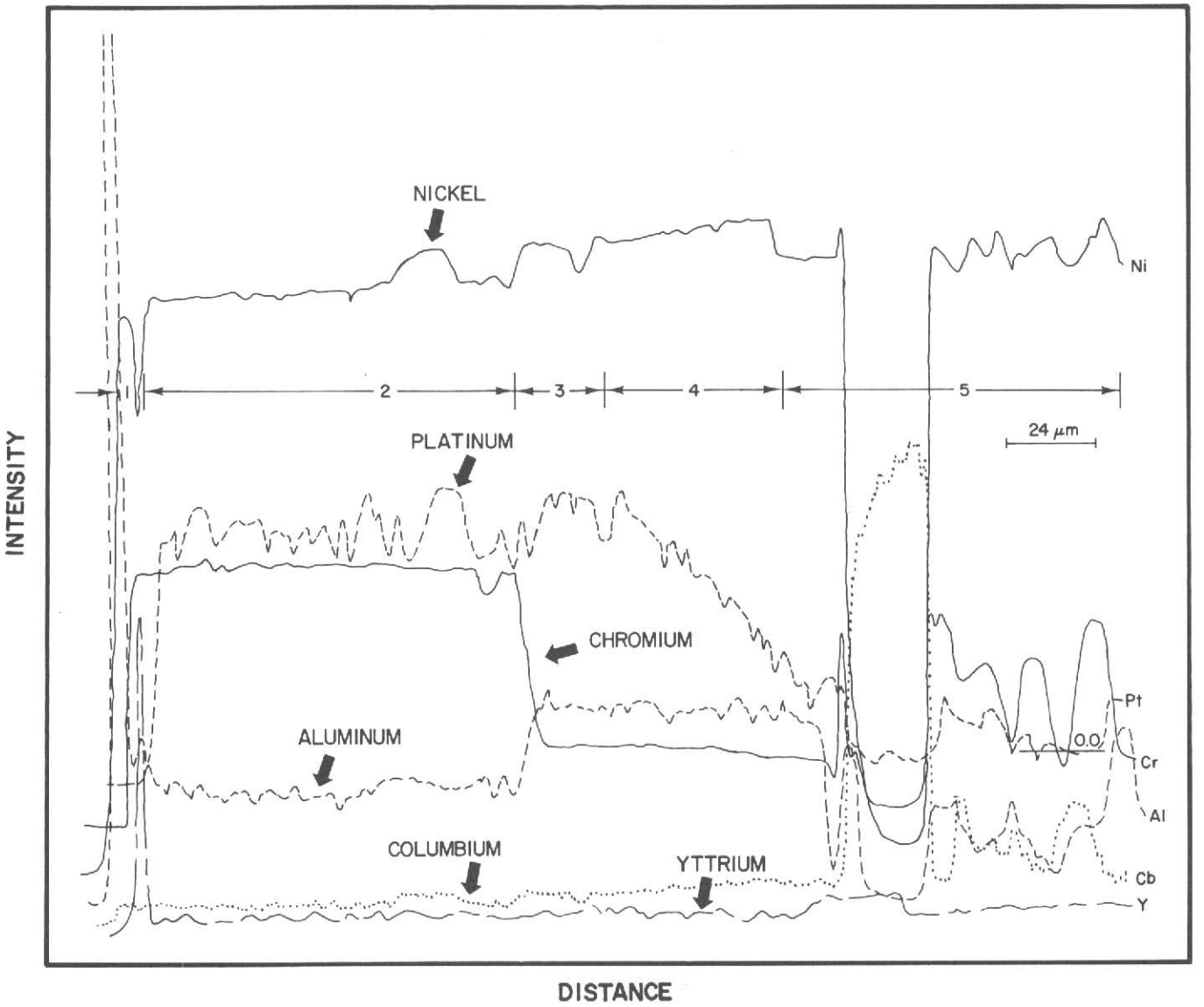

Figure 61 Relative Ni, Pt, Cr, Al, Cb, and Y X-Ray Intensities for NiCrAlY/Pt Coated γ/γ'-δ Specimen R-7414 Which Was Evaluated for 1016 Hours in the Burner Rig 1366°K (2000°F) Cyclic Oxidation Test. (See Figure 59b For Hot Zone Microstructure.)

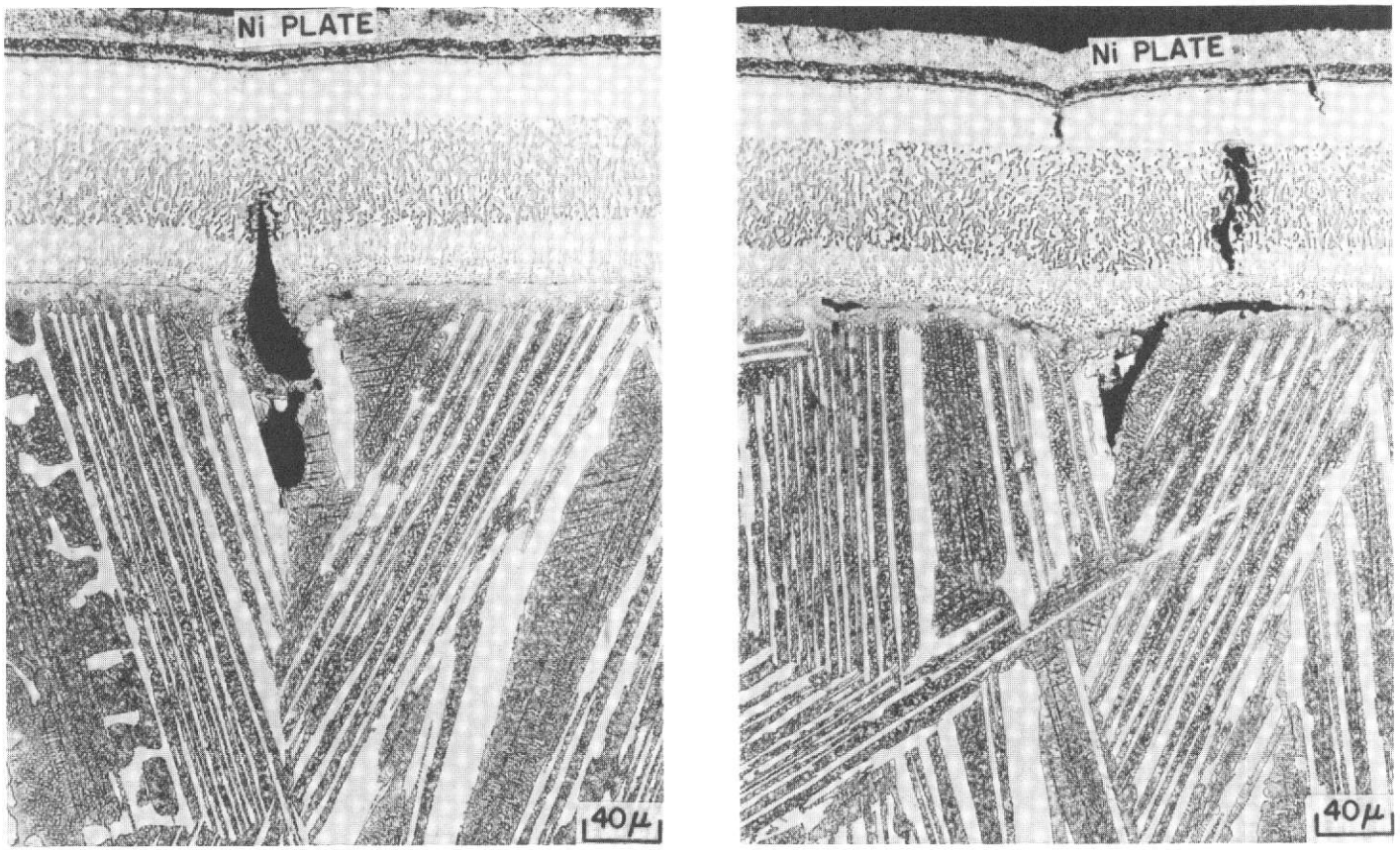

Figure 62 Pre-test Microstructures of Subsurface Defects in NiCrAlY/Pt Coated γ/γ'-δ Specimen (R-7412) Indicate That Porosity in the Cellular Regions of the γ/γ'-δ Substrate Was Contributory to the Formation of Coating Defects During Coating Deposition

parallel to the solidification direction (erosion bar longitudinal axis) may have initiated from similar defects. While the overlay low aluminum NiCrAlY portion of the NiCrAlY/Al coatings on $\gamma/\gamma'-\delta$ may also contain similar defects, the density of these defects appears to be insufficient to account for the large number of cracks which were observed for this system.

Perhaps more significantly, currently available thermal expansion data from internal P&WA programs for PWA 1422, $\gamma/\gamma'-\delta$ and NiCoCrAl (drop cast coating composition), Figure 63, indicate that coating-substrate thermal expansion mismatch strains may provide a partial explanation for the observed coating cracking in the burner rig test. These data indicate that, during cooling from 1366°K (2000°F) to room temperature, thermal expansion mismatch strains in NiCoCrAlY coatings are tensile on both PWA 1422 and $\gamma/\gamma'-\delta$ and have magnitudes of approximately 0.17% and 0.38% strain, respectively. Therefore, in the cyclic burner rig tests, combinations of thermal strains and coating-substrate thermal expansion mismatch strains may reasonably account for the behavior of the NiCoCrAlY coatings which has been observed on these two substrates. Although the magnitude of the coating-substrate thermal expansion mismatch strains are not known for the multi-layered NiCrAlY/Al and NiCrAlY/Pt coatings, it is apparent that the above explanation could be extended to the behavior of these coatings on PWA 1422 and $\gamma/\gamma'-\delta$. If this hypothesis is correct, presumably the NiCrAlY/Pt coating has a better thermal expansion coefficient match. However, for a particular coating-substrate mismatch strain, the tendency to thermal fatigue cracking should also be related to relative coating ductility.

In addition, the rate of thermal fatigue crack penetration into the $\gamma/\gamma'-\delta$ substrate also appeared to be a function of the coating which was present. It is thought that the thermal expansion mismatch strain in the coating, the elastic modulus of the coating, coating thickness, the density of cracks and the oxidation characteristics of a coating crack may be factors contributing to the observed behavior.

In view of the superior performance of the NiCrAlY/Pt coating system in the burner rig evaluation, it appears that incorporation of platinum offers advantages in terms of thermal fatigue and oxidation degradation behavior. The significance of the platinum distribution in the coating and the effect of platinum on the distribution (segregation) of aluminum in the coating merits additional investigation.

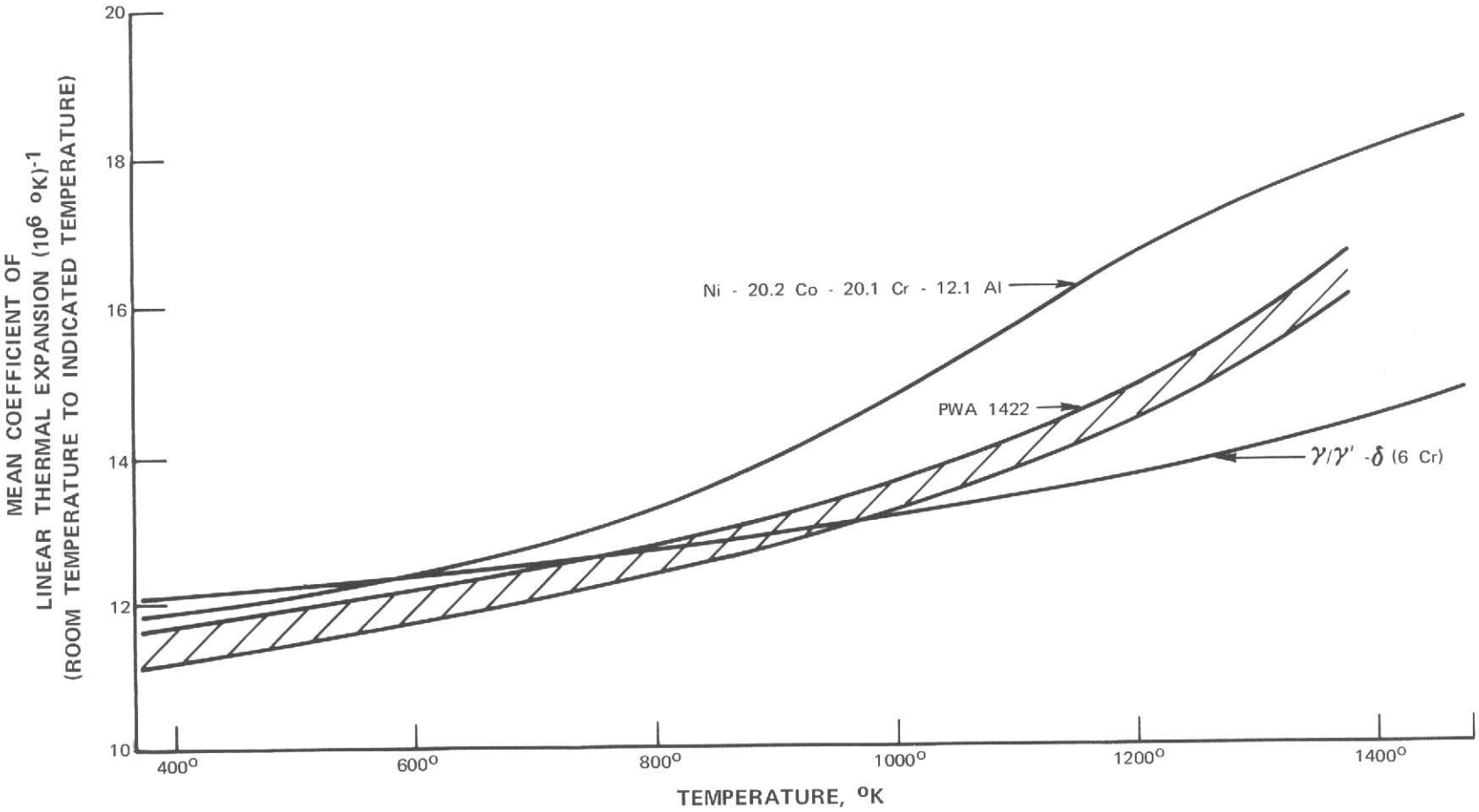

Figure 63 Preliminary Thermal Expansion Data

VII. STRESS-RUPTURE TESTING

Based on the results of the 1366°K (2000°F)/1016 hour burner rig cyclic oxidation test, the NiCrAlY/Pt coating system was selected for the remaining mechanical property evaluations of coated γ/γ'- δ .

A. SPECIMEN PREPARATION

Ten γ/γ'- δ stress (creep)-rupture specimens (Figure 64) were machined from nominal 1.27 cm (0.5 inch) diameter by approximately 15.2 cm (6 inch) long directionally solidified castings, which were prepared by United Aircraft Research Laboratories according to the procedure previously described. These specimens were machined in the same manner as the ductility specimens and the NiCrAlY/Pt coating was then applied using procedures previously described.

Two uncoated and two coated stress-rupture specimens with no prior exposure, were submitted for testing and two uncoated, and two coated specimens were exposed at 1366°K (2000°F) for 500 hours in an inert environment prior to testing. The stress-rupture tests were conducted at 151.7 MN/m^2 (22,000 psi)/1311°K (1900°F) in air in order to provide data pertaining to the influence of the coating system upon the eutectic alloy in the unaged and aged conditions.

In addition, after consultation with the NASA Program Manager, it was agreed that the two stress-rupture specimens designated as spares would be coated, exposed in a furnace at 1366°K (2000°F) for 500 hours in air and tested along with the other specimens. However, since these specimens were fully machined, it was evident that some means of protecting the threaded grips was necessary. To accomplish this, 63.5μ (2.5 mils) of NiCrAlY was applied to the threaded grips (because of dimensional tolerances a full 127μ (5 mils) of coating could not be tolerated on the threads). In addition, the coating on the grips was not peened and platinum was not applied in these areas since considerable time would have been required to modify the fixturing used in the sputtering apparatus. Only one of these specimens was suitable for testing, however.

Some minor problems were encountered in NiCrAlY coating the stress-rupture specimens which required stripping and recoating; in some instances, specimens were reprocessed twice. Stripping of the NiCrAlY coatings was accomplished by remachining of the specimens. In addition to the coating, a few thousandths of an inch of substrate material was also removed so that no residual coating affected substrate material would remain. Thus, no adverse affects related to prior coating were anticipated. However, because of the limited time available, one of the specimens was not reprocessed after the second remachining and recoating operation. Since specimen gage diameters vary, the load applied to the stress-rupture specimens was based upon the uncoated gage diameter for each individual specimen. Table XVI identifies the sequence of processing for each individual stress-rupture specimen and their final uncoated gage diameters.

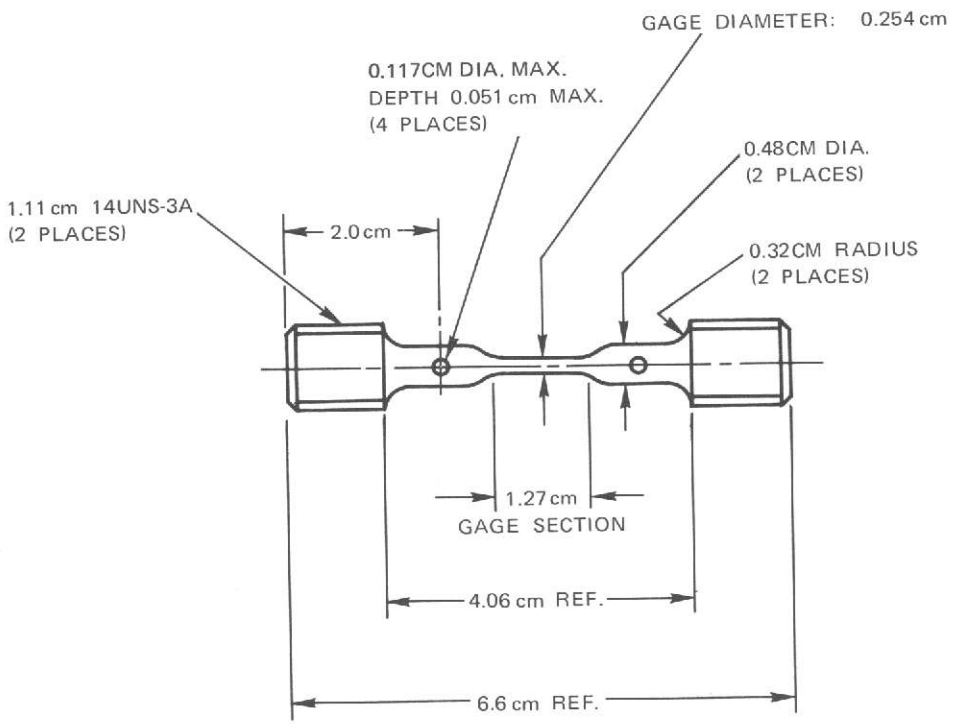

Figure 64 Creep Specimen Design

TABLE XVI

NiCrAlY/Pt COATED STRESS-RUPTURE SPECIMEN PROCESSING HISTORY

Specimen Identification	Uncoated	Times Remachined	Times NiCrAlY Coated	Times Platinum Coated	Pre-Test Condition		Final Uncoated Gage Diameter mm (Inches)
					Unexposed	Exposed	
A73-451-1	Yes	None	None	None	Yes	---	2.51 (0.099)
A73-451-2	Yes	None	None	None	Yes	---	2.51 (0.099)
A73-454-1	Yes	None	None	None	---	Yes[1]	2.54 (0.100)
A73-454-2	Yes	None	None	None	---	Yes[1]	2.54 (0.100)
A73-487-1*	---	2	3	1**	---	Yes[2]	2.31 (0.091)
A73-487-2*	---	2	3	None	---	No***	2.36 (0.093)
A73-502-1	---	2	3	1	Yes	---	2.18 (0.086)
A73-502-2	---	2	3	1	Yes	---	2.31 (0.091)
A73-503-1	---	1	2	1	---	Yes[1]	2.44 (0.096)
A73-503-2	---	1	2	1	---	Yes[1]	2.44 (0.096)

*63.5μ (0.0025 inch) of NiCrAlY on threaded grips.
**Pt deposition interrupted by chamber malfunction.
***NiCrAlY coating chipped from gage during peening--processing terminated.

1. 500 hours at 1366°K (2000°F) - inert environment
2. 500 hours at 1366°K (2000°F) in air

Chemistries of the electron beam overlay coatings are provided in Table XVII; after application of the NiCrAlY overlay coating, the thin 6.35μ (0.25 mil) platinum surface layer was applied by sputtering and then diffused in a 4 hour heat treatment at 1353°K (1975°F) in hydrogen.

B. TEST RESULTS

Results of these stress-rupture tests are summarized in Table XVIII. The NiCrAlY/Pt coated specimens had longer rupture lives than the uncoated $\gamma/\gamma'-\delta$ specimens. In addition, the rupture lives of both the coated and uncoated specimens appeared to be marginally improved when the specimens were in the aged condition. The rupture life data which was generated during this investigation is also compared with average rupture life data, which was generated in other programs, for D.S. $\gamma/\gamma'-\delta$ and D.S. MarM-200 + Hf alloys on a stress versus Larson-Miller parameter, P_{L-M} = (T, °K) (20 + log rupture life) X 10^{-3}, graph shown in Figure 65. While the uncoated $\gamma/\gamma'-\delta$ rupture life data is below average values for the D.S. eutectic alloy, they are similar to the scatter band for the material. Also note that the data for both coated and uncoated D.S. $\gamma/\gamma'-\delta$ which were obtained during this investigation exceed the Larson-Miller parameter values for D.S. MarM-200 + Hf.

Extensometry was inadvertently omitted on the unaged specimens; therefore, only the rupture life and creep ductility data were obtained for these specimens. Creep data was obtained for the aged specimens and times to 0.5% and 1.0% creep are provided in Table XVIII; the data indicates that, in addition to having longer rupture lives, the coated specimens had lower creep rates than the uncoated specimens.

Post-test metallographic examination of the uncoated $\gamma/\gamma'-\delta$ specimens revealed the presence of several surface connected secondary cracks in each specimen; this condition is illustrated in Figure 66a. In addition, during testing of the uncoated specimens, relatively thick surface oxide and oxidation affected substrate layers were formed (see Figure 67a); thicknesses of the depleted alloy zones are given in Table XIX.

Surface initiated secondary cracking appeared to be absent in the NiCrAlY/Pt coated $\gamma/\gamma'-\delta$ specimens. Post-test metallography indicated that some secondary damage was present in the $\gamma/\gamma'-\delta$ substrate adjacent to the coating; however, as shown in Figure 66b, the damage was associated with deterioration and eventual rupture of the δ phase. The size of diffusion affected substrate zones in the NiCrAlY/Pt coated specimens was also less than that of the oxidation affected zones of the uncoated specimens (see Figures 67b, 67c); thicknesses of the diffusion affected substrate zones are also given in Table XIX.

As indicated in Table XIX, post-test metallography revealed that the NiCrAlY layer of the coating was thinner (39.4μ to 106.7μ) than the intended 127μ thickness; a review of processing records did not provide an explanation for this discrepancy, however, it is unlikely that this variation in coating thickness would significantly affect the test results.

TABLE XVII

CHEMISTRIES OF THE ELECTRON BEAM OVERLAY COATINGS ON THE STRESS-RUPTURE SPECIMENS

Specimen Identification	Coating Chemistry
A73-502-1	Ni-17.8Cr-12.5Al-0.05Y
A73-502-2	Ni-21.0Cr-11.8Al-0.06Y
A73-503-1	Ni-18.0Cr-11.3Al-0.30Y
A73-503-2	Ni-18.0Cr-11.3Al-0.30Y
A73-487-1	Ni-18.8Cr-11.9Al-0.08Y

TABLE XVIII

NiCrAlY/Pt COATED γ/γ' - δ STRESS-RUPTURE RESULTS

1311°K (1900°F) - 151.7 MN/m^2 (22,000 psi) - Air

Specimen Identification	NiCrAlY/Pt Coated	Furnace Aged in Argon 2000°F/500 Hours (1366°K/1.8 X 10^6 Sec)	Time to 0.5% Creep (Hours)	Time to 1% Creep (Hours)	Time to Rupture (Hours)	% Elongation	% Reduction in Area
A73-451-1	No	No	Not Obtained*	Not Obtained*	106.2	11.0	21.0
A73-451-2	No	No	Not Obtained*	Not Obtained*	122.9	9.7	21.0
A73-454-1	No	Yes	24.0	46.5	114.7	12.6 (9.3)**	16.4
A73-454-2	No	Yes	21.5	56.0	166.4	15.6 (10.3)**	16.4
A73-502-1	Yes	No	Not Obtained*	Not Obtained*	206.2	9.6	22.5
A73-502-2	Yes	No	Not Obtained*	Not Obtained*	206.1	8.0	23.0
A73-503-1	Yes	Yes	50.0	75.0	213.4	4.8***	22.5
A73-503-2	Yes	Yes	40.0	140.5	287.3	5.7***	36.3
A73-487-1	Yes	Yes (Air)	50.0	185.0	328.8	5.9***	22.2

*Extensometry was inadvertently omitted on the unaged specimens; therefore, only the rupture life and creep ductility data were obtained.

**Last creep extension measurement before rupture.

***Last creep extension measurement before rupture. Specimens were damaged during removal from the test apparatus and it was not possible to determine % elongation by length change.

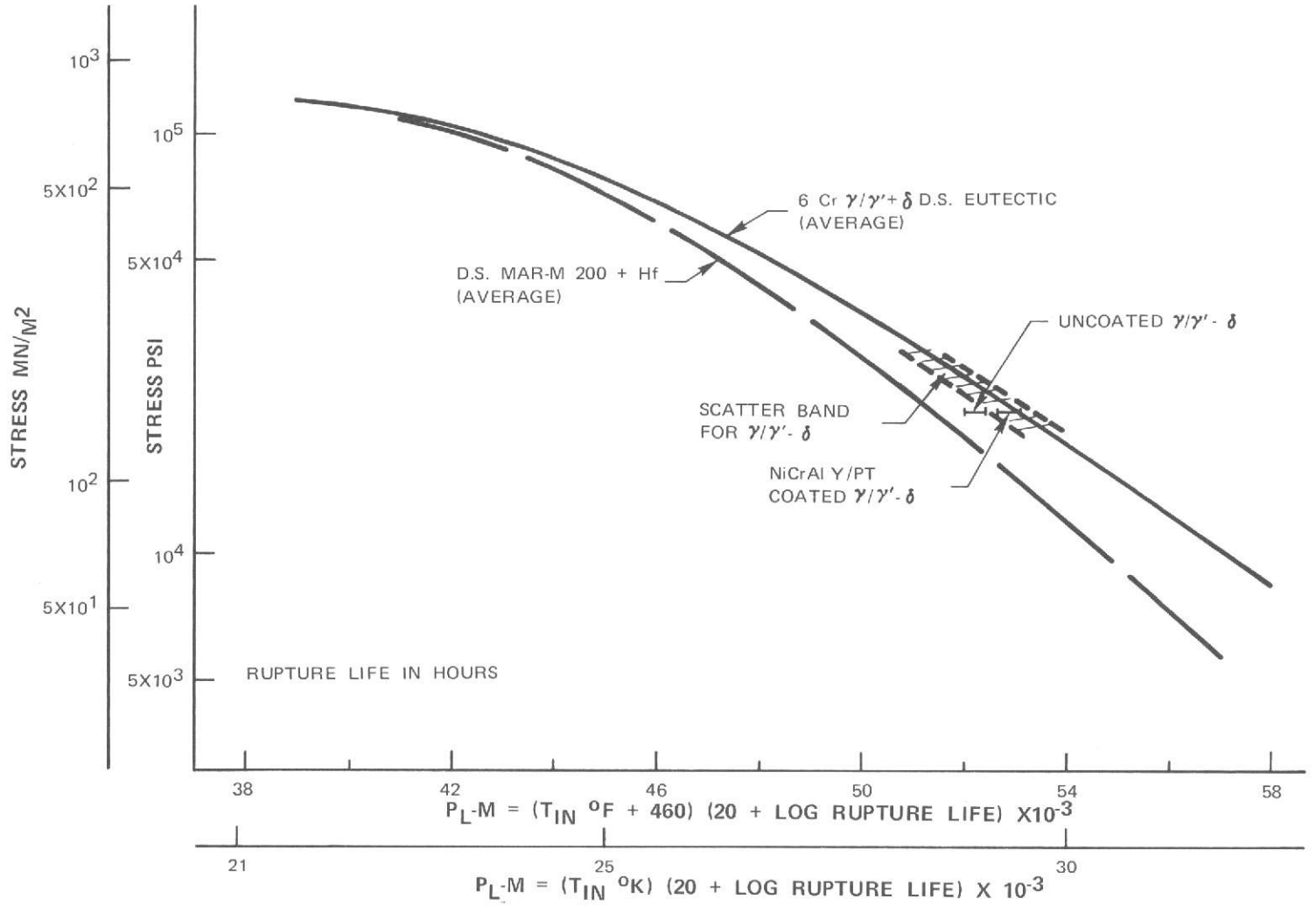

Figure 65 Stress Vs. Larson Miller Parameter Comparison Between Data, For Uncoated and NiCrAlY/Pt Coated γ/γ'-δ Specimens, Obtained in the Current Investigation and Average Data for D. S. γ/γ'-δ And D. S. MAR-M 200 + Hf. (Note: The load applied to the specimens was based upon the uncoated gage diameter of each individual specimen.)

TABLE XIX

1311°K (1900°F) STRESS-RUPTURE RESULTS OF NiCrAlY/Pt COATED γ/γ'- δ
(STRESS LEVEL CALCULATED ON BASIS OF UNAFFECTED SUBSTRATE CROSS SECTION AREA)

Specimen Identification	NiCrAlY/Pt Coated	Furnace Aged in Argon 1366°K (2000°F)/500 Hours	Time to Rupture (Hours)	Coating Thickness Microns (Mils)	Coating or Oxidation Affected Substrate Zone Thickness Microns (Mils)	Recalculated Stress Level* MN/m^2 (psi)
A73-451-1	No	No	106.2	---	67 (2.6)	169.7 (24,600)
A73-451-2	No	No	122.9	---	76 (3.0)	171.7 (24,900)
A73-454-1	No	Yes	114.7	---	67.3 (2.7)	169.0 (24,500)
A73-454-2	No	Yes	166.4	---	80.0 (3.2)	173.1 (25,100)
A73-502-1	Yes	No	206.2	107 (4.2)	27.9 (1.1)	160.0 (23,200)
A73-502-2	Yes	No	206.1	107 (4.2)	25.4 (1.0)	158.6 (23,000)
A73-503-1	Yes	Yes	213.4	39 (1.6)	42.2 (1.7)	162.8 (23,600)
A73-503-2	Yes	Yes	287.3	46 (1.8)	47.0 (1.9)	164.1 (23,800)
A73-487-1	Yes	Yes (Air)	328.8	95 (3.7)	42.7 (1.7)	163.4 (23,700)

*Original 151.7 MN/m^2 (22,000 psi) stress level was calculated on the basis of the gage cross-section area of the uncoated specimen. The new stress level is calculated on the basis of the γ/γ'- δ specimen cross-section which remainded unaffected by either oxidation or diffusion with the coating.

A73-454-2
Rupture Life: 166.4 Hours

A

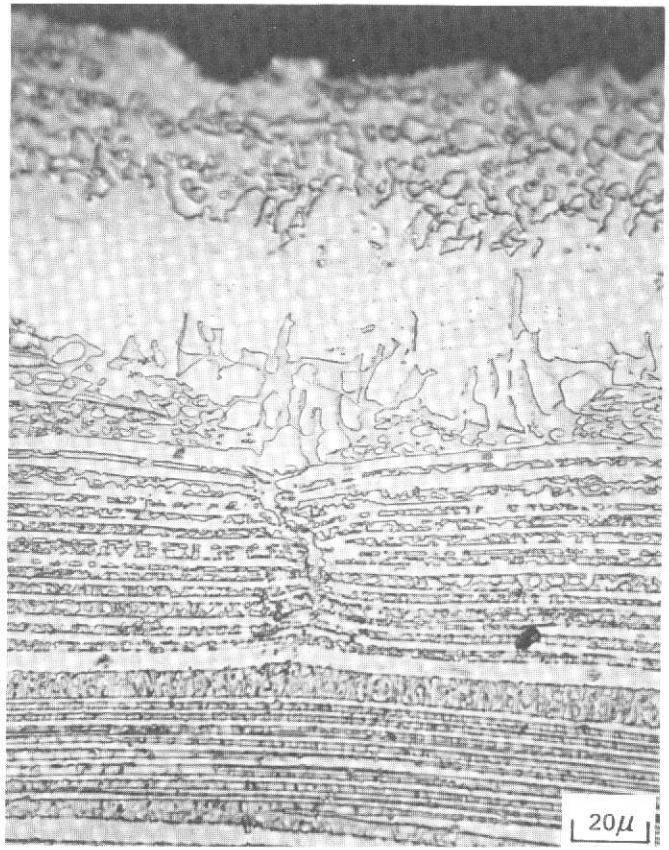

A73-503-2
Rupture Life: 287.3 Hours

B

Figure 66 Post-Test Microstructures of (A) Secondary Cracking in an Uncoated γ/γ'-δ Specimen and (B) Secondary Damage (Rupture of the δ Phase) in the NiCrAlY/Pt Coated γ/γ'-δ Specimen. These Specimens were aged at 1366°K (2000°F) For 500 Hours in Argon and Then Tested at 1311°K (1900°F) At a Stress Level of 151.7 MN/m^2 (22,000 psi)

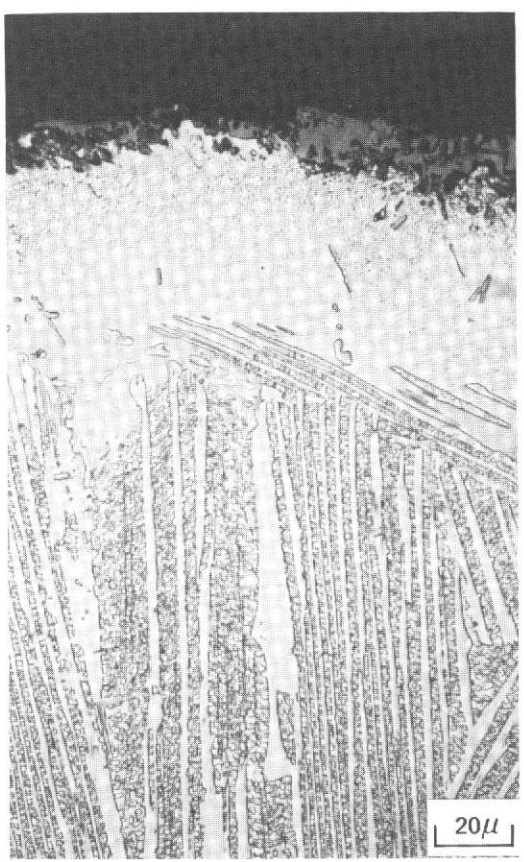

A73-451-2 (UNAGED)
Rupture Life: 122.9 Hours

A

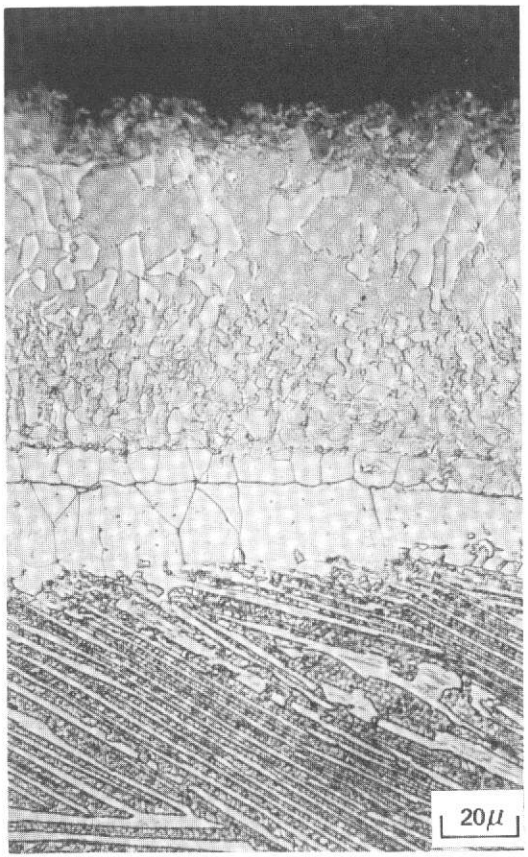

A73-502-2 (UNAGED)
Rupture Life: 206.1 Hours

B

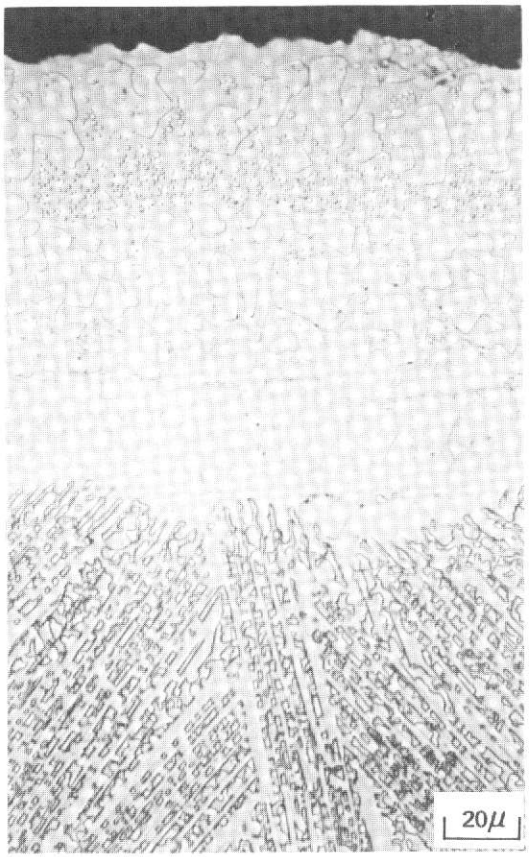

A73-487-1 (AGED)
Rupture Life: 328.8 Hours

C

Figure 67 Post-Test Microstructures of (A) Uncoated and (B, C) NiCrAlY/Pt Coated γ/γ'-δ Stress-Rupture Specimens. Note that the oxidation affected zone in the uncoated specimen is significantly thicker than the interdiffusion affected substrate zones in the coated specimens. The specimens were tested at 1311°K (1900°F) at a stress level of 151.7 MN/m^2 (22,000 psi) in air. Specimen A73-487-1 was aged at 1366°K (2000°F) for 500 hours in air before testing.

Post-test metallographic examination of the unaged γ/γ'-δ specimens indicated that the γ' distribution and particle size were similar to that of the as-cast structure. On the other hand, the γ' particles were significantly coarsened in the specimens which were aged for 500 hours at 1366°K (2000°F) to a size which was approximately equal to the lamellar thicknesses. The lamellar spacing of the δ phase did not appear to be affected by the aging heat treatment. Comparison of rupture life results for the uncoated γ/γ'-δ specimens in both the unaged and aged conditions indicates that the effect of coarsening the γ and γ' phases was of minimal significance.

C. DISCUSSION OF RESULTS

At this point, it should be recalled that the loads for the 151.7 MN/m^2 (22,000 psi) stress were calculated on the basis of the uncoated gage diameters of the specimens. Since these specimens had small cross-sections, the formation of oxidation affected zones in the uncoated specimens and interdiffusion affected zones in the NiCrAlY/Pt coated γ/γ'-δ specimens significantly increased (by 4.5 to 14.1%) the stress on the unaffected γ/γ'-δ substrate. (This statement assumes that the coating, interdiffusion affected substrate and oxidation affected substrate zones support negligible stress at 1311°K.) If the stress, which was applied to each specimen, is recalculated on the basis of the substrate cross-section area which was unaffected by oxidation or interdiffusion with the coating, then the agreement with the average stress versus Larson-Miller parameter data for the γ/γ'-δ alloy is improved significantly as shown in Figure 68 (compare with Figure 65). Even when this procedure is used, the lives for the coated specimens still appear to be somewhat better than those for the uncoated specimens.

In summary, these results indicate application of the NiCrAlY/Pt coating to D.S. γ/γ'-δ specimens is not detrimental and appears to be slightly beneficial from a rupture life standpoint.

VIII. THERMOMECHANICAL FATIGUE TESTING

Airfoil cracking due to the strain-temperature cycling, which occurs on acceleration and deceleration of a gas turbine engine, is one of the major causes of high pressure turbine blade failure. This fatigue cracking is caused by cyclic strains induced by temperature gradients in the airfoil, usually in the vicinity of the leading or trailing edge. For this reason, it is important to evaluate the thermal fatigue properties of all candidate materials for turbine blade applications.

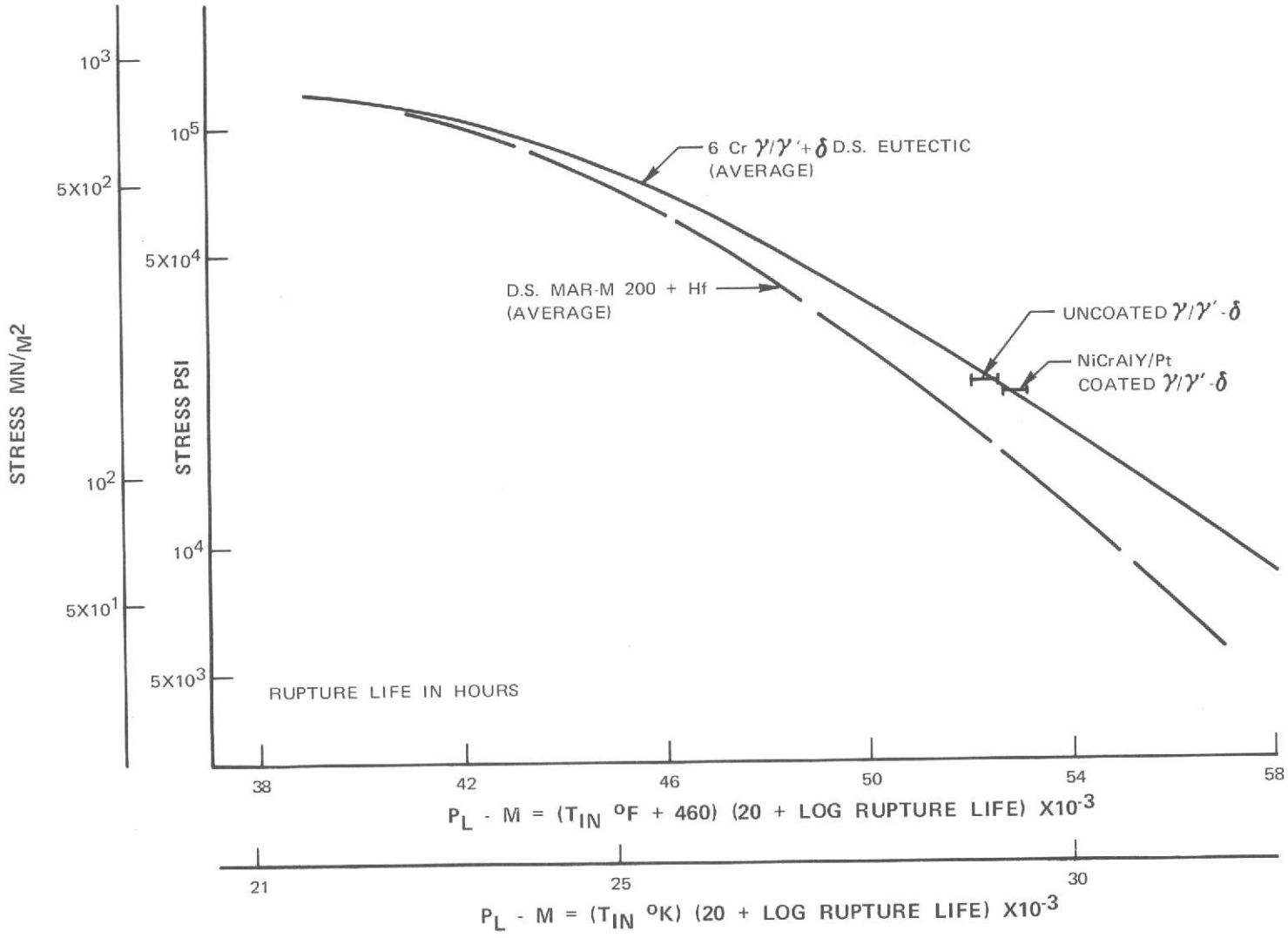

Figure 68 Stress vs. Larson Miller Parameter Comparison Between Data, For Uncoated and NiCrAlY/Pt Coated $\gamma/\gamma'-\delta$ Specimens, Obtained In the Current Investigation and Average Data for D.S. $\gamma/\gamma'-\delta$ and D.S. Mar-M 200 + Hf. In This Case, the Stress on the Specimens was Recalculated Using the Cross Section Area of the $\gamma/\gamma'-\delta$ Substrate Which Was Not Affected By Either Oxidation or Interdiffusion With the Coating.

The test used at P&WA to quantitatively simulate turbine airfoil thermal fatigue is the thermomechanical fatigue (TMF) test. This test allows complete freedom in specifying the relationship between strain and temperature. For example, as shown in Figure 69, the temperature at which the tensile strain peaks can be adjusted to low or high temperatures depending on the strain-temperature history of the particular location of interest in the component under simulation. For the leading edge of some airfoils, the conditions designated as cycle I are appropriate, while cycle II simulates conditions at the midchord or trailing edge of solid and hollow blades.

When significant cycle I type thermomechanical strain conditions are present on an airfoil, it is of particular concern from a coatings standpoint since many coatings have limited ductility at relatively low temperatures. Cycle II, which peaks the tensile strain at relatively high temperatures, is generally of less concern from a coatings viewpoint. Since coating-substrate interaction was of primary interest in this investigation, NiCrAlY/Pt coated γ/γ'- δ thermomechanical fatigue specimens were evaluated under cycle I conditions.

A. SPECIMEN PREPARATION

Directionally solidified 3.5 cm (1.375 inch) diameter bar stock was procured from the United Aircraft Research Laboratories (UARL). Unfortunately cracks developed in these castings during machining. Initially, the basic specimen OD configuration was ground and the ends faced. Then, the ID cavity was EDM machined. Following this operation, the presence of apparent substrate cracks were noted. Since the EDM process induces minimal macroscopic machining stresses, it appeared that relief of residual stress associated with the 3.5 cm diameter cast bars was responsible for the macroscopic cracking observed.

The P&WA Alloy Development Group has reported that TMF specimens, similar in geometry to the former, were successfully machined from castings of modified configuration (smaller diameter and contoured shape). With the NASA Program Manager's approval, the alternate casting configuration was substituted for the initial TMF specimens.

The contoured shape of these castings was facilitated by using alumina investment casting shell molds instead of the high purity alumina crucibles which had been used to cast the 3.5 cm diameter γ/γ'- δ bars. One of the contoured γ/γ'- δ castings (A74-124) was solidified at a rate of 3 cm/hour at the UARL; the second contoured γ/γ'- δ specimen was cast at the Casting Development Section of the MERL at a solidification rate of 1.27 cm/hour. Machining of these castings into thermomechanical fatigue specimens was completed successfully. The TMF specimen geometry is defined in Figure 70.

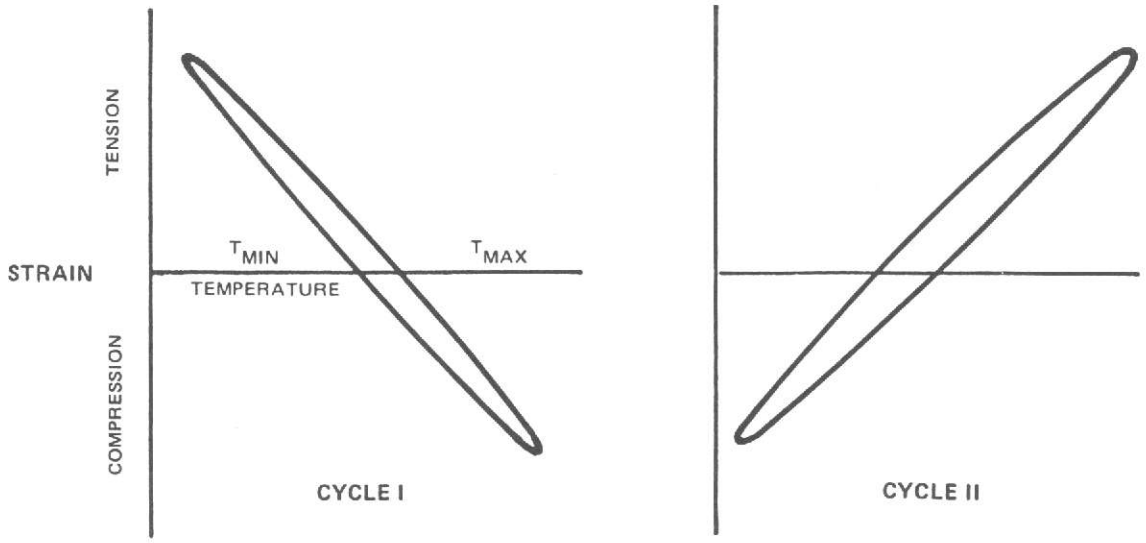

Figure 69 Schematic Diagram of TMF Cycles for Evaluation of Thermal Fatigue Resistance of Turbine Materials

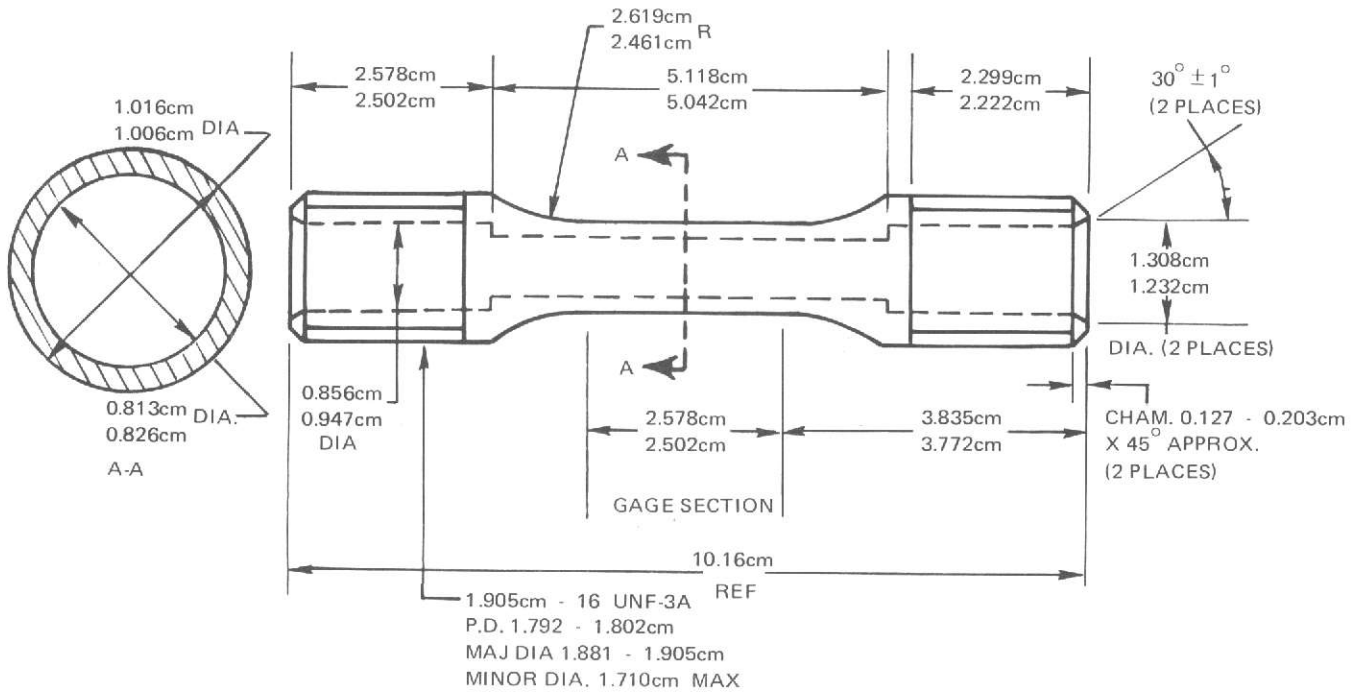

Figure 70 Thermomechanical Fatigue Specimen

The two TMF specimens were then coated on the outside diameter with the NiCrAlY/Pt coating system. The internal cavity of the specimens remained in the uncoated condition. The chemistry of the electron beam overlay coatings were determined to be Ni-18.6Cr-11.4Al-0.16Y; after application of the NiCrAlY overlay coating, the thin 6.35μ (0.25 mil) platinum surface layer was applied by sputtering and then diffused in a 4 hour heat treatment at 1353°K (1975°F) in hydrogen.

B. TEST DESCRIPTION AND RESULTS

Thermal-mechanical-strain cycling tests were performed in a closed loop servo hydraulic CGS (Continuous Growth and Science Corporation) fatigue machine which provided synchronized, independently programmable thermal and mechanical cycling. Cycle I temperature and strain conditions were programmed so that the specimen would be in tension (+0.25% strain) at 700°K (800°F) and in compression (-0.25% strain) at 1311°K (1900°F). Plastic replicas of the coating surface were taken periodically to facilitate detection of coating cracks. An induction coil surrounding the specimen was used for heating and forced air directed on the OD of the specimen was used for cooling. The cycle period was 135 seconds.

Results of these thermomechanical fatigue tests are provided in Table XX; data (from an internal P&WA program) for a directionally solidified MarM-200 + Hf specimen (same geometry) which was coated with Co ~ 18Cr ~ 11Al ~ 0.3Y (nominal composition) on the external surface and a pack aluminide coating on the internal surface is provided for comparative purposes. It can readily be seen from the test data that the cyclic life of the D.S. $\gamma/\gamma'-\delta$ specimens were significantly less than the life of the D.S. MarM-200 + Hf specimen. This situation was related to microstructural defects present in the $\gamma/\gamma'-\delta$ specimens.

Post-test metallographic examination of the UARL specimen, which had a life of 593 cycles, indicated that lamellar and cellular microstructural variations were present along the length of the specimen. Specimen deformation (buckling) appeared to be localized in a cellular band (Figure 71) and specimen failure occurred in this area. The NiCrAlY/Pt coating was in excellent condition and did not contribute to the failure of the specimen.

The $\gamma/\gamma'-\delta$ specimen which was solidified by the Casting Development Section of the MERL had a life of only 119 cycles. Numerous aluminum oxide inclusions were observed during post-test metallographic evaluation of this specimen. Examples of oxide inclusions which were associated with specimen failure and secondary crack initiation are shown in Figure 72. As with the preceding specimen, the NiCrAlY/Pt coating was in generally excellent condition and was not contributory to specimen failure.

TABLE XX

CYCLE I (700-1311°K) THERMOMECHANICAL FATIGUE TEST RESULTS

Specimen Identification	Substrate	External Coating	Internal Coating	Strain Range	Mean Strain	Cycles to 50% Load Reduction	Cycles to Specimen Failure
A-74-124 E-146	D.S. $\gamma/\gamma'-\delta$ D.S. $\gamma/\gamma'-\delta$	NiCrAlY/Pt NiCrAlY/Pt	None None	0.5% 0.5%	0 0	593* 119**	593 119
----	D.S. MarM-200 + HF	CoCrAlY	Pack Aluminide	0.6%	0	1635	> 1635
----	D.S. MarM-200 + Hf	CoCrAlY	Pack Aluminide	0.5%	0	2000 to 3000***	> 2000 to 3000***

*Portions of specimen had a cellular microstructure.
**Specimen contained oxide inclusions.
***Extrapolation of 0.6% strain range data to 0.5%.

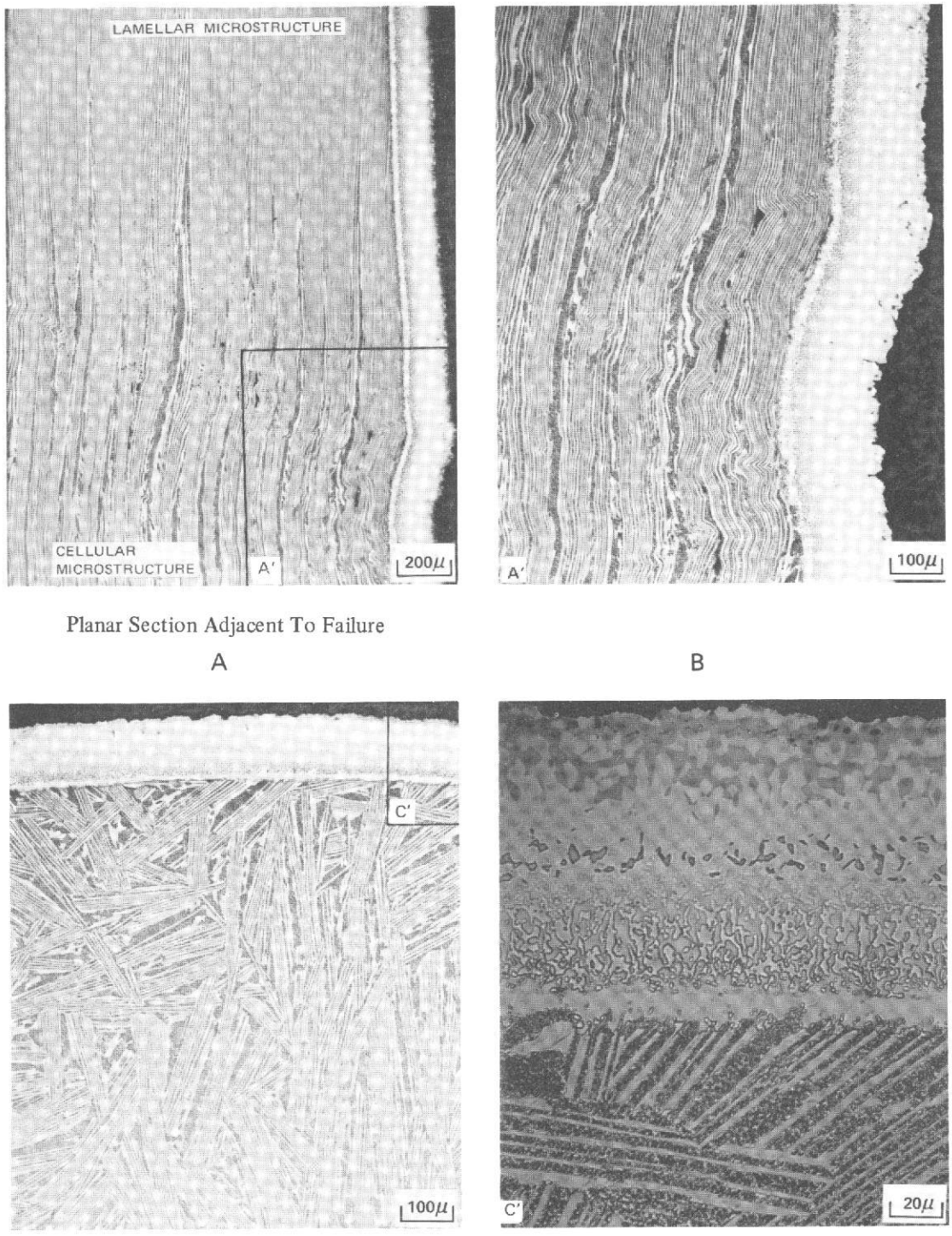

Figure 71 Buckling in a Band of Cellular γ/γ'-δ Was Associated With Failure of the NiCrAlY/Pt Coated γ/γ'-δ TMF Specimen (A74-124) After 593 Cycles of Cycle I (700° - 1311°K, 0.5% Strain Range) Testing. The Buckled Substrate Microstructure is Shown in (A) and (B), The Cellular Microstructure is Shown in Cross Section in (C), and the NiCrAlY/Pt Coating is Shown in (D)

C. DISCUSSION OF RESULTS

The performance of the NiCrAlY/Pt coating in the thermomechanical fatigue test was satisfactory. Oxide inclusions and microstructural inhomogeneities present in the $\gamma/\gamma'-\delta$ substrate were associated with the specimen failures; consequently, evaluation of the thermal fatigue capability of the $\gamma/\gamma'-\delta$ alloy, with an optimum microstructure, remains to be determined. The microstructural conditions which existed for the $\gamma/\gamma'-\delta$ test specimens precluded a meaningful comparison with the thermomechanical fatigue results available for a coated D.S. MarM-200 + Hf specimen.

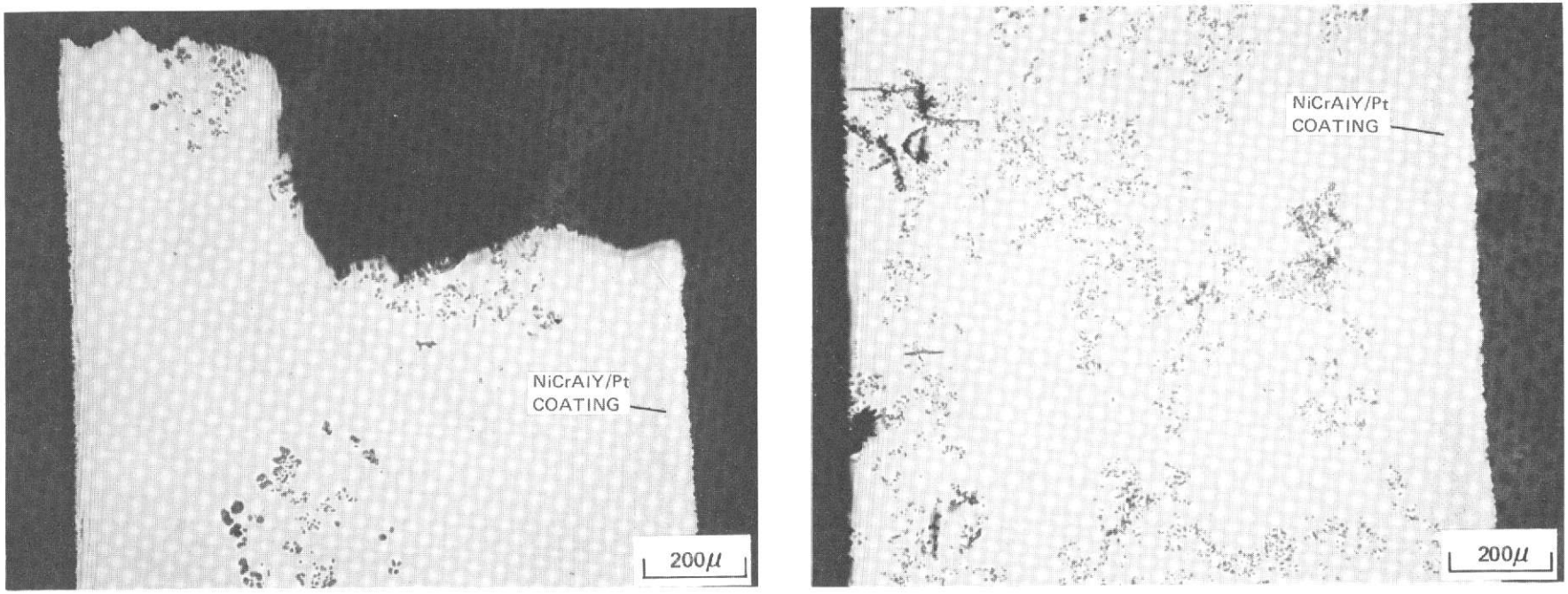

Primary Crack

Secondary Cracks

Figure 72 Post-Test Metallographic Examination Indicates That Numerous Aluminum Oxide (Casting) Inclusions Were Contributory To Failure of the NiCrAlY/Pt Coated γ/γ'-δ Specimen (E-146) Which Was Tested in Cycle I (700° - 1311°K, 0.5% Strain Range) Thermomechanical Fatigue for 119 Cycles.

IX. CONCLUSIONS

A platinum modified NiCrAlY overlay coating provided excellent protection for the $\gamma/\gamma'-\delta$ D.S. eutectic alloy for 1000 hours in 1366°K (2000°F) burner rig testing. This coating also demonstrated adequate overtemperature capability in 1478°K (2200°F) furnace testing, which indicates that the full temperature advantage anticipated with the D.S. eutectic alloy may be realized. The platinum modified NiCrAlY coating caused no significant detrimental effects on mechanical properties as determined by tensile ductility, stress-rupture and thermomechanical fatigue tests. All of the overlay type systems evaluated were superior to the diffusion aluminide coatings in terms of the oxidation protection they afforded the eutectic alloy.

Overlay coatings fabricated by plasma spraying showed potential; however, the oxidation resistance they provided was not comparable to that obtained with those based on electron beam vapor deposition.

Diffusion aluminide coatings appear to offer adequate oxidation protection at intermediate temperatures (1144°K); thus, they may be suitable for internal surface and perhaps blade root protection as well. However, the hot corrosion and higher temperature oxidation protection provided by the diffusion aluminide coatings is limited and improved capabilities in these environments is needed.

A brief summary of the principal findings in this program follows:

1. Laboratory hot corrosion [1144°K (1600°F) - 0.5 mg cm^{-2} Na_2SO_4] and cyclic oxidation [1144°K (1600°F) and 1366°K (2000°F)] furnace screening tests clearly indicated that overlay type coatings, representing a variety of nickel- and cobalt-base compositions applied by various techniques (electron beam, sputtering and plasma spraying), are superior to diffusion aluminide coatings for protecting the $\gamma/\gamma'-\delta$ D.S. eutectic alloy.

2. In the 1144°K (1600°F) hot corrosion testing (0.5 mg cm^{-2} Na_2SO_4), all of the overlay type coatings provided adequate protection for the duration of the test (260 hours). The diffusion aluminide coatings exhibited localized failures and associated substrate attack after 260 hours of exposure.

3. In the 100 hour 1144°K (1600°F) furnace cyclic oxidation testing, the two diffusion aluminides and both of the vapor deposited overlay coatings which were evaluated, provided suitable protection. However, based on weight change data (+0.03 to +0.18 mg cm^{-2} for the vapor deposited overlay coatings versus +0.35 to +0.63 mg cm^{-2} for the diffusion aluminides) and post-test microstructural condition, the overlay coatings performed best.

4. In the 1366°K (2000°F) furnace cyclic oxidation testing, essentially all of the overlay coatings were still adequately protecting the eutectic alloy after 500 hours of exposure. The diffusion aluminides afforded only limited protection with coating failures being observed in 140 hours or less.

5. For protection of internal surfaces, where overlay coatings cannot be applied because of line-of-sight restrictions, current diffusion aluminide coatings may prove adequate. For external airfoil surfaces it is clear that overlay coatings are mandatory for protection of γ/γ'-δ.

6. The 100 hour furnace cyclic oxidation tests at 1422°K (2100°F) and 1478°K (2200°F) indicated that the nickel-base overlay coatings were more diffusionally stable and offered higher overtemperature capability than cobalt-base compositions. Indeed, CoNiCrAlY and Ni/CoCrAlY exhibited incipient melting at the coating/eutectic alloy interface at 1478°K (2200°F). After 100 hours of exposure at 1478°K (2200°F), aluminized low-aluminum NiCrAlY, NiCrAlY/Pt and W/NiCrAlY vapor deposited overlay coatings exhibited about one-third as much interdiffusion with γ/γ'-δ as compared to an unmodified NiCrAlY overlay coating.

7. While the plasma sprayed overlay coatings adequately protected the γ/γ'-δ eutectic alloy, they were not equivalent to the electron beam vapor deposited coatings. Oxidation of the plasma sprayed coatings at 1366°K (2000°F) or higher temperatures was typified by formation of complex oxides (spinels rather than Al_2O_3) which spalled readily. Of the two plasma sprayed compositions evaluated, the NiCrAlSiY coating performed much better than the CoCrAlTaY coating in the 1422°K (2100°F) and 1478°K (2200°F) tests. For example, in the 1478°K (2200°F) test, after 40 hours, the weight loss for the nickel-base composition was about 2 mg cm^{-2} versus about 9 mg cm^{-2} for the Co-base coating (by comparison, the NiCrAlY/Pt vapor deposited overlay coating showed a small weight gain, about 1 mg cm^{-2}, after 100 hours of 1478°K (2200°F) testing).

8. Tensile ductility tests conducted at 578 and 811°K (600 and 1000°F) indicated that substrate failure strains were influenced by the particular coating system present. In general, the aluminized specimens exhibited substrate failure strains which were similar to those for the uncoated alloy (>2%), while those for the overlay coatings varied from less than 1% to about 2% depending upon the particular system. Reducing the thickness of the overlay coating from about 127μ to 63.5μ may provide an acceptable engineering solution for alleviating low temperature, low strain substrate failures.

9. A platinum modified NiCrAlY overlay coating which consists of an inner zone, approximately 127μ (5 mils) of electron beam vapor deposited Ni-18Cr-12Al-0.3Y, and an outer zone, approximately 6.3μ (0.25 mil) of sputter deposited platinum, provided excellent protection for the γ/γ'-δ alloy in 1366°K (2000°F) burner rig test. After 1016 hours in test, this coating was still adequately protecting the eutectic alloy.

10. The platinum modified NiCrAlY overlay coating demonstrated acceptable overtemperature capability in 100 hour cyclic furnace tests at 1422°K (2100°F) and 1478°K (2200°F), which indicates that the full temperature advantage anticipated with the γ/γ'-δ eutectic alloy may be realized.

11. Stress-rupture tests [1311°K (1900°F) - 151.7 MN/m^2 (22 ksi)] conducted on uncoated and NiCrAlY/Pt coated γ/γ'-δ specimens produced average rupture lives of approximately 114 and 206 hours, respectively. Uncoated and NiCrAlY/Pt coated specimens which were aged for 500 hours at 1366°K (2000°F) in inert atmosphere had slightly longer average rupture lives, approximately 140 and 245 hours, respectively, relative to unaged specimens. One NiCrAlY/Pt coated specimen was aged for 500 hours at 1366°K (2000°F) in air and had a rupture life of approximately 328 hours.

12. Thermomechanical fatigue testing of two NiCrAlY/Pt coated γ/γ'-δ specimens (700-1311°K, ± 0.25% strain) indicated no detrimental effects related to the presence of the coating. The cycles to failure (119 and 593 cycles, respectively) were shorter than anticipated and related to undesirable microstructural conditions of the substrate (oxide inclusions and cellular banding, respectively).

X. RECOMMENDATIONS

1. Further development of diffusion aluminide coatings to achieve increased oxidation protection for internal airfoil surfaces and possibly blade roots of γ/γ'-δ D. S. eutectic alloy turbine hardware, particularly in hot corrosion and higher temperature ($>1144°K$) environments, is suggested.

2. Since thinner coatings may be needed to alleviate low temperature, low strain ductility behavior, the oxidation and hot corrosion characteristics of reduced thickness ($<127\mu$) overlay coatings should be determined.

3. In view of the superior performance of the NiCrAlY/Pt coating, the significance of the platinum distribution and the effect of platinum on the distribution of aluminum in the coating merits additional investigation.

REFERENCES

1) Wermuth, F. R. and Stetson, A. R., "Alloyed Coatings for Dispersion Strengthened Alloys", NASA Report CR-120852, Steptember 1971.

2) Gedwill, M. A. and Grisaffe, S. J., "Oxidation Resistance Claddings for Superalloys", NASA Technical Memorandum X-67925.

3) Felten, E. J., "The Role Played by Tantalum During the Oxidation of Nickel and Cobalt Alloys", AMRDL Report 69-043.

4) David, A. and Coutsouradis, D., AGARD Conference Proceedings No. 120, p. 222. Report of Specialist Meeting held at the Technical University of Denmark, April 1972.

5) Grisaffe, S. J. and Merutka, J. P., "Coatings for Aircraft Gas Turbine Engines and Space Shuttle Heat Shields: A Review of Lewis Research Center Programs", NASA Technical Memorandum X-68007.

6) Lowell, C. E. and Miner, R. V., "Improvement in Cyclic Oxidation of the Nickel-Base Superalloy B-1900 by Addition of One Percent Silicon", NASA Technical Memoranium X-68191.

7) Lehnert, G. and Meinhardt, H., Electrodeposition and Surface Treatment 1, 71 (1972/73).

8) Lehnert, G. and Meinhardt, H., Electrodeposition and Surface Treatment 1, 189 (1972/73).

9) Felten, E. J. and Pettit, F. S., "High Temperature Oxidation Behavior of Directionally Solidified Eutectic Alloys", to be published.

10) Lemkey, F. D., "Eutectic Superalloys Strengthened by δ, Ni_3Cb Lamellae and γ', Ni_3Al Precipitates", Final Report, Contract NAS3-15562, January 1973.

11) Talboom, F. P., Elam, R. C., and Wilson, L. W., "Evaluation of Advanced Superalloy Protection Systems", NASA CR-72813, Contract NAS3-12415, December 2, 1970.

12) Maissel, L. I. and Glang, R., "Handbook of Thin Film Technology", McGraw-Hill Book Company, New York, 1970.

13) Holland, L., "Vacuum Deposition of Thin Films", Chapman and Hall, Ltd., London, 1966.

14) Pigrova, G. D. and Levin, Ye. Ye., Fiz. Metal. Metalloved., 28, 858 (1969).

15) Komura, Y., Sly, W. G. and Shoemaker, D. P., Acta Cryst., 13, 575 (1960).